

Brain Functionality via Complex Systems Theory

Gabriel Crumpei¹, Alina Gavriluț², Maricel Agop³, Irina Crumpei⁴

¹Psychiatry, Psychotherapy and Counselling Center Iași, Romania
(E-mail: crumpei.gabriel@yahoo.com)

²Faculty of Mathematics, A.I. Cuza University from Iași, Romania
(E-mail: gavrilut@uaic.ro)

³Gheorghe Asachi Technical University of Iași, Department of Physics, Romania
(E-mail: m.agop@yahoo.com)

⁴Psychology and Education Sciences Department, "A.I. Cuza" University from Iași, Romania
(E-mail: irina.crumpei@psih.uaic.ro)

Abstract. The evolution of research in the field of brain study and function has had a series of stages during the 20th century, starting with the age of great anatomical discoveries, passing through phrenology and continuing with the behaviourist and new cognitivist stages. Accordingly, in the last decades neurosciences attempted to encompass the phenomenology of psychological reality within an interdisciplinary approach. This wide interdisciplinary necessity comes from the need to apply the principles of complex systems to brain activity as well. From such perspective, it is necessary to overcome the paradigm according to which psychological activity is an exclusive product of neuronal activity. The detailed understanding of the way in which the main types of neurons function, will not help us entirely understand the mental. The theory of complex systems comes with totally different assumptions. In the complex systems generated by a great number of elements, the properties of the systems cannot be found in the sum of the properties of constitutive elements. The emergence property is the one that creates a link between the multitude of components and the properties of the complex system. As a result, even if we describe all the properties of all neurons, we will not be closer to understanding the mental.

In this paper we shall demonstrate that the psychological system has all the necessary elements in order to associate it with a complex system. That is the reason why we shall bring anatomical, neurophysiological and pathophysiological arguments, as well as data from the latest research in neurosciences using functional MRI. We shall also analyze the theories from the last century concerning the structure of the psyche in which we find elements that support a new theory of the mental from the perspective of the complex system theory.

Memorizing takes place at the interface of the spectral field with the contribution of certain information patterns as well as new information from the complex space which represents the potential, unstructured, non-differentiable, unpredictable parts. Such hypothesis is possible using a new vision on information according to which information is made up of energy patterns included in a topological dynamics.

We shall conclude that the complex space (from mathematical view point) is a real physical space and not an abstract one and that the brain dynamics between the complex space and the real one represents what we call the psyche and consists of the information processing in neural networks.

Keywords: Complex system theory; Brain; Fractals; Chaos; Topology; Complex space.

1 Introduction

The aim of this paper is to apply the theory of complex systems in order to sustain the hypothesis of the complex space as a physical space. Thus, the dynamics of the complex systems and especially that of the complex and of the real space (from the inner part of the systems) may lead to new hypotheses and theories about the structure of psyche and about its functioning.

The whole collection of the analyzers manages the transfer of information from its wave form into corpuscular form. This allows for the information processing to be accomplished both in a corpuscular, material network, the neuronal network, but also in a spectral network, of the coherent field associated to the neuronal network. Through the waves of the spectral field the dynamical link to the complex space is realized, situation which allows for the occurrence of the superior psychic processes, which are specific to the human being, and which need multidimensional development in order to be formed, a situation which is only allowed by the complex space. The mental reality represents thus the permanent dynamics between the neuronal (material) network, the associated spectral field (the fractal potential) and the infinite dimensional complex space.

The dynamics between the complex and the real space (the neuronal network) through the spectral field (wave field represented by the totality of the waves associated to corpuscles within the neuronal network) lies at the basis of the psychological system functioning. This paradigm can generate new hypotheses which should explain the mysteries of the psychological life, just as the old "mind-body" duality. The new topical



structure of the psychism associated with the theory of complexity and simplicity applied on fractal geometry through which reality is structured allows for the brain to have access to the knowledge of the fractal in its wholeness (when the mathematical model is reduced as a number of informational bytes, or a symbol, to put it differently). Through the analysis and synthesis ability, it can conceptualize the fractal at any point and at any scale, but with the price of extensive informational data.

2 Complex systems from the perspective of modern physics

Complex systems include many components which mutually interact and which have the ability to generate a new macroscopic collective behaviour modality, whose result is the spontaneous formation of distinct temporal, spatial and functional structures. Such examples of systems can be widely frequent and can be correlated with the climate, the coherent issuance of light by lasers, chemical systems of reaction-diffusion, biological cell networks, the statistics and prediction of earthquakes, the human brain etc.

A complex system has a behaviour of an emergent type, which means that the modality in which the system manifests itself cannot be deduced from the behaviour of its components. Nevertheless, the system's behaviour is contained in the behaviour of the components, if they are studied in the context in which they find themselves. From a qualitative viewpoint, in order to understand the behaviour of a complex system, we must understand both the behaviour of its components as well as the way in which they interact in order to generate the collective action. Complex systems are difficult to study because we cannot describe the „whole” without describing each component and because every component must be described through its relation with the other components.

From a quantitative viewpoint, the „complexity” of a system represents the information quantity necessary to describe it and it depends on the details necessary to describe the respective system. In other words, if we have a system with several possible states and we want to determine its state precisely, then the number of binary numbers (bytes) which is necessary to determine the respective state is dependent on the number of possible states. The positions and the impulses of the particles are real numbers whose specification may need an infinite number of bytes. Nevertheless, the information necessary for stating the microstate of a system is not infinite. This fact is due to quantum physics, which attributes a unique value to entropy and, thus, also to the information necessary to express a state of the system. First of all, the microscopic states are indiscernible if their positions and impulses do not differ through a discrete quantity given by Planck's constant. Secondly, quantum physics indicates the fact that particles (such as nuclei or atoms) found in the fundamental state are uniquely determined by this state and cannot be differed from each other. There is no additional information which is necessary in specifying their internal structure. Under normal conditions, all nuclei are, without exception, in the state of minimum energy. The relationship between information and entropy consists in the fact that the entropy of a physical system is maximum when it is in equilibrium, thus we can infer that the most complex system is in equilibrium state. This assertion is in contradiction with the perception of complex systems. Systems in a state of equilibrium do not have a spatial structure and do not change with the lapse of time. Complex systems have a substantial internal structure which is permanently modified as time passes.

Another challenge in the case of complex systems is the difficulty of predicting their behaviour even when the initial conditions are known, because the strength of interactions among the components of the systems completely screen the specific individual properties. It is not yet exactly known if this type of system respects some strict laws similar to the ones of the classical systems, nevertheless the development of some methods which allow for determining some of the dynamic properties of complex systems came to be possible. We should focus on representing the an-organization of complex systems which are manifested upon the passage from „complicated” to „complex” and which is based on the new paradigm of the passage from the classical space of the trajectories to more abstract spaces of the trajectories associated with the natural invariance of systems, which is characteristic to the dynamics of complex systems, which represent a separate class of entities with non-linear behaviour ([15]).

A complex system cannot be analyzed in principle by fragmentation into parts, because it is made up of elements which make sense only in within the privacy of the system. It has an unpredictable evolution, it can suffer sudden transformations which can be as big as possible, without obvious external causes; it manifests different aspects, depending on the analysis scale. It is principally different from a complicated system because the difficulty of prediction is not to be found in the inability of the observer to consider all the variables which would influence its dynamics, but in the sensitivity of the system to initial conditions (initial conditions which are slightly different can lead to extremely different types of evolution), to which the effect of an auto-organization process is to be added (process determined by the very interactions

between the component subsystems and which has, as an effect, the spontaneous emergence – on principle unpredictable – of some order relations).

A complex system can be shaped and studied in an equivalent topological space, called the phase space, in which specific notions can be defined: attractors and repulsors, attraction basin, trajectories, limit cycles, etc. In this context, one can talk about functional modelling, which is a lot more abstract and "unleashed" of the constraints imposed by a concrete "anatomy" and "physiology". While classical modelling starts by approximating what "is seen", functional modelling involves the identification of an equivalent dynamical system, whose behaviour can be analyzed through specific methods, with an extremely heightened generalization degree.

In systems composed of a great number of elements, the properties of the systems cannot be found in the sum of the properties of constituent elements. The emergence property is the one which creates a connection between the multitude of components and the properties of the complex system.

3. An approach to psychism from the perspective of complex systems theory

In complex systems structure there is a potential part with chaotic aspect and a structured, causal, Newtonian part, as well as different intermediate phases. From here there results a certain uncertainty in the structure of reality. Incertitude principle of Heisenberg [16] can also be found in Gabor [14] in communication theory (the information quantum); the non-linear, potential and apparently chaotic part corresponds to the unconscious, the structured causal part corresponds to the conscious and the intermediate phases, as well as the structures which process both the information from reality and from the unconscious are represented by what Freud was calling SuperEgo. This is not only an instance of censorship of impulses and wishes with only a moral significance, but we find there the processing structures of the representation of physical reality, such as tri-dimensional vision, the synesthesia, that is the processing which structures the imaginary reality according to the capacity of our analyzers to perceive reality.

In complex systems, the chaotic part is structured through attractors according to the constraints of the system (for instance, the way some physiological needs generate, during the dream, some dream structure (thirst, hunger, sexual abstinence etc.)). These mechanisms are also highlighted in daydreaming, when the fantasies are much more adapted to the conditions of reality. Thus, there is no longer the breakage of physical laws and of causality, but only a modification of these according to subject's wish-aspiration tendency. During the wakefulness state there is a dynamics with the chaotic part, potentially unconscious in the background and which allows accessing the information, memories, the logical links (for example, a speech). Recent studies linked to the role of the unconscious when awake and monitoring the cognitive and motric activity demonstrates that there is a permanent involvement from the unconscious through different ground reactions (such as reactions of defense from a potential danger or the involvement of a psychotrauma through the unconscious in the current activity (such as blind seeing, missed facts, slips of memory, compulsive-neurotic behaviours)).

The whole cosmologic and biological evolution is resumed to a dynamical link between chance and necessity, between diversity (chance mutation) and selection, between chaos and structuring, as in the human body (permanent renewal of cells and tissues, as well as the dynamics between inflammation (disorder) and structuring). Thus, old age, disease, epilepsy, rhythm troubles can be interpreted as losses of the fractal character, through the reduction of the chaotic character.

Information represents codified energy which is expressed under the form of patterns, structure patterns, initiated by attractors which activate in the phase space, between the chaotic and the structured part. The information is stored in the spectral space and expresses the patterns in the structure of atoms, molecules, macromolecules and cells. It has a potential existence which is expressed through substance and energy in certain conditions (of local coherence).

The virtual projection from optics or from projective geometry can be associated, so that when the whole physical (Newtonian) reality to which we have access through our sense organs, through perception, represents a projection in the imaginary space. We could thus build a mathematical model of this space using imaginary numbers, complex (imaginary) geometry, imaginary time, topology etc.

A virtual, Newtonian reality as projection of physical reality is completed by the unstructured, a-causal, apparently chaotic component: the imagination, the dream, the failed acts, the subliminal mechanisms, the unconscious etc., which can be associated with the a-causal, potential, unstructured and non-differentiable component of complex systems, the source of inspiration, of creation and of access to non-euclidean realities to holospace. These potentialities can become conscious through patterns (see the archetypes and the collective unconscious of Jung [17]) and they can be found in logical, algorithmic, organized and systematic form in everything that is creation (from making a speech, conversation,

improvisation, to creating new musical pieces, new artistic work, new scientific work). The chaotic, unpredictable part does not only contain the Newtonian reality to which we all have access, but much more, maybe even the structure of the whole Universe, at potential informational level. The brain has access to the implicit part (the implicit reality of Bohm [9]), if we associate this part to what the classics called unconscious. From here derives the capacity for mathematical reasoning, for physics, for reasoning reality in n-dimensional spaces, a-temporal realities, a-spatial realities.

The fractal geometry of reality confirms the older intuitions connected to the structuring of the Universe, which would have the same functioning and forming principles, irrespective of the scale. The physics of black holes and the astrophysics of the last years, as well as the theory of Big Bang, have brought arguments to support the idea that the fundamental principles of quantum mechanics can be found in the structure of the Universe.

By continuing to look for elements in order to sustain the unity of the Universe, it is necessary to analyze the theory of complex systems and, also connected to it, (as a physical approach), the complex functions or the complex space from a mathematical perspective. The complex analysis is absolutely necessary in describing the spinning movement, including that of the magnetic vector from the electromagnetic wave, as well as in the fluid dynamics.

Complex space could then describe a physical reality which integrates newtonian reality, as well as quantum mechanics or cosmology. For instance, Yang [21] considers the complex space as a physical entity, in which one can describe an entire variety of phenomena, among which one can find classical mechanics or relativistic mechanics.

The unpredictable, a-causal, unstructured part, which is potential in the complex systems structure, can be found in the structure of the spectral field associated to the corpuscle from the structured, causal, newtonian, predictable part. This spectral component contains, through the imaginary component of the wave formula which describes the phase (the dynamics of the magnetic vector), the access towards the complex spaces, where the whole information is to be found, as it is structured in the topological geometry of the energy configurations. The infinite dimensional possibility of these complex spaces, just as the infinite diversity of topological transformation within these spaces, together with their scale invariance allows for the estimation that in this complex space which is dimensionally infinite we can have access to all the information in the Universe.

Thus several theories are gathered together in a unitary approach: the theory of complex systems, which comes from a physical perspective in the physics of the fluids, the fractal theory, the theory of chaos and topology, with the complex analysis and the complex functions which use complex numbers with their imaginary component and which describe, in physics, the imaginary, unpredictable, potential, non-differentiable part, which can be found in the theory of complex systems. The semantic confusion, the apparent different significance of the word *complex* within the two theories or approaches is proved to be, on the contrary, a coincidence which is not random, but is connected to the synchronicities of Jung.

As in Mathematics the information can be stored or processed by algebraical equations or by trigonometrical functions, also in the physical reality information can be structured either algebraically or geometrically. The Fourier series and the Fourier transform achieve this through the interface between a spatial and temporal reality and a spectral reality. Because spectral reality is a-temporal, a-spatial, the Fourier transform and the reverse of the Fourier transform make this switch between the algebraical description and the geometrical one. The mathematical model for complex spaces includes the existence of topological transformations in an infinite dimensional space. As a result, the reality of the wave formula as being a-temporal, a-spatial, it represents an interface between the Newtonian reality and the complex "reality", that of complex spaces (Hilbert space).

The dynamics between the complex space and the physical one is an expression of the mathematical description of reality by algebraical or trigonometrical equations. The potentiality can be encompassed, codified in trigonometrical equations and it expresses the information in an a-spatial, a-temporal reality, which is specific to the wave and is algebraically transformed into a geometrical form when a spatio-temporal reality emerges, as it happens when the wave is collapsed into a corpuscle. In both cases, topological transformations are possible (and in an a-spatial, a-temporal situation which is trigonometrically expressed, but also in a spatial and temporal situation which is algebraically and geometrically expressed).

The discontinuity of reality which is described by Planck as an energy quanta, by Gabor in information quanta, the non-differentiability which is specific to fractal dynamics, just as the property of complex systems together with deterministic chaos, all are due to a continuous interference between the physical reality and the complex one, by means of spectral field. Depending on the local field conditions, of force field and of scale structure, under the action of attractors, the information (patterns of qualitative energy, diversified through topological transformations) is taken over in order to structure the quantum or cosmic Euclidean space.

4. The imaginary space as a physical and mathematical reality, from a psychological perspective

Complex systems can be identified at different scales, a method which can be applied also to the imaginary space. In the imaginary space, time has a spatial dimension property, which allows for movement in both senses of its axis. The construction of this imaginary space is made by the same methods as the ones used for the space of physical reality, although it has additionally elements which elude to it, that is the implicit reality of Bohm, such as, for example, n-dimensional spaces, fractal developments beyond what we can find in physical reality, plus mechanisms specific to deterministic chaos and generally speaking to complex systems.

The complex analysis is essential for the description of physical reality, of spectral, wave, field phenomena, which together with the corpuscular ones contribute to building the physical reality. The electric field corresponds to the real part, whereas the magnetic field corresponds to the imaginary component. The magnetic vector has a rotation movement around its own axis, movement which is described by the complex systems. At a 90-degree rotation (multiplication by i), an inversion of the components of the complex number occurs, event which in physics involves a Wick rotation. By multiplication with i , frequency and phase are mutually modulated, and their correlation is achieved by means of information.

Complex analysis describes physical phenomena which take into account the spinning movement. This phenomenon is present first of all in the electromagnetic waves and thus it can be found in many theoretically and technologically described situations. If we accept that there exists, in the real world and also in the functioning of the brain a spectral, wave component, then the description of the phenomena at this level requires the use, in mathematical modelling, of complex numbers with their imaginary part, of complex plans and so of complex spaces. Thus, the imaginary space, which encompasses the space of psychic activity, can be described by complex analysis, so that the syntagm "imaginary space" is not only a metaphor, but a real physical space.

All these are associated in the description of different physical realities and phenomena, which are, in one way or another, connected to the spectral reality of the field and wave associated to every particle. Surprising as that may sound, these complex spaces coexist with our Newtonian reality, as they are present in our every-day reality, as we are delved into a spectral, electromagnetic reality, to which we are closely-linked. As a consequence, a reality co-existing with us is the a-spatial and a-temporal reality, described by the wave formula and which is involved in the phenomenon of visual perception, in which the undertaking of spatial and temporal information is achieved by light through the modulation of its frequency, a phenomenon which is described by the Fourier transform, while the stimulation of the retina involves the collapse of the wave formula and the emergence of corpuscles which stimulate cells in the retina through the reverse of the Fourier transform. As a result, all we look at and all we see, in order for it to be seen, passes through an a-temporal and a-spatial phase, within the time lapse which is necessary for light to reach us, coming from that object. This lapse can be millions of light years for cosmic objects, or infinitely small second fractions when we look at our friends, our house or our garden.

The imaginary time represents only one of the dimensions of the imaginary space, the other ones being spatial dimensions which can be described as imaginary dimensions of the complex space. At small distances, at speeds within our Newtonian space, time can be seen and represented as a size which measures the succession of some events or the interval between them. If we use the equations of the relativity theory (space-time continuum) for very long distances (the distance Sun-Earth and the light velocity), then the time resulted from these formulas is described by a complex number, with a significance of imaginary time. This would lead to the conclusion that practically speaking, we as people use only this imaginary space, or, to put it differently, our representations of time actually use the imaginary time in Einstein's relativity theory. This imaginary time, or the time from the imaginary space is a time which, as compared to the Newtonian reality, does not have a single sense. In the imaginary space, time has the characteristics of a spatial dimension, as it can be run in both senses, in the past and in the present.

If in the space of physical reality, time is run in only one sense, because of the dynamics towards an increase in entropy triggered by the Big Bang, in the imaginary space it seems that it makes an enclave, a break from the cosmic dynamics of the Universe expansion, as long as evidently, in our brain we can evolve in living and updating the past, but also construct variants of the future. Without this possibility, neither memory nor the conscious action oriented towards the aim would exist, there would not be psychological life as we know it, as the neurological studies have demonstrated that without memory neither new experiences could be assimilated which are based on old ones, nor coherent and focused actions could be achieved, if they need the experience of the past.

For almost a century it is known about the existence, on the cortex, of projections of the sensory and motric structure of the body of that which is classically named sensitive and motric humunculus. Research on psychopathological situations such as the situation of the syndrome of the phantom limb, bring arguments on a spatial projection at brain level of every segment in the body. The fact that this cerebral

representation of the segment remains functional for a longer or shorter period of time demonstrates both the existence and the persistence of such representations.

The mirror box technique applied by Ramachandran [18] for the persistent, painful and spasmodic phantom limb cases shows that the representations of the segments of the body have a spatial character, as long as they can be influenced by the illusion of topological modifications, outside the imaginary space. The fact that the cerebral image of the lost limb segment persists away from the normal period after an amputation shows that some circular reverberant circuits maintained by remembrances marked by pain, contraction and suffering, are involved in the persistence of this structure which is spatially cerebral. These experimental facts lead to the conclusion that in the imaginary space there is a projection of the spatial structure of our body, to which it participates along with sensoriality and motricity, with the sensory organites and the corresponding neuromotric plaque and the affective, positive or negative processes. In fact, Davidson [13] demonstrated in his research that affection is involved in all the cognitive processes, including in the projection of the body and of the whole reality, at the level of imaginary space.

On the other hand, at an overview, the phenomena of suggestion and suggestibility from the modern theories point of view are involved in the Ramachandran [18] technique of improving the residual or complicated phantom limb symptom. A whole series of studies have demonstrated that we are willing to accept and to believe, as long as there is a motivation, be it affective-emotional or even logical, rational. In order to be able to reconstruct the action of a book or film, of a speech or of a lecture, it is necessary that, in our brain, we have a virtual reality, an imaginary one, which describes what in fact we call imaginary space. In the last decade the so-called mirror neurons have been highlighted and they recently acquired scientific validity through research with functional RMN and which brought objective proof for the existence of a virtual or imaginary projection of the Newtonian geometric space in which we live. Excitation of these neurons in the motric, sensitive or sensorial area to the actions and the behaviour of the others comes to sustain the previous so-called theory of the mind, which was trying to explain our ability of intuition, of perceiving the feelings and thoughts of the other. Mirror neurons come as objective arguments which sustain this theory, which was explained previously by psychologists as being a result of relationships with the others, communication and our specificity as social beings. They also represent a proof of the existence of spatial and temporal structures in our imaginary.

5. An explanation of psychism from the new paradigms perspective

Complex space, which is considered to be a purely mathematical, imaginary, abstract one, can actually be a physical space (without which quantum physics would not have any coherence any more) and which includes the real space which it generates and maintains through permanent dynamics. This change of paradigm is also important for macro reality from our Newtonian level and even cosmical, through the theory of scale relativity and, just as we described before, by interfering in the dynamics of complex systems through the scale invariance of fractality and topology. Thus, the notion of "complex" in the complex systems theory conceived in order to describe the systems with an indefinitely high number of elements in order to distinguish them from the complicated ones gains a significance which overlaps the one in the mathematics of the complex space.

Tegmark [19] maintains that mathematical structures and the relationships between them lie at the basis of reality. The elementary particles themselves are mathematical structures which can be perfectly described only by mathematical properties; all these form something that we generically call information. Another argument of the physical character of the complex space is the description of the wave function and of the wave function equation, which impose the existence of the Hilbert space. This abstract space allows for the inclusion of both the real part of the wave but also the imaginary, complex part of the wave (Schrödinger). This space requires the inclusion of both the real part of the wave, but also of the imaginary, complex part. As a result, the Hilbert space has properties of the complex space (the infinite dimensional character), the description using complex analysis, but also the real part which includes the wave amplitude and the potential capacity of becoming real in the collapse of the wave formula.

Another element which belongs to the real part is the space-time continuum, which we find in the Minkowski space, but which we also find in the Hilbert space concentrated in the expression of characterizing the wave as being "a-spatial", "a-temporal". In our view, the Hilbert space is an interface between the real and the complex space and a proof that the complex space is a physical space connected through a permanent dynamics with the real space, as long as we accept a wave as being real, with its wave function and equation.

The very notion of complexity needs also another approach. From the general theory of systems from the 60s conceived by Bertalanffy, in the last decades, the theory of complex systems or the complexity

theory are more and more mentioned, as they include a whole series of theories which imposed in the last decades (the chaos theory, the fractal theory or fractal geometry with non-linear dynamics, non-differentiability and topology).

All these theories are trying to describe as close to reality as possible the intimacy of the systems functioning with a huge number of elements, which interacts with other systems (dissipative systems) and which in fact can be found anywhere in the physical reality. These systems have a series of properties, among which emergence is a property with special implications, but also the dynamic structure they presuppose, generally characterized by a structural, causal, Newtonian, predictable component and another unpredictable, a-causal, non-structured, potential component. Physical experiments (the ones in the plasma tubes but also in the dynamics of fluids, etc.) highlighted these components as well as the dynamics between them, which presuppose a tendency of auto-structuring through the attractors, within a space called the phase space. There is still an important question related to the source of information which allows for the auto-structuring and thus the dynamics between the potential and the predictable component. The current explanation for the source of this information is that it comes from the privacy of the system. However, in the structure of the system (if we remain at the more simple model of the plasma tube), there are only particles and their attached wave component. If we consider that the information contained by the particle comes from the coherent wave, the obvious question is where the information at wave level comes from. Currently, in every day life, in the information technology era, the information is transmitted via waves, by means of their analogic transformation into waves which modulate a carrying wave. Modulation can be the amplitude modulation (little used because it is too easily affected by noise, but anyway the amplitude is in inverse ratio to frequency), the generally-used way is that of angle modulation, which means modulation of either the frequency, or of the phase, which is transmitted in the end to the modulation of the magnetic vector angle. The phase is recognized as being an imaginary, complex component of the wave formula. The movement of the magnetic vector, described by the complex equations, generate a complex plan, which connects the wave to the complex space, which allows for the storage of information in the topological modifications from this infinite dimensional space. To put it different, the information in the complex systems is to be found in the complex space, which renders the potentiality, non-differentiability, a-causality characteristics from the description of complex systems ([1-7], [11], [12], [14]). Coming back to the plasma tubes, the intimacy of the system from where the information comes is represented by the coherent waves phase with every particle (wave corresponding to every particle from the wave-particle duality), which represents the connection to the complex space, where it can be found at the potential mode, as information, the whole physical reality. According to the constraints of the system from the complex space, through the wave phase, the information which reaches the particle that generates the auto-structuring pattern is undertaken.

The topic of the dynamics between the two components (the structured, causal, differentiable, Newtonian component and the potential, unstructured, a-causal component) is to be found in the psycho-analytic conception over the psychological system (see also [10]), which is then repeated under different forms in the theories of psychism, namely the unconscious (id), subconscious (superego) and the conscious (ego). The unconscious represents the unstructured, a-causal, potential, unpredictable part which we can highlight in what we can call dreams, failed acts, lapses (as Freud himself describes), and the structured, causal, differentiable and Newtonian part is what was called conscious. In the psycho-analytic view, the super-ego is considered to be partially conscious, partially unconscious and it contains (according to Freud) the totality of the norms, rules, social laws, moral laws, which are constructed in the psychological space through education, as they represent elements with a value of law, faith, the nucleus of convictions through which the environment information is processed. From the complexity theory viewpoint, this superego could be associated to the phase space, where these convictions and values help with processing the information in conscious mental structures. Compared to Freudian theory, the theory of complexity would suppose that, at this level (superego) there are not only the moral and social values and norms, but also the processing patterns of the Newtonian laws connected to space, time, movement, just as the other rational precepts which science offered to the modern man in order to help one adapt to the environment.

The analyzers achieve, on principle, the transformation of wave information in the corpuscle, thus generating the tri-dimensional and spatial-temporal vision of reality, but the processing, at brain level, is also spectrally-made (de Valois [20]).

From a physical viewpoint, at any scale, there is a differentiable hydro-dynamic description mathematically modelled through hydro-dynamic equations, but also a stochastic, potential description, expressed through the equation of the wave formula. If we accept that the Hilbert space presents both the properties of the Minkowski space as well as those of the Euclidean one, but also of the infinite dimensional complex space, then it results that the Hilbert space represents the interface between the real space with all its descriptions and the complex space with its whole potentiality. Thus, the whole psychological life can be considered to be developed in this Hilbertian space which allows also for a Minkowskian perspective, a

spatio-temporal continuum, under the form of fractal space-time, where the trigonometrically-stored information is a-spatial and a-temporal, thus creating the conditions of a stable memory, but also a tri-dimensional spatial and temporal perspective which represents sections in time and space of this continuum. This material component of the neuronal network allows for the processing of information but for superior psychological processes, the processing is made in the complex space, so that the synthesis, generalization, abstractization and conceptualization suppose a multi-dimensional perspective, which can be achieved only in the complex, infinite dimensional space.

What we find, at quantum level, described by the Hilbert space, the real component, along with the fractal space-time and the complex component, at the level of the brain the interface of the neuronal network, the spectral field and the complex space, at a cosmic level, the Euclidean and Minkowskian spaces, together with the Riemannian one, connected to the complex space which from now on will be called matter and black energy. This hypothesis follows the principles of fractal development, which remains scale invariant.

On the other hand, as specialists in neurosciences sustain, just as the anthropologists, a radical qualitative leap for the development of the human species was the emergence of mirror neurons. They are present in other mammals, too, but it seems that in the case of human beings, through a genetic modification, they reached a degree of numerical development or maybe qualitative development which made this leap possible; it was expressed through a radical development of the social life, but which most of all permitted the transmission of information, abilities and behaviours, within the same generation and which, being transmitted to future generations, gradually constituted what we call today culture. The mirror-neurons which were highlighted about 20 years ago were recognized as being present at humans in the last 10 years, with the help of functional MRN. The study of these neurons is still ongoing, but just as the wave-corpucle duality of one century ago, mirror neurons also start to raise some epistemologic problems. They allow for a connection between the subjects in a relationship, a connection which explains, for example, "the old theory of the mind", built by the psychologists a long time ago in order to explain the empathy, compassion and intuition phenomena of the feelings of others. There remains a great problem, connected to the physical way in which mirror neurons are connected, in one person or another, especially because the last researches highlight the fact that the involvement of the visual sense and of other senses is not necessary, as long as the stimulation of mirror neurons with an individual is achieved by the intentionality of the action of the other individual. It may seem that a form of communication is involved, discussed until now more in the sphere of parapsychology, but which could find a scientific explanation in the dynamics of the psychological system between the neuronal network, the spectral field (the fractal potential) and the complex space.

The processing of information is made for the information supplied by the analyzers in a differentiable, causal, algorithmical form at the level of the neuronal network, whereas outside the analyzers, within a complementary network found in the complex space, mediated by the fractal potential from the spectral field of neurons. As a result, the qualitative leap represented by the emergence of culture would not be generated only by the emergence of mirror neurons which are present also with other animals, but by the development of genetic patterns which allowed for a better connection between the two networks. Not randomly, the appearance of articulate speech is associated with this qualitative leap in the development of humans. The speech centre seems to represent a system of information processing which allows for the connection to the infinite dimensional and complex space and thus the possibility of superior psychological processes. The study of mimic and gesture language of individuals with deafness highlighted the fact that, when learning this language, there is a first phase of learning of a mimic and gesture behaviour which is processed in the right hemisphere, specialized on spatial representations, and it becomes a real language only when it is undertaken by the speech center from the left emisphere. Then the mimic and gesture is undertaken at a level of notions and concepts and superior processes of abstractization, synthesis and generalization can be achieved. It results then that the centre of speech can be such a module which allows for the connection of the neuronal network with the corresponding one from the complex system, thus explaining the leap towards Homo sapiens. The centre which demonstrates the connection with the infinite dimensional spaces of the complex systems is the centre of speech (the deaf and dumb language), music processing and intuition, imagination, the ability to know some realities beyond the Euclidean space.

In the field of knowledge, fractal theory highlighted the fact that, in spite of the apparent infinite complexity of reality, this is in fact built on the basis of a fractal geometry in which the iteration of an extremely simple structure or configuration (the generating equation) combined with the topological modifications at every dimensional leap can reduce this whole complexity for a fractal collection which could theoretically lead to a single fractal, to a single configuration, to *One*.

Tegmark [19] proposes that this immeasurable complexity is generated by our approach of an extremely reduced sector from the scale section of a fractal. This is the aspect of reality that the positivist is trying to get to know through the scientific experiment. The analysis and description of this aspect of reality

needs an immense number of informational bytes and at this level the generalization and abstractization capacity of mathematics allows us to build models to approximate this reality. We started from the premise that science researches an extremely reduced sector of the scale section of a fractal. If we consider the whole fractal, all is reduced to a simple equation (Mandelbrot's equation $F(z)=z^2+c$). It seems that we have the possibility to represent our reality also at the level of complete fractal. It is what mystics, philosophy and metaphysics did for millennia. The place where the undeployed fractal can be found, where the "wrapped" reality of Bohm is, is the complex space, where there is the whole reality enveloped in potential under the form of mathematical structures which represent the equations of fractal generation. The first form of deployment of information from the complex system takes the form of the energy we find in the physical field under non-differentiable continuous form, but also at quantum level and at Minkowskian level. The next deployed form of the fractal is to be found under spatial and temporal form, under corpuscular form at quantum level or Euclidean form at tri-dimensional level. The representation of knowledge - through its scientific theories but also the philosophical and religious concepts - consists of two complementary aspects which physicists of a century ago presented under the form of the wave-corpuscle duality, while those of current day give a differentiable description which is mathematically modelled through the equations of hydrodynamics, as well as a stochastic, potential description expressed through the equation of the wave formula.

6. Is brain a computer?

The neuronal network development is made on fractal criteria, just as all the other apparatuses and systems of the human body. In the brain, the transmission of sense perception is spectrally and vibration-achieved [20]. As a consequence, the spectral field formed by the waves corresponding to corpuscles from the neuronal network are coherent, allowing for the processing of information both in the neuronal network and in the spectral space (Hilbert space), where at any scale there are the two types of realities, a differentiable and a non-differentiable one, highlighted through the hydrodynamic model of Madelung and the stochastic model, respectively. The a-spatial, a-temporal component allows for memorization, whereas the complex component offers the possibility of multi-dimensional processing which can explain superior psychological processes, such as, for example, conceptualization, semantics, abstractization and generalization, etc.

As opposed to the electronic computer whose hard structure is structured after some artificial algorithms (Barabassy [8]), the spectral component corresponding to corpuscles from the hardware has the same artificial character, deprived of the fractality specific to natural development, as a result there is no coherence between the substance corpuscle network and the spectral wave one.

Another essential difference between the electronic computer and the human brain is given by the analogical specific of the psychological processing, as opposed to digital processing. Analogical processing is doubled by the configurative topological character of the processing, practically speaking it is not numerical processing or only numerical processing, it is also a processing which belongs more to topological geometry. The dimensional dynamics from the 0 dimension to the infinite dimensional, which in our reality is achieved only up to three dimensions, can be achieved in the psychological reality in a multidimensional way in the complex space (through the fractal potential).

In the structure of psychism, the access from neuronal network to spectral (fractal) field and through Hilbert space to complex space allows for multidimensional dynamics which is not met at the electronic computer and which can explain superior psychological processes such as conceptualization, semantics, abstractization and generalization, etc., but also what is specifically human, creativity, intuition and adaptability.

References

- [1] M. Agop, C. Buzea, C. Gh. Buzea, L. Chirilă, S. Oancea, *On the information and uncertainty relation of canonical quantum systems with $SL(2R)$ invariance*, Chaos, Solitons & Fractals, Vol. 7, Issue 5, 659-668, 1996.
- [2] M. Agop, V. Griga, B. Ciobanu, C. Buzea, C. Stan, D. Tatomir, *The uncertainty relation for an assembly of Planck-type oscillators. A possible GR quantum mechanics connection*, Chaos, Solitons & Fractals, Vol. 8, Issue 5, 809-821, 1997.
- [3] M. Agop, V. Melnig, *L'energie informationelle et les relations d'incertitude pour les systemes canoniques $SL(2R)$ invariants*, Entropie, no. 188/189, 119-123, 1995.
- [4] M. Agop, A. Gavriluț, G. Ștefan, *$SL(2R)$ invariance of the Kepler type motions and Shannon informational entropy. Uncertainty relations through the constant value of the Onicescu informational energy*, Rep. Math. Phys, Vol. 75 (2015), No. 1, 101-112.

- [5] M. Agop, A. Gavriluț, E. Rezuș, *Implications of Onicescu's informational energy in some fundamental physical models*, International Journal of Modern Physics B, Vol. 29, No. 0 (2015), DOI: 10.1142/S0217979215500459.
- [6] M. Agop, A. Gavriluț, G. Crumpei, B. Doroftei, *Informational Non-differentiable Entropy and Uncertainty Relations in Complex Systems*, Entropy, 16 (2014), 6042-6058, DOI:10.3390/e16116042.
- [7] M. Agop, A. Gavriluț, C. Gh. Buzea, L. Ochiuz, D. Tesloianu, G. Crumpei, C. Popa, *Implications of quantum informational entropy in some fundamental physical and biophysical models*, chapter in the book Quantum Mechanics, IntechOpen, 2015, in print.
- [8] A.L. Barabassy, *Bursts: The Hidden Pattern Behind Everything We Do*, Penguin Group (USA) Inc., 2010.
- [9] D. Bohm, *Meaning And Information*, In: P. Pylykänen (ed.): The Search for Meaning: The New Spirit in Science and Philosophy, Crucible, The Aquarian Press, 1989.
- [10] F. Capra, *The Tao of Physics: An Exploration of the Parallels Between Modern Physics and Eastern Mysticism*, Shambhala Publications of Berkeley, California, 1975.
- [11] G. Crumpei, A. Gavriluț, M. Agop, I. Crumpei, L. Negură, I. Grecu, *New Mathematical and Theoretical Foundation in Human Brain Research. An interdisciplinary approach in a transdisciplinary world*, Human and Social Studies, Vol. 3, no. 1 (2014), 45-58.
- [12] G. Crumpei, A. Gavriluț, M. Agop, I. Crumpei, *An Exercise in a Transdisciplinary Approach for New Knowledge Paradigms*, Human and Social Studies, Vol. 3, no. 3 (2014), 114-143.
- [13] R. Davidson, *Affective neuroscience and psychophysiology: Toward a synthesis*, Psychophysiology, 40 (2003), 655–665.
- [14] D. Gabor, *Theory of communication*, Journal of the Institute of Electrical Engineers, 93, 429-441, 1946.
- [15] A. Gavriluț, M. Agop, *A Mathematical Approach in the Study of the Dynamics of Complex Systems* (in Romanian), Ars Longa Publishing House, Iași, 2013.
- [16] W. Heisenberg, *The Physical Principles of the Quantum Theory*, Courier Dover Publications, 1949.
- [17] C.G. Jung, *The Undiscovered Self: The Problem of the Individual in Modern Society*. New American Library, 2006.
- [18] V.S. Ramachandran, *Mirror neurons and imitation learning as the driving force behind "the great leap forward" in human evolution*, Edge Foundation web site. Retrieved October 19, 2011.
- [19] M. Tegmark, *Our Mathematical Universe: My Quest for the Ultimate Nature of Reality*, 2014.
- [20] R.L. De Valois, K.K. De Valois, *Spatial vision*, New York: Oxford University Press, 1988.
- [21] C. D. Yang, *Complex Mechanics*, Progress in Nonlinear Science, Vol. 1, 2010, 1-383.

An Approach on Information from Topological View

Gabriel Crumpei¹, Alina Gavriluț², Maricel Agop³, Irina Crumpei⁴

¹Psychiatry, Psychotherapy and Counselling Center Iași, Romania
(E-mail: crumpei.gabriel@yahoo.com)

²Faculty of Mathematics, A.I. Cuza University from Iași, Romania
(E-mail: gavrilut@uaic.ro)

³Gheorghe Asachi Technical University of Iași, Department of Physics, Romania
(E-mail: m.agop@yahoo.com)

⁴Psychology and Education Sciences Department, "A.I. Cuza" University from Iași, Romania
(E-mail: irina.crumpei@psih.uaic.ro)

Abstract. To define information is not easy task due to the diverse forms in which it can be expressed and identified. The main forms that occur (data, information and knowledge) do not represent a mere structure with increasing complexity which implies the integration of information in knowledge and that of data within information. For data to represent information a processing system is necessary. For information to construct knowledge, the human psychic is necessary. On the other hand, Shannon's theory which is the basis of informational phenomena implies the approach of information from quantitative view and less from a qualitative one.

We shall demonstrate that this qualitative aspect is generated by the topology of the geometrical space which, in its turn, organizes the informational dynamics and explains the unity of reality from the informational point of view due to scale invariant feature of topology. We shall argue that from the qualitative point of view, information is made up of energy patterns situated at different topological configurations, while according to the quantitative approach, besides entropic elements, information is implied in fractal dynamics, the topology of geometrical space interfering in dimensional change. Such hypothesis will be supported by implying topology in all scales and reality levels, using the string theory and quantum physics, a new perspective of wave-corpucle duality, as well as considering the molecular, biochemical, biological and mental levels, i.e. those places where information is permanently retrieved within topological dynamics.

We conclude regarding the hypothesis according to which topology as a mathematical discipline applied on information at different scales can offer a coherent perspective and an answer to the question "What is reality?"

Keywords: Information; Topology; Complex system theory; Fractals; Chaos.

1. Introduction

In our paper, we want to treat the information correlated to the substance and the energy, by applying the theory of complex systems, of complex analysis and of topology. We aim to highlight the fact that information can be found in the complex space of the wave phase spectral field. As a result, this complex space can be found anywhere and at every level of the reality. In our view, it is infinitely dimensional, as it can contain all the information in the Universe. From a mathematical viewpoint, the real space is included in and intertwined with the complex space generated by the electromagnetic waves. At quantum level, this intertwining can be achieved by the collapsing of the wave formula into the complex space of the wave phase and it can be transmitted into the complex space of the spin rotation, by transferring the whole information. This phenomenon is specific to reality at the level of the whole knowable universe, as everywhere there are electromagnetic waves and also at every level of the reality, including the human brain.

Our hypothesis is that the complex space is a physical space, which includes the real space which it generates and maintains through permanent dynamics. Thus, the complex space describes in fact a physical reality which integrates Newtonian reality, quantum mechanics and cosmology etc.

2. Information. Definitions and concept-making

In an etimological sense, the information is what gives shape to the spirit. It comes from the Latin verb *informare*, which means "to give shape" or "to form an idea on something". The perception on the information is as heterogenous as possible, the concept of information being a subject for reflection and analysis in: information theory, communication theory, knowledge theory, logics, semantics, philosophy, theology etc. Mainly, data forms information and information constitutes knowledge. Actually, the phenomena is not reduced only to an inclusion of a field into another. The information needs data and



operation and memory systems, whereas knowledge supposes an accumulation of information, but also of superior psychological systems, such as generalization, abstractization, synthesis, correlation and significance. This diversity under which information is presented determines both the defining difficulty and a unitary understanding of its significance at different levels of reality.

With quantum mechanics, the necessity emerged to define information at quantum level. In the theories which appeared in the second half of the twentieth century (the theory of chaos, the theory of fractals and of non-linear dynamics), all united into what is called the theory of complex systems, the necessity to define information appears more imperatively, especially because this theory is applied irrespective of the scale, to all levels of reality. The science of complexity, which attempts at modelling the structure of matter at different scales or reality levels, needs a new approach of information as a defining notion along with energy and substance. This is the reason why defining information becomes even more complicated from the perspective of the new paradigms. Traditionally speaking, there are two meanings of the information notion. One with the aristotelic acception, which designates the formation and structuring of a specific form, of an organization within an initially non-homogenous matter, the other signifying the transmission of a message. Information can also be seen as a proper fact, as a relation fact, as a fact of action transmission. That is why we are talking about an objective information transmission which is related to the structure of the Universe, be it macroscopic or microscopic, but also of a subjective meaning, which involves human communication, not only between human beings, but also between them and the various information technology devices and technologies.

The theory of information is connected to Shannon and Weaver [21], who defined, in the 50s and 60s, information as an entity which is neither true nor false, neither significant nor insignificant, neither credible nor doubtful, neither accepted nor rejected. As a result, it is not worth studying anything else than a quantitative component of information, but not also the semantic part, which allows for the association of information with the second theory of thermodynamics, with entropy, the information or the quantity of information being in inverse ratio with it.

Weaver connected Shannon's mathematical theory with the second thermodynamic law and asserted that entropy is the one which determines the information generation ratio. The formula of information is identical to the one of entropy elaborated by Boltzmann, but considered with a minus sign:

$$H = - \sum_{k=1}^i p_k \log p_k$$

where p represents the probability of an element or event k within the system.

Information is, thus, entropy. It is important to notice that Onicescu [17] also formulated the hypothesis regarding the fact that the degree of organizing a system can be "measured" with the help of informational energy, thus defined:

$$E = - \sum_{j=1}^n p_j^2(A)$$

where p represents the probability of appearance of the event A .

This quantitative approach of information is applied in the field of telecommunication and of information technology. Under this approach it is important to establish the quantity of information and its true or false character in transmitting information, to which probability notions can be connected in order to find, with the receptors, the source-transmitted information. Even within this technological approach, two aspects of information are highlighted: information as a product, which reflects a static overview, and the approach as a process, which highlights the genesis and the scope of information. In fact, the two aspects represent the information as potentiality and the information expressed and involved in the dynamics of the becoming and structuring of matter.

Upon attempting to structure the multiple informational approaches, Introna [15] distinguishes two archetypes: the informational and the communicational one. The first was patented with the explosive development of informational technology and is connected to the making (development) of "productive"

informational systems. The second has its origins in the communicational frame of Shannon and Weaver [21], being less important in the field of informational system field, but it is more widely accepted in the theories of communication. Similarly, Stonier [18] is of opinion that the fundamental aspect of information is connected to the fact that this is not a mental construction, but a fundamental property of the Universe. Any general theory of information must start with the study of the physical properties of information, as it is manifested in the Universe. This action must be taken before attempting to understand the variants and the more complex forms of human information. The next step must involve the examination of the evolution of informational systems beyond the physical systems, first in the area of biology, then in the human, cultural area.

The scientific approach of the information theory starts from the classical opinion that mathematics is the general language of nature. The structure of the Universe is written in the mathematical language, and its letters are geometrical forms, symbols and mathematical relations. Tegmark [19] maintains that at the basis of reality there are mathematical structures and the relationships between them and that elementary particles are mathematical structures which can be perfectly described only by mathematical properties. Thus, these mathematical structures and the relationships between them define what we call today information, whereas science does not do anything else but decypher the information contained in the structure of the matter, by physical-mathematical modelling. According to this paradigm, information is to be found in nature, outside of, beyond and independently of the observer. As a consequence, information must have existed before the appearance of human conscience.

To put it different, the information is the fundamental component of reality, such as matter and energy, as the nature is filled with information. On a larger scale, information exists before, or, in other words, knowledge is "more fundamental" than its observer and interpreter. Thus, the reunited concepts of matter (substance and energy) and information can explain the emergence, the forming, structure and dynamics of mind and knowledge, but also of the whole structure of the Universe. Information has an objective natural existence; people absorb it in their minds and the computer memory modifies and multiplies it through thought and bring it to the "middle" of society via the language.

At the opposite end of this materialistic-objective approach of information is the belief according to which information is something one person communicates to another, whereas the meaning of information can be understood only if we take into account the presence of alive beings endowed with reason, placed into a socio-cultural context and analyzed from a historical perspective.

A fundamental trait of information is connected to its subjectivity. Whatever can be information for a person can mean nothing to other people. Whatever is considered as information for a person can be data for another person. On the other hand, starting from the same set of data, different individuals, through different processing, can infer different information. If the data has a physical, tangible existence, the information exists only with the receptor, thus it is intangible. Information is the product of human or artificial intelligence and what constitutes information for one person can represent mere data for another person. No matter how difficult the definition and significance of information is, a possible modality of understanding what information represents in its essence is to be able to define the connection between energy, substance and information.

3. The place of information in the wave-corpucle duality

The paradoxes highlighted by quantum mechanics in the first half of the 20th century include, apart from the uncertainty relations of Heisenberg [14], a strange involvement of the observer in developing quantum phenomena. These facts suggest that the splitting into subjective and objective information is artificial and that they should be regarded as aspects of the same phenomenon. In order to uphold this idea, we must take into consideration another paradox of quantum mechanics, which is just as exciting and linked to the entanglement phenomenon, which, as a result of repeated experiments, highlighted a reality which is hard to infer, that is that all the particles which interacted at a certain point remain connected.

All these paradoxes that quantum mechanics imposed, along with the wave-corpucle duality, determined a new approach in physics, mathematics and in the scientific approach in general. If during the 20th century it was studied from the elementary particles' point of view, of the wave component from the spectral viewpoint and materially under the form of substance and energy, the information was not treated at its true value, according to the role it has in quantum mechanics. The information technology era, as well as the theory of complex systems, with the chaotic aspects in which information has a potential character, but which explains the dynamic evolution patterns of the system which is highlighted in the phase space, have all imposed the comeback on the role of information at quantum level.

The complex systems theory imposes re-analyzing the wave-corpuscle duality from the perspective of fractal geometry and of non-linear dynamics, which also need the involvement of information as a third element in the wave-corpuscle duality.

In Scale Relativity Theory, the dynamics of any physical system is described through dimensions which can be expressed through fractal functions, that is functions which are dependent both on coordinates and on time, but also on resolution scales. Moreover, any quantity can be written as sum between a differentiable part, i.e., dependent only on coordinates and time, but also on a fractal part, i.e. dependent on both coordinates and time, but also on resolution scales. In such a context, the differentiable part is proved to be compatible only with the predictable states of the physical system, while the fractal part is proved to be compatible only with the unpredictable states of the same physical system.

The analysis of wave-corpuscle duality in de Broglie's theory involves the simultaneous existence of two types of movements: a deterministic movement, which is predictable and associated to a continuous movement of hydrodynamic type along a continuous line, which is specific to the corpuscle character, and a zig-zag random and unpredictable movement, which is specific to the wave character. De Broglie's model introduces the two types of movements only as hypotheses, but the real problem, how much it is wave, how much corpuscle, as well as the wave-corpuscle structural compatibility (the structure of the wave should be compatible with the corpuscle structure) has not been solved yet.

A new approach modality of the problematics involved in the wave-corpuscle duality resides, in our view, in supposing that the movement of a particle takes place along continuous and non-differentiable curves. This means passing from a classical approach of movement within an euclidean space to a non-conventional, non-standard approach, with the assumption that movement takes place within a fractal space-time.

Thus, de Broglie's difficult problem can be solved, meaning that this could not justify the uniform movement of the particle within the wave field (incompatibility with the straight-line, uniform movement of the wave-corpuscle duality). The postulate through which motions are introduced on continuous and nondifferentiable curves solves this problem of the straight and uniform movement, meaning that on the new fractal manifold the movement is free (on geodesics). By accepting such a postulate, on the basis of the model of Scale Relativity Theory, it results that the geodesics of a fractal space-time supports a double representation, a stochastic, unpredictable one, described by Schrödinger type equations and specific to the wave character, and at the same time a deterministic, predictable representation, through the fractal hydrodynamic model, which is specific to the corpuscular character.

In Schrödinger's representation, only the modulus of the square wave function has physical significance, while in the second case we talk about average movements of some fluid particles which are submitted to a datum force, a force which is induced by the unpredictable part (non-differentiability of the motion curves). Non-predictability, described through the non-differentiability of motion curves can be related to a Shannon-type fractal informational entropy, which, based on a maximization principle, leads to an egalitarian uncertainty principle. Within this uncertainty principle, the interaction constants are specified on the basis of an Onicescu-type informational energy. Now, we mention the fact that only the constant value of the Onicescu informational energy settles the interaction constants within the uncertainty relations.

Through the maximization principle, the integrally invariant functions are simultaneously probability density and movements on constant energy curves. Practically speaking, through the principle of informational maximization, the unpredictable, wave character given by the probability density is linked to the corpuscle character given by the energy.

The unpredictable part must be directly correlated to non-differentiability and is manifested through the existence of a potential, also called fractal potential. The principle of maximization of the informational energy gives a concrete form to the potential and the latter, introduced in the fractal potential, gives complete form to the force field. As a result, the informational energy not only stores and transmits the information through interaction, but also connects it directly to the deterministic part through interaction. So, practically speaking, the owner of all "mysteries" is the fractal potential, which imposes the intelligent, fractal medium and the informational energy which gives the force.

As above-specified, on the basis of the non-predictable component, one can define a fractal entropy in Shannon's sense and, starting from here, a fractal informational energy in the sense of Onicescu. By using a maximization principle of fractal entropy in Shannon's sense, one can demonstrate that, if fractal informational energy in Onicescu's sense is constant, then the ratio between the corpuscle energy and the frequency of the associated wave is a constant at any resolution scale. As a result, the wave-corpuscle duality is achieved through movements on curves of informational energy constant in Onicescu's approach (for details, see [1-7, 11-13]).

4. Information as an expression of topological transformations. Different levels of reality

Topology studies the deformations of the space through continuous transformation, practically-speaking the properties of sets which remain unchanged at some transformations. Movement is a fundamental aspect of the real world and any elaborate study of dynamics leads to topology, as long as there is a dimensional space. Nevertheless, applications of the topological ideas appear in various fields, such as the theory of chaos, the quantum theory of fields, molecular biology, where the description and analysis of twists and deformations of the DNA molecule needs topological concepts. More specifically, the so-called topology of the knots allows for understanding the way in which the two spiral chains which make the double helical structure of the DNA molecule can be unfolded when the genetic plan controls the development of the living being.

Starting from quantum microcosm towards our Newtonian reality, we meet the information under the same topological forms at every scale. Atoms form molecules and macromolecules, whose spatial configuration suffers topological modifications which grant them some properties. Organic macromolecules in protein and enzyme form "ship" the information to cellular receptors, under the form of topological structures. Any modified radical determines a reconfiguration of spatial structures, which generates a certain property necessary in the chain of metabolic transformations which in this way are topologically equivalent, as they are obtained through topological transformations.

Any biochemical structure represents a graph, every cellular structure represents a network which forms knots and whose dynamics can be described by the network topology, which explicitly mentions the vicinities of every point. All this information comes from the structure of the DNA. The latter, apart from the succession of nitrate bases which form the genes, has a topologically-complex structure, in agglomerations which form the chromosomes, but which also influence the coding functions. The same information transmission mechanisms from DNA to RNA messenger and RNA ribosome and the constituting of protein and neurotransmitters we can also find within the structuring and functioning of the nervous system. We meet networks, knots, graphs, thus topological transformations also in this instance. All these represent only one part of the reality, because atoms, molecules, macromolecules, etc., are bodily aspects of the wave-corpuscle duality. All these structures have also a wave part, they are practically doubled by a spectral reality, of electromagnetic field.

The term topology is used also for establishing the projecting manner of a network. In order to highlight the physical (real) and logical (virtual) inter-connections between the knots, one can distinguish two corresponding types of topologies: a physical and a logical one, respectively. The physical topology of the network refers to the configuration of the transmission environments, of computers and peripheral devices, whereas the logical topology represents the method used to transfer information from one computer to another. The theory of domains developed within lattices represents a modality of modelling the topological concepts in a computational form, which allows for the processing of information.

Now, coming back to the wave-corpuscle problem, an analysis of the particle behaviour can be made from the perspective of fractal space-time, with the unpredictable and non-linear evolution, allowing that, on the basis of the informational theory of Shannon, we connect it to entropy and further, through a maximizing process, to the informational energy in the acception of Onicescu. There still remains an essential question: where can we search for and find the information in this quantum dynamics. It must be present both in the wave structure and in the particle properties. This connection cannot be made otherwise than in the phasic component of the wave, which is to be found in the spinning of the particle and which allows for the transfer of information from the spectral reality to the corpuscular reality, as it is demonstrated by the transform and the reverse of the Fourier transform. The phase is given by the magnetic component of the electromagnetic field and it represents the unpredictable, potential part, described by the complex function of Schrödinger's wave formula, as these characteristics can be explained both through the fractal theory and through the topological transformations supported by the phase from the electromagnetic wave, respectively by the spin from the particle description.

The spinning movement is mathematically modelled using the complex analysis. This model is dynamic, as it undergoes transformations at the level of topological dimensions through the successive passage from the topological dimension 0 (of the point) to the topological dimension 1 (of the line) etc. Thus, a complex, infinitely-dimensional space is made, which explains the difficulty of highlighting the informational component. The successive passage through Euclidean, fractal and topological dimensions determines a quantitative, but also qualitative dynamics of energy. The moment in which this qualitative diversity is expressed is given by the moment of topological transformations at every dimension. This diversity which is practically unlimited renders quality, apart from quantity, to energy in its dynamics. From the perspective of complex systems we can find, in the statements above, the main characteristics specific to complex systems: non-linear dynamics, fractal geometry, with a latent informational energy which is

potential, along with a dynamics of a practically infinite diversity, obtained by topological transformations in the phase complex space.

If we accept that topological transformations are invariant as compared to the scale and that these topological transformations represent energy patterns, configurations through which information is expressed, it should happen that, irrespective of the level of reality and of scale, the information has as an underlayer these topological transformations. The consequence of this is the ubiquity of information, just as the substance and energy, both at the level of microcosm and at macrocosm level.

Obviously, there exists structural information which, along with energy and substance, structures the matter at different scales and aggregation states. It is a structural information, which is achieved through topological transformations in fractal dynamics and even in euclidean dynamics. The topological space represents the place where information gains diversity, whereas energy gains a qualitative character. Qualitative variations of energy appear here, which constitute the informational energy or the psychological energy at mental level. Jung, in his research [16] over the unconscious and archetypes considers psychological energy to be a form of energy described through qualitative, not through quantitative ones, as physical energy was described. We will detail these considerations further below.

5. Dynamics of the real space – complex space in the structure of reality and psychism

Complex functions mathematically describe physical phenomena which assume the rotation movement around the own centre, including the movement of the magnetic vector of the electromagnetic wave, as well as from the fluid dynamics, and they sustain such hypotheses, theories and phenomena that the modern technology presupposes. This phenomenon is present first of all in the electromagnetic waves and thus it can be found in many situations which are theoretically and technologically described. The electric field corresponds to the real part, whereas the magnetic field corresponds to the imaginary component. The magnetic vector has a spinning movement, which is described by complex functions. At a 90-degree rotation (multiplication by i), an inversion of the components of the complex number takes place, a movement which in physics implies a Wick rotation. By multiplication with i , the amplitude and the phase are mutually modulated and their correlation is achieved by information.

The unpredictable, a-causal, unstructured, potential part of the complex systems structure can be found in the structure of the spectral field, associated to the corpuscle from the structured, causal, Newtonian, predictable part. This spectral component contains, through the imaginary component of the wave formula that describes the phase (the dynamics of the magnetic vector) the access to complex spaces, where the whole information can be found, structured in the topological geometry of energy configurations. The infinitely-dimensional possibility of these complex spaces, just as the infinite diversity of topological transformation within these spaces, along with their scale invariance allows for the estimation that in this infinitely-dimensional complex space we can have access to the whole information of the Universe. Thus, in a unitary approach, one can find the theory of complex systems, which comes from a physical perspective of the fluid physics, fractal theory, chaos theory and topology, with the complex analysis and the complex functions which use complex numbers with their imaginary component and which describe, in physics, the imaginary, unpredictable, potential, non-differentiable part, which can be found in the theory of complex systems.

As in mathematics information can be stored or processed by algebraical equations or by trigonometrical functions, in physical reality also information can be either algebraically or geometrically structured. The Fourier series and the Fourier transform achieve this through the interface between a spatial-temporal reality and a spectral one. Because the spectral reality is a-temporal, a-spatial, the Fourier transform and the reverse of the Fourier transform make this switch between the algebraical and the geometrical description. The mathematical model for the complex spaces includes the existence of topological transformations within an infinitely-dimensional space. As a result, the reality of the wave formula as being a-temporal, a-spatial, represents an interface between the newtonian reality and the complex "reality" of the complex spaces (Hilbert space).

The discontinuity of reality described by Planck as an energy quanta, by Gabor as information quanta, the non-differentiability specific to fractal dynamics, as well as the property of complex systems with deterministic chaos, all are due to a continuous interference between the physical and the complex reality through the spectral field. Depending on the local field conditions, of forces and scale structure, with the action of attractors, information from the complex space is absorbed (qualitative energy patterns, diversified through topological transformations), in order to structure the quantum or cosmic Euclidean space.

The dynamics between the complex and the physical space is an expression of the mathematical description of reality through algebraic or trigonometric equations. The potentiality can be encompassed, codified in trigonometric equations and it expresses the information in an a-spatial, a-temporal reality which is specific to the wave and which is algebraically transformed in geometric form when a spatio-temporal reality appears, as it happens when the wave collapses into a corpuscle. In both cases, topological transformations are possible (in an a-spatial, a-temporal situation trigonometrically expressed, but also in a spatial-temporal one, expressed algebraically or geometrically).

Another argument of the physical character of the complex space is the wave function and wave function equation description which impose the existence of the Hilbert space. This abstract space allows for the description of the wave function and of the Schrödinger wave function equation. This space imposes the inclusion of both the real part of the wave and of its imaginary, complex one. As a result, the Hilbert space has properties of the complex space (the infinitely-dimensional character), the description by complex functions (complex analysis), but also the real part which includes the amplitude of the wave and its potential capacity of becoming real in the collapse of the wave formula. Another element which belongs to the real part is the space-time continuum character which we can find in the Minkowski space, but which we also find concentrated in the Hilbert space in the characterizing expression of the wave as being ,’’a-spatial’’, ’’a-temporal’’. In our view, the Hilbert space is an interface between the real space and the complex space and a proof that the complex space is a physical space connected through a permanent dynamics with the real space, as long as we accept the wave as real, with its wave function and wave equation.

The dynamics between the complex and the real space (the neuronal network), by way of the spectral field (wave field represented by the totality of the waves associated to the corpuscles in the neuronal network) is the basis of the psychological system functioning. This paradigm can generate new hypotheses which should explain the mysteries of the psychological life, just as the old ’’mind-brain’’ duality. This new topic structure of psychism, associated with the theory of complexity and simplicity, applied to fractal geometry, through which reality is structured, allows the brain to have access also to the knowledge of the fractal as a whole, when the mathematical model is reduced as a number of informational bytes, to put it different as a symbol, but also, through the analysis and synthesis capacity, to be able to conceptualize the fractal at any point or at any scale, with the cost of an enormous informational content.

From a physical viewpoint, at any scale, there is a differentiable hydrodynamic description mathematically modelled by hydrodynamic equations, but also a stochastic, potential description, expressed by the equation of the wave formula. If we accept that the Hilbert space presents both the properties of the Minkowski space and the ones of the Euclidean space, just as of the infinitely-dimensional complex space, then it results that the Hilbert space represents the interface between the real space with all its descriptions and the complex space with all its potentiality.

Thus, the whole psychological life can be considered to take place in this Hilbert space which allows also for a Minkowskian perspective, a spatial-temporal continuum, under the form of the fractal space-time, where the information trigonometrically stored is a-spatial and a-temporal, thus creating the conditions of a stable memory, but also a spatial-temporal tri-dimensional perspective which represents sections in time and space of this continuum. This material component of the neuronal network allows for the processing of information, but for the superior psychological processes, the processing is achieved in the complex space, so that the synthesis, generalization, abstractization, conceptualization, all assume a multidimensional perspective, which can be made only in the infinitely dimensional complex space. More precisely, the dimensional dynamics from the 0 dimension to infinitely dimensional which in our reality is realized only up to three dimensions, can be realized multidimensionally in the psychological reality in the complex space (through the fractal potential).

6. An approach from the perspective of the complex systems theory for the processing, storage and transmission of information at brain level

As we already know, a complex system cannot be analyzed on principle through the part fragmenting, as it is made up of elements which make sense only within the privacy of the system. It has an unpredictable evolution (than, mostly, within a short time frame called temporal horizon), can suffer sudden transformations, no matter how big, without obvious external causes and it manifests different aspects according to the analysis scale. It is on principle different from a complicated system because the difficulty of prediction is not to be found in the inability of the observer to analyze all the variables which would influence its dynamics, but in the sensitivity of the system to initial conditions (slightly different initial conditions which lead to extremely different evolution possibilities), to which one can add the effect of an

auto-organization process (process determined by the very interactions between the component sub-systems and whose effect is the spontaneous emergence – principled unpredictable – of some order relations).

A complex system can be modeled and studied within a topologically-equivalent space, called the phase space, in which specific notions are defined: attractors and repulsors, attraction basin, trajectories, limit cycles, etc. In this context, one can talk about a functional modeling, which is much more abstract and "unbound" from the constraints imposed by a concrete "anatomy" and "physiology". While classical modeling starts by approximating what "can be seen", functional modeling involves the identification of an equivalent dynamic system, whose behavior can be analyzed through specific methods with an extremely high degree of generalization.

In the systems composed by a great number of elements, the properties of the systems cannot be found in the total amount of the complex systems properties. The emergence property is what creates a link between the multitude of the components and the properties of the complex systems.

All these theories are trying to describe, as close to the reality as possible, the privacy of the functioning of systems with a great number of elements, which interacts with other systems (dissipative systems) and which in fact are widely-met in the physical reality. These systems have a series of properties, among which the emergence is one with special implications, but also the dynamic structure they presuppose, generally characterized by a structured, causal, Newtonian, predictable component and an unpredictable, a-causal, unstructured, potential one. Physical experiments (the ones in the plasma tubes but also in the fluid dynamics, etc.) have highlighted these components just as the dynamics between them, which presuppose an auto-structuring tendency by means of the attractors within a certain space called the phase space. However, there remains an important question connected to the source of information which allows for the auto-structuring and thus the dynamics between the potential component and the predictable one. In the plasma tubes experiments, the phenomena can be more easily observed because upon modification of the system constraints (modification of electrical tension to the two ends of the tube) we can obtain different particle organisation patterns which presuppose the interference of some informational structures. The current explanations for the source of this information is that it comes from the privacy of the system. However, in the structure of the system (if we stay with the more simple model of the plasma tube) there are only particles and their attached wave component. Considering that the information contained by the particle comes from the coherent wave, the question which arises is where the information comes from, at wave level. In everyday life, today, in the information technology era, the information is transmitted via waves, by their analogical transformation into waves which modulate a carrying wave. Modulation can be the modulation of the amplitude (little employed because it is too easily affected by noise, but anyway the amplitude is in inverse ratio to frequency), the generally-employed modality is that of angle modulation, which presupposes a modulation of either the frequency or of the phase, which is finally transmitted to the modulation of the magnetic vector angle. The phase is recognized as being an imaginary, complex component of the wave formula. The movement of the magnetic wave described by complex equations generate a complex plan, which connects the wave to the complex space and allows for the storage of information in the topological modifications from this infinitely-dimensional space. To put it different, the information in the complex systems is to be found in the complex space, which gives the characteristics of potentiality, non-differentiability, a-causality from the description of complex systems. Coming back to the plasma tubes, the privacy of the system from which information comes is represented by the coherent wave phase with every particle (the wave corresponding to every particle from the wave-particle duality) which represents the connection to the complex space, where the whole physical reality is to be found at the potential mode, under the form of information. This is the consequence of permanent dynamics between the complex and the real space, by means of information. Depending on the system constraints from the complex space through the wave phase, the information which reaches the particle generating the auto-structuring patterns is undertaken.

In the structure of complex systems there is a potential part with a chaotic aspect and a structured, causal, newtonian part, as well as different intermediary phases. From there it results that a certain uncertainty exists in all the structure of reality. Moreover, we find the uncertainty principle (Heisenberg [14]) in Gabor's theory of communication (the information quanta). At brain level, the non-linear, potential, apparently chaotic part corresponds to the unconscious, whereas the structured, causal part corresponds to the conscious; the intermediary parts, as well as the structures which process both the information from reality and from the unconscious, all are represented by what Freud called SuperEgo.

The chaotic part is structured via attractors, depending on the constraints of the system (for example, the way in which some physiological needs generate, during the dream, a certain structure). During the wakefulness there is a dynamics with the chaotic, potentially unconscious part in the background and which allows accessing the information, the memories, the logical links (for example, a discourse).

We must therefore accept that, also in the living world, including the brain functioning, there exists a spectral, wave component and the transmission of senses is achieved spectrally, by vibrations [9, 10].

Thus, a reality which coexists with us is the a-spatial a-temporal one, described by the wave formula and which is involved in the visual perception phenomenon, in which the undertaking of the spatial-temporal information is made by light through modulation of its frequency, a phenomenon which is described by the Fourier transform, while the stimulation of the retina involves the collapse of the wave formula and the emergence of corpuscles which stimulate the retina cells by inverting the Fourier transform. As a result, all we look at and see, in order to be seen, goes through an a-temporal and a-spatial phase, in the interval necessary for the light to reach from the object to us. This interval can be million of light years for cosmic objects or minutely small fractions of a second when we look at our friends, our home or our garden.

Information is codified energy which is expressed as pattern, structure templates, initiated by attractors which are active in the phase space, between the chaotic part and the structured one. The information lies stored in the spectral space and it expresses the patterns in the structure of atoms, molecules, macro-molecules and cells. It has a potential existence which is expressed by substance and energy under certain conditions (of local coherence).

A virtual, Newtonian reality as projection of physical reality is completed by the unstructured, a-causal, apparently chaotic component: the imagination, the dream, the failed acts, the subliminal mechanisms, the unconscious etc., which can be associated with the causal, potential, unstructured and non-differentiable component of complex systems, the source of inspiration, of creation and of access to non-Euclidean realities to holospace. These potentialities can become conscious through patterns (see the archetypes and the collective unconscious of Jung) and they can be found in logical, algorithmic, organized and systematic form in everything that is creation (from making a speech, conversation, improvisation, to creating new musical pieces, new artistic work, new scientific work). The chaotic, unpredictable part does not only contain the Newtonian reality to which we have access, but more, maybe even the structure of the whole Universe, at informational potential level. The brain has access to the implicit part (the implicit reality of Bohm [9]), if we associate this part to what the classics called unconscious. From here derives the capacity for mathematical reasoning, for physics, for reasoning reality in n dimensional spaces, a-temporal realities, a-spatial realities.

The development of the neuronal network is made according to fractal criteria, just as all the other apparatuses and systems of the human body. As a result, the spectral field formed by the waves corresponding to corpuscles form the neuronal network are coherent, allowing for the processing of information both in the neuronal network and in the spectral space (the Hilbert space), where both the a-spatial a-temporal components exist, as they allow memory to develop, but also the complex component which offers the possibility of a multi-dimensional processing which can explain the superior psychological processes (conceptualization, semantics, abstracting and generalization etc.). At any scale we can find the two types of realities: a differentiable one and a non-differentiable one, highlighted by the Madelung hydrodynamic model Madelung and respectively by the stochastic model.

Analyzers manage on principle the transformation of wave information in the corpuscle, thus generating the tri-dimensional and the spatial and temporal vision upon reality, but the processing at brain level is also spectrally made (de Valois [20]). Because the whole of the analyzers achieve the information transfer from a wave form to a body form, the processing of information is achieved both within a material, corpuscle network, the neural network, but also in a spectral network, of the coherent field associated to the neuron network. Through the waves of the spectral field the dynamic link to the complex space is made, process which allows for the occurrence of the superior psychological processes, specific to the human being, which need multidimensional development in order to be formed, development which is only allowed by the complex space. The psychological reality represents the permanent dynamics between the neuronal (material) network, the associated spectral field (the fractal potential) and the complex space (infinitely-dimensional).

The processing of information for the information provided by analyzers is made in a differentiable, causal, algorithmical form at the level of the neuronal network (Barabassy [8]), whereas beyond the analyzers it is made within a complementary network found in the complex space, which is mediated by the fractal potential from the spectral potential of neurons. As a result, the qualitative leap represented by the appearance of culture would not have generated only the appearance of mirror neurons which are present also in some animals, but the development of genetic patterns which allowed for a better connectivity between the two networks. It is not a matter of chance that the appearance of articulate speech is associated to this qualitative leap in human development. The centre of speech appears to represent a system of processing information which allows for connecting to the infinite and complex-dimensional space and thus to the possibility of emergence of superior psychological processes. The study of the mimic-gesture language of the deaf individuals highlighted the fact that, in learning this language, there is a first phase of learning of a mimic-gesture behaviour which is processed in the right hemisphere, which is specialized in spatial representations and becomes truly language only when it is undertaken by the speech centre from the left hemisphere. Then the mimic-gesture is processed at the level of notions and concepts

and superior processes can be achieved, such as abstractization, synthesis and generalization. The result is that the centre of speech can be such a module which allows for the connection of the neuronal network with the one corresponding in the complex system and thus the leap towards Homo sapiens can be explained.

Concluding remarks

The complex systems dynamics and especially that of the complex and of the real space (from the inner part of the systems) may lead to new hypotheses and theories about the structure of psyche and about its functioning.

The whole collection of the analyzers manages the transfer of information from its wave form into corpuscular form. This allows for the information processing to be accomplished both in a corpuscular, material network, the neuronal network, but also in a spectral network, of the coherent field associated to the neuronal network. Through the waves of the spectral field the dynamical link to the complex space is realized, situation which allows for the occurrence of the superior psychic processes, which are specific to the human being, and which need multidimensional development in order to be formed, a situation which is only allowed by the complex space. The mental reality represents thus the permanent dynamics between the neuronal (material) network, the associated spectral field (the fractal potential) and the infinite dimensional complex space.

The aim of this paper is to apply the theory of complex systems in order to sustain the hypothesis of the complex space as a physical space. We want to treat the information correlated to the substance and the energy, by applying the theory of complex systems, of complex analysis and of topology. We aim to highlight the fact that information can be found in the complex space of the wave phase spectral field. As a result, this complex space can be found anywhere and at every level of the reality. In our view, it is infinite dimensional, as it can contain all the information in the Universe. From a mathematical viewpoint, the real space is included in and intertwined with the complex space generated by the electromagnetic waves. At quantum level, this intertwining can be achieved by the collapsing of the wave formula into the complex space of the wave phase and it can be transmitted into the complex space of the spin rotation, by transferring the whole information. This phenomenon is specific to reality at the level of the whole knowable universe, as everywhere there are electromagnetic waves and also at every level of the reality, including the human brain.

References

- [1] M. Agop, C. Buzea, C. Gh. Buzea, L. Chirilă, S. Oancea, *On the information and uncertainty relation of canonical quantum systems with $SL(2R)$ invariance*, Chaos, Solitons & Fractals, Vol. 7, Issue 5, 659-668, 1996.
- [2] M. Agop, V. Griga, B. Ciobanu, C. Buzea, C. Stan, D. Tatomir, *The uncertainty relation for an assembly of Planck-type oscillators. A possible GR quantum mechanics connection*, Chaos, Solitons & Fractals, Vol. 8, Issue 5, 809-821, 1997.
- [3] M. Agop, V. Melnig, *L'energie informationelle et les relations d'incertitude pour les systemes canoniques $SL(2R)$ invariants*, Entropie, no. 188/189, 119-123, 1995.
- [4] M. Agop, A. Gavriluț, G. Ștefan, *$SL(2R)$ invariance of the Kepler type motions and Shannon informational entropy. Uncertainty relations through the constant value of the Onicescu informational energy*, Rep. Math. Phys, Vol. 75 (2015), No. 1, 101-112.
- [5] M. Agop, A. Gavriluț, E. Rezuș, *Implications of Onicescu's informational energy in some fundamental physical models*, International Journal of Modern Physics B, Vol. 29, No. 0 (2015), DOI: 10.1142/S0217979215500459.
- [6] M. Agop, A. Gavriluț, G. Crumpei, B. Doroftei, *Informational Non-differentiable Entropy and Uncertainty Relations in Complex Systems*, Entropy, 16 (2014), 6042-6058, DOI:10.3390/e16116042.
- [7] M. Agop, A. Gavriluț, C. Gh. Buzea, L. Ochiuz, D. Tesloianu, G. Crumpei, C. Popa, *Implications of quantum informational entropy in some fundamental physical and biophysical models*, chapter in the book Quantum Mechanics, IntechOpen, 2015, in print.
- [8] A.L. Barabassy, *Bursts: The Hidden Pattern Behind Everything We Do*, Penguin Group (USA) Inc., 2010.
- [9] D. Bohm, *Meaning And Information*, In: P. Pyllkkänen (ed.): The Search for Meaning: The New Spirit in Science and Philosophy, Crucible, The Aquarian Press, 1989.
- [10] F. Capra, *The Tao of Physics: An Exploration of the Parallels Between Modern Physics and Eastern Mysticism*, Shambhala Publications of Berkeley, California, 1975.
- [11] G. Crumpei, A. Gavriluț, M. Agop, I. Crumpei, L. Negură, I. Grecu, *New Mathematical and Theoretical Foundation in Human Brain Research. An interdisciplinary approach in a transdisciplinary world*, Human and Social Studies, Vol. 3, no. 1 (2014), 45-58.
- [12] G. Crumpei, A. Gavriluț, M. Agop, I. Crumpei, *An Exercise in a Transdisciplinary Approach for New Knowledge Paradigms*, Human and Social Studies, Vol. 3, no. 3 (2014), 114-143.

- [13] A. Gavriluț, M. Agop, *A Mathematical Approach in the Study of the Dynamics of Complex Systems* (in Romanian), Ars Longa Publishing House, Iași, 2013.
- [14] W. Heisenberg, *The Physical Principles of the Quantum Theory*, Courier Dover Publications, 1949.
- [15] L. Introna, *Phenomenological Approaches to Ethics and Information Technology*, The Stanford Encyclopedia of Philosophy (Spring 2005 Edition).
- [16] C.G. Jung, *The Undiscovered Self: The Problem of the Individual in Modern Society*. New American Library, 2006.
- [17] O. Onicescu, *Energie informationnelle*, C. R. Acad. Sci. Paris A 263 (1966), 841-842.
- [18] T. Stonier, *Information and the Internal Structure of the Universe*, Springer Verlag, Londra, 1990, p.155.
- [19] M. Tegmark, *Our Mathematical Universe: My Quest for the Ultimate Nature of Reality*, 2014.
- [20] R.L. De Valois, K.K. De Valois, *Spatial vision*, New York: Oxford University Press, 1988.
- [21] W. Weaver, C.E. Shannon, *The Mathematical Theory of Communication*, Univ. of Illinois Press, 1963.

Measuring quasiperiodicity

Suddhasattwa Das*, Yoshitaka Saiki†, Evelyn Sander‡, James A Yorke‡

January 15, 2016

Abstract

A map on a torus is called “quasiperiodic” if there is a change of variables which converts it into a pure rotation in each coordinate of the torus. We develop a numerical method for finding this change of variables, a method that can be used effectively to determine how smooth (i.e., differentiable) the change of variables is, even in cases with large nonlinearities. Our method relies on fast and accurate estimates of limits of ergodic averages. Instead of uniform averages that assign equal weights to points along the trajectory of N points, we consider averages with a non-uniform distribution of weights, weighing the early and late points of the trajectory much less than those near the midpoint $N/2$. We provide a one-dimensional quasiperiodic map as an example and show that our weighted averages converge far faster than the usual rate of $O(1/N)$, provided f is sufficiently differentiable. We use this method to efficiently numerically compute rotation numbers, invariant densities, conjugacies of quasiperiodic systems, and to provide evidence that the changes of variables are (real) analytic.

1 Introduction

Let X a topological space with a probability measure μ and $T : X \rightarrow X$ be a measure preserving map. Let $f : X \rightarrow E$ be an integrable function, where E is a finite-dimensional real vector space. Given a point x in X , we will refer to the long-time average of the function f along the trajectory at x

$$\frac{1}{N} \sum_{n=0}^{N-1} f(T^n(x)), \quad (1)$$

as a **Birkhoff average**. The Birkhoff Ergodic Theorem (see Theorem 4.5.5. in [1]) states that if $f \in L^1(X, \mu)$, then (1) converges to the integral $\int_X f d\mu$ for μ -a.e. point $x \in X$. The Birkhoff average (1) can

*Department of Mathematics, University of Maryland, College Park

†Graduate School of Commerce and Management, Hitotsubashi University

‡Department of Mathematical Sciences, George Mason University

§Institute for Physical Science and Technology, University of Maryland, College Park



be interpreted as an approximation to an integral, but convergence is very slow, as given below.

$$\left| \frac{1}{N} \sum_{n=1}^N f(T^n(x)) - \int_X f d\mu \right| \leq CN^{-1},$$

and even this slow rate will occur only under special circumstances such as when $(T^n(x))$ is a quasiperiodic trajectory. In general, the rate of convergence of these sums can be arbitrarily slow, as shown in [2].

The speed of convergence is often important for numerical computations. Instead of weighing the terms $f(T^n(x))$ in the average equally, we weigh the early and late terms of the set $1, \dots, N$ much less than the terms with $n \sim N/2$ in the middle. We insert a weighting function w into the Birkhoff average, which in our case is the following C^∞ function that we will call the **exponential weighting**

$$w(t) = \begin{cases} \exp\left(\frac{1}{t(t-1)}\right) & \text{for } t \in (0, 1) \\ 0 & \text{for } t \notin (0, 1). \end{cases} \quad (2)$$

Let \mathbb{T}^d denote a d -dimensional torus. For $X = \mathbb{T}^d$ and a continuous f and for $\phi \in \mathbb{T}^d$, we define what we call a **Weighted Birkhoff (WB_N) average**

$$\text{WB}_N(f)(x) := \frac{1}{A_N} \sum_{n=0}^{N-1} w\left(\frac{n}{N}\right) f(T^n x), \text{ where } A_N := \sum_{n=0}^{N-1} w\left(\frac{n}{N}\right). \quad (3)$$

Note that the sum of the terms $w(n/N)/A_N$ is 1, that w and all of its derivatives are 0 at both 0 and 1, and that $\int_0^1 w(x) dx > 0$.

Quasiperiodicity. Each $\vec{\rho} \in (0, 1)^d$ defines a **rotation**, i.e. a map $T_{\vec{\rho}}$ on the d -dimensional torus \mathbb{T}^d , defined as

$$T_{\vec{\rho}} : \theta \mapsto \theta + \vec{\rho} \pmod{1} \text{ in each coordinate.} \quad (4)$$

This map acts on each coordinate θ_j by rotating it by some angle ρ_j . We call the ρ_j values “**rotation numbers.**”

A vector $\vec{\rho} = (\rho_1, \dots, \rho_d) \in \mathbb{R}^d$ is said to be **irrational** if there are no integers k_j for which $k_1\rho_1 + \dots + k_n\rho_n \in \mathbb{Z}$, except when all k_j are zero. In particular, this implies that each ρ_j must be irrational. The rotation numbers depend on the choice of the coordinate system. In any other coordinates in which the system is also a rotation, the rotation vector $\vec{\rho}$ is $A\vec{\rho}$, for some matrix A whose entries are integers such that the determinant of A is ± 1 . Conversely, any such matrix corresponds to a coordinate change which also changes $\vec{\rho}$ to $A\vec{\rho}$.

A map $T : X \rightarrow X$ is said to be **d -dimensionally C^m quasiperiodic** on a set $X_0 \subseteq X$ for some $d \in \mathbb{N}$

iff there is a C^m -diffeomorphism $h : \mathbb{T}^d \rightarrow X_0$, such that,

$$T(h(\theta)) = h(T_{\vec{\rho}}(\theta)). \quad (5)$$

where $T_{\vec{\rho}}$ is an irrational rotation. In this case, h is a conjugacy of T to $T_{\vec{\rho}}$. In particular, a (pure) **irrational rotation**, (a rotation by an irrational vector $\vec{\rho}$) is a quasiperiodic map.

Invariant measure for quasiperiodic maps. An irrational rotation $T_{\vec{\rho}} : \mathbb{T}^d \rightarrow \mathbb{T}^d$ on the torus has a unique invariant measure, which is the Lebesgue probability measure. This measure also turns out to be the unique ergodic measure. It follows that if a dynamical system $T : X_0 \rightarrow X_0$ is d -dimensionally C^1 quasiperiodic, there is a unique T -invariant measure on X_0 which, under change of variables, becomes the Lebesgue probability measure on \mathbb{T}^d .

Diophantine rotations. An irrational vector $\vec{\rho} \in \mathbb{R}^d$ is said to be **Diophantine** if for some $\beta > 0$ it is **Diophantine of class β** (see [3], Definition 3.1), which means there exists $C_\rho > 0$ such that for every $\vec{k} \in \mathbb{Z}^d$, $\vec{k} \neq 0$ and every $p \in \mathbb{Z}$,

$$|\vec{k} \cdot \vec{\rho} - p| \geq \frac{C_\rho}{\|\vec{k}\|^{d+\beta}}. \quad (6)$$

For every $\beta > 0$ the set of Diophantine vectors of class β have full Lebesgue measure in \mathbb{R}^d (see [3], 4.1). The Diophantine class is crucial in the study of quasiperiodic behavior, for example in [4] and [5].

Continued fractions. Every irrational number $\alpha_0 \in (0, 1)$ has a representation known as its continued fraction expansion $[n_1, n_2, n_3, \dots]$, where n_1, n_2, n_3, \dots are positive integers. It can be defined inductively as follows

$$\begin{aligned} n_1 &= \lfloor \frac{1}{\alpha_0} \rfloor; \alpha_1 := \frac{1}{\alpha_0} - n_1; \\ n_{k+1} &:= \lfloor \frac{1}{\alpha_k} \rfloor; \alpha_{k+1} := \frac{1}{\alpha_k} - n_{k+1}. \end{aligned}$$

Continued fractions as approximations. The **k-th convergent** of an irrational $\alpha_0 \in (0, 1)$ is the number p_k/q_k defined as follows.

$$\frac{p_k}{q_k} = [n_1, \dots, n_k] := \frac{1}{n_1 + \frac{1}{\dots + \frac{1}{n_k}}}. \quad (7)$$

Then for every integers $q, k \geq 0$, integer p , if $q\alpha - p$ is strictly between $q_k\alpha - p_k$ and $q_{k+1}\alpha - p_{k+1}$, then either $q \geq q_k + q_{k+1}$ or both p, q must be zero. In other words, the best approximation of α by a fraction p/q with q not exceeding q_k , is the k-th convergent p_k/q_k . We rely on the continued fraction expansion of a number to decide whether it is rational or not. Every rational number has a finite number of terms in its continued fraction expansion. If α is irrational, then the sequence continues forever, while if it is rational, it stops when some α_k is zero.

The Diophantine class β of an irrational number is a measure of how closely it can be approximated

by a rational number. The Diophantine class of an irrational number can be deduced from its continued fractions. This is because the k -th convergent p_k/q_k provides the best rational approximation among all rational numbers whose denominator is $\leq q_k$.

We will now state our main theorem about fast convergence of weighted Birkhoff sums (3). We will first define a notion of fast convergence called super-convergence.

Definition. Let $(z_N)_{N=0}^\infty$ be a sequence in a normed vector space such that $z_N \rightarrow z$ as $N \rightarrow \infty$. We say (z_N) has **super-polynomial convergence** to z or **super converges** to z if for each integer $m > 0$ there is a constant $C_m > 0$ such that

$$|z_N - z| \leq C_m N^{-m} \text{ for all } m.$$

Theorem 1.1 *Let X be a C^∞ manifold and $T : X \rightarrow X$ be a d -dimensional C^∞ quasiperiodic map on $X_0 \subseteq X$, with invariant probability measure μ . Assume T has a Diophantine rotation vector. Let $f : X \rightarrow E$ be C^∞ , where E is a finite-dimensional, real vector space. Assume w is the exponential weighting (see Eqn. (2)). Then for each $x_0 \in X_0$, the weighted Birkhoff average $WB_N f(x_0)$ has super convergence to $\int_{X_0} f d\mu$.*

Other studies on weighted averages. The convergence of weighted ergodic sums has been discussed, for example, [6], [7] and [8]), but without any conclusions on the rate of convergence. In [9], a convergence rate of $O(N^{-\alpha})$, ($0 < \alpha < 1$), was obtained for functionals in $L^{2+\epsilon}$ for a certain choice of weights. A series of our applications of the method discussed in this paper appear in [10], and the details of the proof of our theorem appears in [11].

The use of a temporal weight in ergodic averages has been a subject of study for several decades, usually using more generic weighting sequences in the form of

$$T_N(f) := \sum_{n=0}^{\infty} \nu_N(n) U^n(f), \text{ where } \nu_N \text{ is a probability distribution on } \mathbb{N}. \quad (8)$$

In our theorem, the probability measure ν_N are the values of the weight function w sampled at the points $\{n/N : 0 \leq n < N\}$ and divided by the normalizing constant A_N , as defined in (3). In [6], sufficient conditions were derived for (8) to converge in weighting sequences of a similar kind. Equations (3) and (8) arise from the study of functionals on the Hilbert Space L^2 . On the other hand, [12] considered the convergence of (8) for invertible operators on Banach spaces. It was shown that for a particular choice for $(\nu_N)_{N \in \mathbb{N}}$, the operators converge in the strong operator topology to an idempotent operator.

Remark. Our results apply to C^m or smooth functions, which are L^2 , and carry the assumption that the underlying dynamics is quasiperiodic. We are interested in exploring the applicability of the theorem to other dynamical systems, while keeping in mind that various counter-examples exist in which weighted ergodic averages do not converge. For example, in [13], the authors derived a property called *strong*

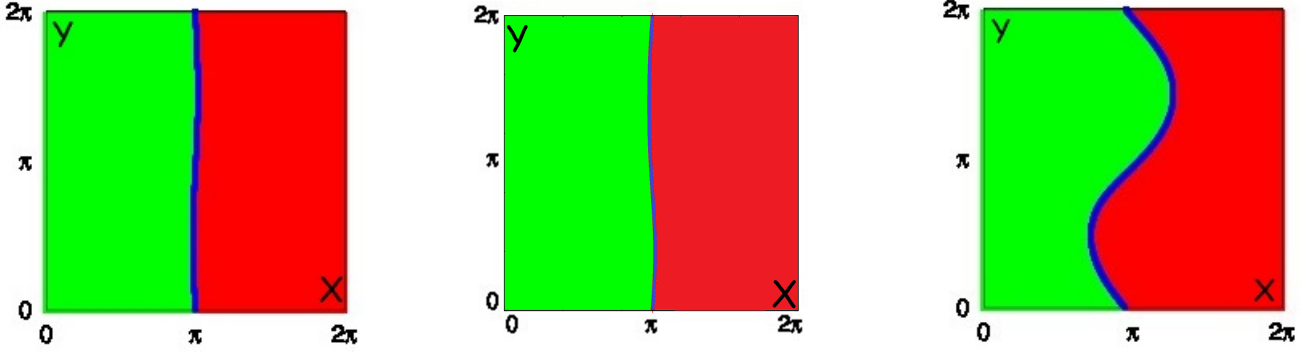


Figure 1: **Invariant circles** in the cylinder map (9), for values of $(\sigma, \delta, \epsilon)$ equal to a) $(0.1, 0.1, 0.1)$, b) $(0.2, 0.8, 0.8)$ and c) $(1.0, 0.1, 0.1)$. Points in the region on the right of the curves diverge to $x = +\infty$, while points on the left diverge to $x = -\infty$. Therefore, these circles are quasiperiodic repellers and we are interested in the classification of the dynamics on these curves as periodic or quasiperiodic.

sweeping property for the operators in (8), under the assumption that each ν_N is a *dissipative probability measure* and certain other conditions on the underlying dynamical system (X, T) . The strong sweeping out property implies that the limits do not converge but attain values over an interval of numbers. In [14] similar results are obtained to prove the lack of convergence of (8) for a dense set of L^1 characteristic functions, in the context of ergodic rotations of the unit circle.

2 Application I of Theorem 1.1 - Rotation numbers

To illustrate some applications of Theorem 1.1, we will work with the following dynamical system for the rest of the paper.

A cylinder-map. Consider the infinitely long cylinder $\mathbb{R} \times S^1$, where S^1 is the standard topological circle. Consider the following map on this cylinder, first studied in [15].

$$\begin{aligned} x_{n+1} &= 3x_n + \sigma(x_n, y_n) \\ y_{n+1} &= y_n - \delta \sin(y_n) + \epsilon(1 - \cos(x_n)) \pmod{2\pi}. \end{aligned} \tag{9}$$

Here σ is a small perturbation term, δ and ϵ are parameters satisfying $0 < 2\delta < \epsilon$. It turns out that for every such parameter value, if σ is sufficiently small, then there exists an invariant topological circle. Note that if $\sigma \equiv 0$, then this is the circle whose points are $\{(\pi, y) : y \in S^1\}$. Though the map is C^∞ , the invariant circle may not be smooth. We are however interested in demonstrating that the dynamics on it is C^∞ -conjugate to a rotation. See Fig. 1 for some of these curves.

2.1 Rotation Number as a weighted Birkhoff sum.

Rotation number. Let $\bar{F} : \mathbb{R}^d \rightarrow \mathbb{R}^d$ be the lift of a quasiperiodic map $F : \mathbb{T}^d \rightarrow \mathbb{T}^d$. It is well known (see for example, [16]) that the following limit exists and is a constant independent of $\bar{z} \in \mathbb{R}^d$.

$$\bar{\rho}(F) := \lim_{n \rightarrow \infty} \frac{\bar{F}^n(z) - \bar{z}}{n}. \quad (10)$$

This limit is called the **rotation number** of F . The limit in (10) is a means of approximating ρ , but its convergence is bounded by the $O(1/N)$, where N is the number of iterates taken into account. We propose a better method based on the weighting factor w .

Note that in the example under discussion, X_0 is a one-dimensional quasiperiodic curve embedded in $X = \mathbb{R}^2$. Let X_0 be given the coordinates θ of a circle S^1 (in this case, θ could be the Y -coordinate of each point on the invariant curve divided by 2π). Given two angles $\theta_1, \theta_2 \in [0, 1)$, $\theta_2 - \theta_1$ denotes the positive angle difference between these two angles, i.e., with value in $[0, 1)$. We are interested in the limit $\rho := \lim_{N \rightarrow \infty} \frac{1}{N} \sum_{n=0}^{N-1} [\theta_{n+1} - \theta_n]$, which can be obtained as the super-convergent limit of

$$\text{WB}_N((\theta_{n+1} - \theta_n)) := \frac{1}{A_N} \sum_{n=0}^{N-1} w\left(\frac{n}{N}\right) [\theta_{n+1} - \theta_n].$$

More generally, let X_0 be a quasiperiodic curve embedded in $X = \mathbb{R}^2$. Let $C := C_B \cup C_U$ be the complement of X_0 in \mathbb{R}^2 , where C_B and C_U are the bounded and unbounded components of C respectively. For $p \in \mathbb{R}^2$, define $\phi(\theta) = (\theta - p)/\|\theta - p\|$. Therefore $\phi(\theta) \in S^1$. Let $\bar{\phi} : \mathbb{R} \rightarrow \mathbb{R}$ be the lift of ϕ . If $p \in C_B$, then $\bar{\phi}$ is of the form

$$\bar{\phi}(\bar{\theta}) = \pm \bar{\theta} + \bar{g}(\bar{\theta}),$$

where $\bar{\theta} \in \mathbb{R}$ is a lift of $\theta \in C$. Notice that the real valued function $\bar{g} : \mathbb{R} \rightarrow \mathbb{R}$ is period one and hence factors into a smooth function $g : X_0 \rightarrow \mathbb{R}$. Define a limit ρ_ϕ as follows.

$$\rho_\phi := \text{WB}_N(g(\theta)) = \frac{1}{A_N} \sum_{n=0}^{N-1} w\left(\frac{n}{N}\right) [(\theta_{n+1} - \theta_n) + g(\theta_n)].$$

Then ρ_ϕ is ρ or $1 - \rho$, depending on the orientation of θ , both being legitimate representations of ρ . We have illustrated this construction in Fig. 2. If $p \in C_U$, then $\rho_\phi = 0$.

2.2 Error bound for the unweighted method.

Given a one-dimensional quasiperiodic trajectory (x_n) on the circle $S^1 = [0, 1)$, one can define a trajectory on the real line \bar{x}_n for $n = 0, \dots, N$, where $\bar{x}_0 = x_0$, \bar{x}_n is a lift of x_n and $\bar{x}_{n+1} - \bar{x}_n \in (0, 1)$. It therefore follows

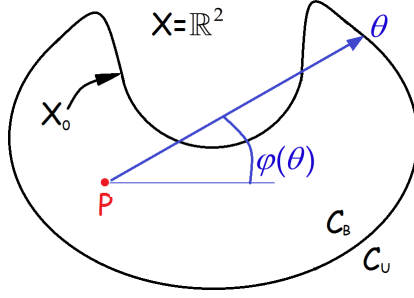


Figure 2: **Rotation number on a quasiperiodic curve.** The numbers $\phi_n = \phi(\theta_n)$ can be used to calculate the rotation number, as stated in Application 1.

that $\bar{x}_{n+1} = \bar{F}(\bar{x}_n)$. Let

$$k_n := \bar{x}_n - x_n \quad (11)$$

be the winding number of the n -th iterate. Let the (x_n) iterates be sorted in increasing order as

$$x_{n_0} = 0 < x_{n_1} < \dots < x_{n_N} < 1.$$

If ρ is the true rotation number, then the iterates $\theta_n = n\rho \pmod{1}$, for $n = 0, \dots, N$ have the same cyclic order as the x -orbit. In other words, $0 = \theta_{n_0} < \theta_{n_1} < \dots < \theta_{n_N}$. We can determine the interval of ρ values for which that is true. First note that

$$0 < x_{n_1} \text{ so } \rho < k_{n_1}/n_1$$

$$x_{n_N} < 1 \text{ so } \rho > (k_{n_N} + 1)/n_N.$$

Suppose $n_i < n_{i+1}$, then $(n_{i+1} - n_i)\rho = k_{n_{i+1}} - k_{n_i} + \epsilon_{n_i}$, for some $\epsilon_{n_i} \in [0, 1)$. Similarly, if $n_i > n_{i+1}$, then $(n_i - n_{i+1})\rho = k_{n_i} - k_{n_{i+1}} - \epsilon_{n_i}$. These two identities give the following two inequalities respectively.

$$\rho > \frac{k_{n_{i+1}} - k_{n_i}}{n_{i+1} - n_i}, \quad (12)$$

$$\rho < \frac{k_{n_i} - k_{n_{i+1}}}{n_i - n_{i+1}}. \quad (13)$$

For each of the $N - 1$ consecutive pairs $(x_{n_i}, x_{n_{i+1}})$, we get such an inequality and they combine to give the possible range of values of ρ . Note that instead of consecutive x -s from the sorted list, we could have taken distant x -s, but the following inequality shows that that would not have yielded a sharper bound.

$$\text{If } a_1, a_2, b_1, b_2 > 0, \text{ then } \frac{a_1 + a_2}{b_1 + b_2} \text{ lies in-between } \frac{a_1}{b_1} \text{ and } \frac{a_2}{b_2}. \quad (14)$$

2.3 Another calculation of the rotation number using unweighted Birkhoff sums

Let $F : \mathbb{T}^d \rightarrow \mathbb{T}^d$ be a homeomorphism, where \mathbb{T}^d is the n -torus, obtained from the n -cube $[0, 1]^d$ by taking each coordinate modulo 1. Using the weighting methods, an initial estimate $\vec{\rho}'$ of the rotation number $\vec{\rho}$ of F , by analysing a dense trajectory $\vec{z}_0, \dots, \vec{z}_{N-1}$. This section describes how to obtain a better estimate $\vec{\rho}''$ of $\vec{\rho}$ from $\vec{\rho}'$.

Let $\vec{z}_{n_1}, \vec{z}_{n_2}, \dots, \vec{z}_{n_{d+1}}$ be $d+1$ points on the trajectory which are close to the origin O and whose convex hull contains O . Then there are constants $\alpha_i \in (0, 1)$, for $i = 1, \dots, d+1$ such that O is a convex combination of the points \vec{z}_{n_i} , i.e.,

$$\vec{0} = \sum_{i=1, \dots, d+1} \alpha_i \vec{z}_{n_i}. \quad (15)$$

Since the map is quasiperiodic, there is a homeomorphism $G : \mathbb{T}^d \rightarrow \mathbb{T}^d$ such that for every $k = 0, \dots, d+1$, $\vec{z}_k = G(k\vec{\rho} \bmod 1)$. If the points $\vec{z}_{n_1}, \vec{z}_{n_2}, \dots, \vec{z}_{n_{d+1}}$ are very close to the origin, G can be considered to be linear in a neighborhood containing these points. for every $i = 1, \dots, d+1$. Therefore, $\vec{z}_{n_i} = G(n_i\vec{\rho} \bmod 1) \approx dG(0)(n_i\vec{\rho} \bmod 1)$. If both sides are multiplied by $dG(0)^{-1}$ then, (15) becomes

$$\vec{0} \approx \sum_{i=1, \dots, d+1} \alpha_i dG(0)(n_i\vec{\rho} \bmod 1). \quad (16)$$

Now let the integral part of $n_i\vec{\rho}$ be \vec{k}_i , i.e., $n_i\vec{\rho} = \vec{k}_i + \vec{\epsilon}_i$, where \vec{k}_i is a vector with integer entries and the entries of $\vec{\epsilon}_i$ lie in $(-0.5, 0.5)^d$ and are very small. Therefore $n_i\vec{\rho} \bmod (2\pi) = \vec{\epsilon}_i$. Therefore (16) becomes

$$\vec{0} = \sum_{i=1, \dots, d+1} [\alpha_i (n_i\vec{\rho} - \vec{k}_i)]. \quad (17)$$

Therefore, the equation can be solved to ρ as

$$\vec{\rho} = \frac{\sum_{i=1, \dots, d+1} \alpha_i \vec{k}_i}{\sum_{i=1, \dots, d+1} \alpha_i n_i}. \quad (18)$$

Note that for every $i = 1, \dots, d+1$, \vec{k}_i/n_i is a close approximation to ρ , so the sum (18) is an optimal combination of these optimizations.

2.4 Fine tuning the rotation number.

Let (x_n) be a quasiperiodic trajectory on a circle $S^1 = [0, 1)$. If we attempt to graph the conjugacy map $h(\theta)$ from (5), we have only N points and they are not equally spaced. We can compute the slopes between successive points and choose $\hat{\rho}$ so as to minimize the fluctuations in the derivatives of successive slopes.

Define points $\theta_n = n\hat{\rho} \pmod 1$. As before, let the (x_n) iterates be sorted in increasing order as

$$x_{n_0} = 0 < x_{n_1} < \dots < x_{n_N} < 1.$$

This ordering will be the same (cyclically) as that of $\theta_0, \dots, \theta_{N-1}$. Therefore, if consider the graph of h , the successive points of the graph are $p_j := (\theta_j, x_{n_j})$. The slope from p_j to p_{j+1} is:

$$S_i = \frac{\Delta x}{\Delta \theta} := \frac{x_{n_{i+1}} - x_{n_i}}{n_{i+1}\hat{\rho} \pmod 1 - n_i\hat{\rho} \pmod 1}.$$

From each estimate $\hat{\rho}$ of ρ , a circle map $h : S^1 \rightarrow S^1$ be constructed which maps $n\hat{\rho} \mapsto y_n$. From h , one can construct the map $h : S^1 \rightarrow S^1$ defined as $g(\theta) = h(\theta) - \theta$. When the function h is lifted to \mathbb{R} it becomes a function with period one. The closer $\hat{\rho}$ is to the true rotation number ρ , the smoother h is going to be. The following is used as a measure of smoothness of the h .

$$\sigma(\hat{\rho}) := \sum_{i=0, \dots, N} \left[\left(\frac{\Delta x}{\Delta \theta} \right)_i - \left(\frac{\Delta x}{\Delta \theta} \right)_{i-1} \right]^2, \quad (19)$$

where the indices -1 refers to the index N . The sequence of quantities $(\Delta x / \Delta \theta)_i$ is defined as,

$$\left(\frac{\Delta x}{\Delta \theta} \right)_i := \frac{[x_{n_i} + k_{n_i} - n_i\hat{\rho}] - [x_{n_{i-1}} + k_{n_{i-1}} - n_{i-1}\hat{\rho}]}{[n_i\hat{\rho} \pmod 1] - [n_{i-1}\hat{\rho} \pmod 1]}, \quad (20)$$

where the sequence (k_n) is as in (11). Equation (19) is a measure of the smoothness of h in terms of the sum of the squares of the difference between successive slopes of the map h . If h is smooth, the slope changes slowly and the sum is expected to be small. We can change ρ to minimize the quantity $\sigma(\rho)/\rho$.

3 Other applications of Theorem 1.1.

We will now describe a computationally efficient method of determining whether invariant tori show quasiperiodic behavior, and we will numerically estimate the analyticity of the conjugacy to a pure rotation. There is a large volume of literature about determining invariant periodic or quasiperiodic sets, these being two of the three types of typical recurrent behavior. An algorithm was introduced in [17], which uses the Newton's method to determine all periodic orbits up to a fixed period along with their basins of attraction. Variants of the Newton's method have been employed to determine quasiperiodic trajectories in various other settings. For example, [18] used the monodromy variant of Newton[U+2019]'s method to locate periodic or quasi-periodic relative satellite motion. In [17], a quantity called local Lyapunov exponent distribution was defined and used to locate basins of small period/quasiperiodic trajectories which lie in the vicinity of larger quasiperiodic trajectories. This step is followed by an application of the

Newton method. They used this method to locate co-existing quasiperiodic and periodic trajectories in the standard map. In [19], the authors defined an invariance equation involving partial derivatives. The invariant tori are then computed using finite element methods of PDE-s. See Chapter 2, [19] for more references on the numerical computation of invariant tori.

The analysis is based on the use of Theorem 1.1 for performing fast integration of smooth, periodic functions on the torus.

Application II, computing the integral of a periodic C^∞ function. A C^∞ periodic map $f : \mathbb{R}^d \rightarrow E$ can be integrated with respect to the Lebesgue measure quickly and accurately in the following manner. We first rescale coordinates so that its domain is a d -dimensional torus $\mathbb{T}^d = [0, 1]^d \text{ mod } 1$. We next choose any $\vec{\rho} = (\rho_1, \dots, \rho_d) \in (0, 1)^d$ of Diophantine class $\beta \geq 0$. For example, a good choice for the case $d = 1$ is $\rho = \frac{\sqrt{5}-1}{2}$, the golden ratio, for which $\beta = 0$. Let $T = T_{\vec{\rho}}$ be the rotation by the Diophantine vector ρ on \mathbb{T}^d . Let w be the exponential weighting function Eq. (2). Then by Theorem 1.1, for every $\theta \in \mathbb{T}^d$, $WB_N(f)(\theta)$ has super convergence to $\int_{\mathbb{T}^d} f d\mu$ and convergence is uniform in θ .

3.1 Application III, Fourier Series of the embedding.

After computing the rotation number ρ by the method explained in Application 1, we can construct the parameterization $\phi = h(\theta)$, where $h : S^1 \rightarrow \mathbb{R}$, for which $x_{n+1} = T(x_n)$ is conjugate to the pure rotation $\theta_{n+1} = \theta_n + \rho$. The map h is not known explicitly, but its values $(x_n := h(n\vec{\rho} \text{ mod } 1))_{n=0,1,2,\dots}$ are known. Let $\bar{h} : \mathbb{R} \rightarrow \mathbb{R}$ be a lift of the map h . Consider the following function $g : \mathbb{R} \rightarrow \mathbb{R}$ defined as

$$g(\theta) := \bar{h}(\theta) - \theta. \quad (21)$$

The continuity and the degree of differentiability of h is the same as that of g , and the latter can be non-rigorously estimated by observing the rate of decay of the Fourier series coefficients of the function g . For every $k \in \mathbb{Z}$, the k -th Fourier coefficient of g is described below.

$$a_k(h) := \int_{S^1} h(\theta) e^{-i2\pi k\theta} d\theta.$$

For every $\theta \in S^1$, h has the Fourier series representation

$$h(\theta) = \sum_{k \in \mathbb{Z}} a_k e^{i2\pi k\theta}.$$

To study the decay rate of the coefficients a_k with $|k|$, we need to accurately calculate each term a_k . By Theorem 1.1, $a_k(h)$ can be approximated by a weighted Birkhoff sum that has super convergence to

$a_k(h)$,

$$a_k(h) = \lim_{N \rightarrow \infty} \text{WB}_N[h(\theta)e^{-i2\pi k\theta}] = \lim_{N \rightarrow \infty} \sum_{n=0}^{N-1} w\left(\frac{n}{N}\right) x_n e^{-i2\pi nk\rho}.$$

Instead of computing the complex-valued Fourier coefficients, we will compute the Fourier sine and cosine series. Given a periodic map $f : S^1 \rightarrow \mathbb{R}$, the Fourier sine and cosine representation of f is the following. For every $t \in S^1$,

$$f(t) = \frac{a_0}{2} + \sum_{n=1,2,\dots} a_n \cos(2n\pi t) + \sum_{n=0,1,2,\dots} b_n \sin(2n\pi t), \quad (22)$$

where the coefficients a_n and b_n are given by the following formulas.

$$a_n = 2 \int_{\theta \in S^1} f(\theta) \cos(2n\pi\theta) d\theta, \quad (23)$$

$$b_n = 2 \int_{\theta \in S^1} f(\theta) \sin(2n\pi\theta) d\theta. \quad (24)$$

See Fig. 4 for the decay of the Fourier sine and cosine coefficients with k .

Role of length of trajectory. Using a higher number of iterates enables a more accurate computation of the higher order Fourier terms (up to 400 terms), up to the accuracy limit which is possible with the precision being used. Fig. 3 shows that the sine and cosine series decay exponentially, as expected in an analytic conjugation.

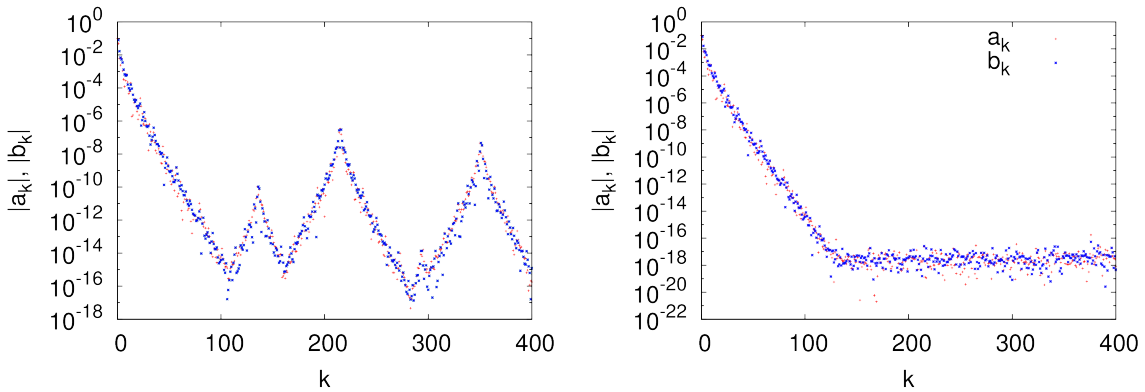


Figure 3: **Accuracy of Fourier series, orbit length and computer arithmetic.** In all these figures, the Fourier sine and cosine terms of the map $h(\theta) - \theta$ were calculated up to 400 terms, with $\epsilon = 0.8$, $\delta = 0.8$, $\sigma = 0.2$. In Figs (a) and (b), 10^4 and 2×10^5 iterates respectively were used along with double precision. The earlier Figure 4 shows the highest accuracy, as it used 2×10^5 iterates and quadruple precision. From these results, it becomes apparent that increasing the number of iterates leads to an accurate calculation of higher order Fourier terms. Use of double precision limits the accuracy of the results to 10^{-16} while the accuracy limit for quadruple precision is around 10^{-32} , as seen in Fig. 4.

3.2 Smoothness of conjugacies

In [20], Denjoy proved that if a C^2 , orientation-preserving circle diffeomorphism has an irrational rotation number α , then it is topologically conjugate to the pure rotation $T_\alpha : z \mapsto z + \alpha$, via some continuous map h . We are interested in inferring more about the smoothness class of h . The question of smoothness of conjugacy to a pure rotation is an old problem. While we have described here a non-rigorous method, the papers [3], [21], [22] and [23] arrive at rigorous conclusions on the differentiability of f by making various assumptions on the smoothness of the quasiperiodic map T and the Diophantine class of its rotation number ρ . We will give a brief summary of some of the classical results before describing our approach.

The **Arnold family** is a commonly studied in the context of existence of quasiperiodic trajectories. In this seminal work ([16]), Arnold studied the following 2-parameter family of circle diffeomorphisms where ϕ is a T -periodic real analytic function with period one, meaning $\phi(y + 1) \equiv \phi(y)$:

$$A_{\omega, \epsilon} : y \mapsto y + \omega + \epsilon\phi(y) \pmod{1} \text{ for } y \in [0, 1] \text{ and } \epsilon \text{ in } [0, 1]. \quad (25)$$

One of the main theorems about this generic family of maps is that was that for ω belonging to a certain, full-measure set of irrational numbers, for all small values of the parameter ϵ , the map (25) will be analytically conjugate to the pure rotation T_ρ (4). By “small” ϵ , we mean all ϵ which are less in magnitude than a positive constant ϵ_0 which depends on ω . Subsequently, several other conjugacy results have been established. They differ in their claims on the degree of smoothness of the conjugacy (C^0, C^1, C^2, \dots , or C^∞ or C^ω); as well as in their assumptions on f .

Consider the following four assumptions on the circle map F which will serve as the hypothesis of some of the known results we are going to cite. The subscripted variables, namely r and ν denote parameters which are a part of their respective assumptions.

(A1) _{r} F is C^r .

(A2) _{ν} $\rho(F)$ is irrational and there is some $\nu > 0$ such that the continued fraction expansion k_1, k_2, \dots of the rotation number satisfies : $\{k_n n^{-\nu} : n \in \mathbb{N}\}$ is bounded.

(A3) _{β} There is $\beta \geq 0$ and a $c > 0$ such that for every $n \in \mathbb{Z} - \{0\}$, $|e^{2\pi i n \rho} - 1| > c|n|^{-\beta-1}$. Equivalently, ρ is Diophantine with Diophantine class β .

$$(A4) \lim_{B \rightarrow \infty} \limsup_{N \rightarrow \infty} \left[\begin{array}{c} \sum_{1 \leq i \leq N} \ln(1 + a_i) / \sum_{1 \leq i \leq N} \ln(1 + a_i) \\ a_i \geq B \end{array} \right] = 0. \text{ A4 is a full-measure condition.}$$

In [3], Herman proves that F is C^1 -conjugate to a pure rotation if it satisfies (A1) _{r} for some $r > 2$. By [21], if F satisfies (A1) _{r} for some $r > 2$ and (A3)₀, then h is absolutely continuous. According to [22] if F

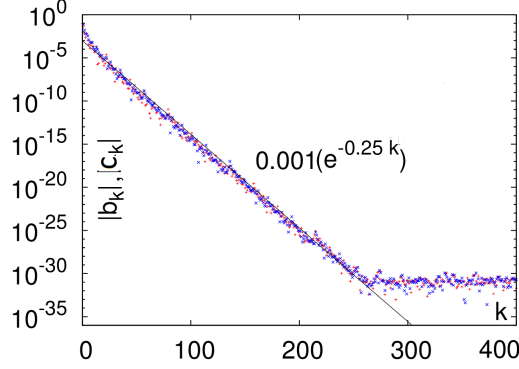


Figure 4: **Exponential decay of Fourier coefficients for the cylinder-map (9)**. The figure shows the magnitude of the Fourier coefficients of the periodic function g in (21). The first 400 Fourier sine and cosine terms were calculated and the magnitude of the n -th sine and cosine terms was plotted as a function of n , in a log(base 10)-linear scale. All calculations were carried out in quadruple precision computer arithmetic. The graph shows that the Fourier coefficients decay according to the law in (26), with $c = -0.25$. The tail of the graph appears flat because the higher order Fourier coefficients could not be calculated to values with magnitude less than the limits of quadruple precision.

satisfies more generally $(A1)_r$ for some $r > 2$ and $(A3)_\tau$, then h is $C^{r-1-\tau-\epsilon}$ for every $\epsilon > 0$.

In [24], the following smoothness result is derived for rotation numbers belonging to a full measure subset of \mathbb{R} . There exists $\epsilon > 0$ and $C > 0$ such that for $\forall \beta > 0$, if F satisfies $(A1)_5$, $(A3)_\beta$ and if $\|f - R_\alpha\|_{C^5} \leq \epsilon\gamma$, then h is C^3 and satisfies

$$\|D^3 h\|_{L^2} \leq \frac{C}{\gamma} \|f - R_\alpha\|_{C^5}.$$

In [23], it is shown that if F satisfies $(A3)_\beta$ for some $\beta \geq 0$ and $(A1)_r$, for $r \geq 3$ and $r > 2\beta + 1$. Then h is $C^{r-1-\beta-\epsilon}$ for every $\epsilon > 0$. As a corollary, it follows that under the same hypothesis, if F is C^∞ , then so is h .

In [25], the following conclusions are made about h :

- If F satisfies $(A1)_r$ for some $r \geq 3$ and α satisfies (A4), then h is $C^{r-1-\epsilon}$, for every $\epsilon > 0$.
- F is conjugate to a rotation if and only if the sequence $(F^n)_{n \in \mathbb{N}}$ is bounded in the C^1 -topology.

In our case, we conclude that h is real analytic if $\|a_k\|$ decreases exponentially fast, i.e.,

$$\log \|a_k\| \leq A + B|k| \tag{26}$$

for some A and B , to the extent checkable with a given computer precision. In this section, $F : S^1 \rightarrow S^1$ is a circle diffeomorphism and $\alpha := \rho(F)$ is its rotation number.

References

- [1] M Brin and G Stuck. *Introduction to Dynamical Systems*. Cambridge University Press, 2002.
- [2] U Krengel. On the speed of convergence in the ergodic theorem. *Monatshefte für Mathematik*, 86 (1):3–6, 1978.
- [3] M R Herman. Sur la conjugaison différentiable des difféomorphismes du cercle des rotations. *Publications Mathématiques de l'Institut des Hautes Études Scientifiques*, 49 (1):5–233, 1979.
- [4] C Simó. *Averaging under fast quasiperiodic forcing*. Plenum Pub. Co., New York, 1994.
- [5] C Simó, P Sousa-Silva, and M Terra. Practical stability domains near $L_{4,5}$ in the restricted three-body problem: Some preliminary facts. *Progress and Challenges in Dynamical Systems*, 54:367–382, 2013.
- [6] M Lin and M Weber. Weighted ergodic theorems and strong laws of large numbers. *Ergodic Theory and Dynamical Systems*, 27 (02):511–543, 2007.
- [7] A Bellow, R Jones, and J Rosenblatt. *Almost everywhere convergence of weighted ergodic averages*. ProQuest, 2009.
- [8] A Bellow and V Losert. The weighted pointwise ergodic theorem and the individual ergodic theorem along subsequences. *Annales de l'Institut Fourier*, 52 (2):561–583, 2002.
- [9] F Durand and D Shneider. Ergodic averages with deterministic weights. *Transactions of the American Mathematical Society*, 288 (1):307–345, March, 1985.
- [10] S Das, E Sander, Y Saiki, and J A Yorke. Quantitative quasiperiodicity. *Preprint : arXiv:1508.00062 [math.DS]*, 2015.
- [11] S Das and J A Yorke. Super convergence of ergodic averages for quasiperiodic orbits. *Preprint : arXiv:1506.06810 [math.DS]*, 2015.
- [12] E Berkson and T A Gillespie. Spectral decompositions, ergodic averages, and the hilbert transform. *Studia Math*, 144:39–61, 2001.
- [13] Mustafa Akcoglu et al. The strong sweeping out property for lacunary sequences, riemann sums, convolution powers, and related matters. *Ergodic Theory and Dynamical Systems*, 16 (02):207–253, 1996.
- [14] M D Ha. Weighted ergodic averages. *Turkish Journal of Mathematics*, 22 (1):61–68, 1998.

- [15] E J Kostelich, I Kan, C Grebogi, E Ott, and J A Yorke. Unstable dimension variability: A source of nonhyperbolicity in chaotic systems. *Physica D*, 109, (1-2):81 [U+2013]90, 1 November 1997.
- [16] V Arnold. Small denominators. i. mapping of the circumference onto itself. *Amer. Math. Soc. Transl. (2)*, 46:213–284, 1965.
- [17] J R Miller and J A Yorke. Finding all periodic orbits of maps using Newton methods: sizes of basins. *Physica D: Nonlinear Phenomena*, 135 (3):195–211, 2000.
- [18] V M Becerra, J D Biggs, S J Nasuto, V F Ruiz, W Holderbaum, and D Izzo. Using Newton’s method to search for quasi-periodic relative satellite motion based on nonlinear Hamiltonian models. *7th International Conference On Dynamics and Control of Systems and Structures in Space*, 7, 2006.
- [19] F Schilder, H M Osinga, and W Vogt. Continuation of quasi-periodic invariant tori. *SIAM Journal on Applied Dynamical Systems*, 4 (3):459–488, 2005.
- [20] A Denjoy. Sur les courbes definies par les equations differentielles a la surface du tore. *J. Math Pures et Appl.*, 11:333–375, 1932.
- [21] Y Katznelson and D Ornstein. The absolute continuity of the conjugation of certain diffeomorphisms of the circle. *Ergodic Theory and Dynamical Systems*, 9:681–690, 1989.
- [22] Y Katznelson and D Ornstein. The differentiability of the conjugation of certain diffeomorphisms of the circle. *Ergodic Theory and Dynamical Systems*, 9:643–680, 1989.
- [23] J C Yoccoz. Conjugaison differentiable des diffeomorphismes du cercle dont le nombre de rotation verifie une condition diophantine. *Annales scientifiques de l’[U+00C9]cole Normale Sup[U+00E9]rieure*, 17 (3):333–359, 1984.
- [24] M Herman. Simple proofs of local conjugacy theorems for diffeomorphisms of the circle with almost every rotation number. *Boletim da Sociedade Brasileira de Matem[U+00E1]tica*, 16 (1):45–83, 1985.
- [25] M R Herman. Resultats recents sur la conjugaison differentiable. *Proceedings of the International Congress of Mathematicians, Helsinki*, 2:811–820, 1978.

Analytical results in type I, II and III intermittency theory

Ezequiel del Rio¹ and Sergio Elaskar²

¹ Dpto. Fisica Aplicada, ETSI Aeronauticos, Universidad Politecnica de Madrid, Spain

(E-mail: ezequiel.delrio@upm.es)

² Dpto. de Aeronautica, Facultad de Ciencias Exactas, Fisicas y Naturales, Universidad Nacional de Cordoba, Argentina

(E-mail: sergio.elaskar@gmail.com)

Abstract. The concept of intermittency has been introduced by Pomeau and Maneville and are usually classified in three classes called I, II, and III. The main attribute of intermittency is a global reinjection mechanism described by the corresponding reinjection probability density (RPD), that maps trajectories of the system from the chaotic region back into the local laminar phase. We generalize the classical RPD for Type-I, II, or III intermittency. As a consequence, the classical intermittency theory is a particular case of the new one. We present an analytical approach to the noise reinjection probability density. It is also important to note that the RPD, obtained from noisy data, provides also a complete description of the noiseless system.

Keywords: Intermittency, chaos, one dimensional map, noise.

1 Introduction

Intermittency is a particular route to the deterministic chaos characterized by spontaneous transitions between laminar and chaotic dynamics. For the first time this concept has been introduced by Pomeau and Maneville in the context of the Lorenz system Manneville[1], Pomeau and Manneville[2]. Later intermittency has been found in a variety of different systems including, for example, periodically forced nonlinear oscillators, Rayleigh-Bénard convection, derivative nonlinear Schrödinger (DNLS) equation, and the development of turbulence in hydrodynamics (see e.g. Refs. Dubois *et al.*[3], del Rio *et al.*[4], Stavrínides *et al.*[5], Krause *et al.*[6], Sanchez-Arriaga *et al.*[7]).

Beside this, there are other types of intermittencies such as type V, X, on-off, eyelet and ring Kaplan[8], Price and Mullin[9], Platt *et al.*[10], Pikovsky *et al.*[11], Lee *et al.*[12], Hramov *et al.*[13]. A more general case of on-off intermittency is the so-called in-out intermittency. A complete review of on-off and in-out intermittencies can be found in Stavrínides and Anagnostopoulos[14].

Proper qualitative and quantitative characterizations of intermittency based on experimental data are especially useful for studying problems with partial

⁸*th* CHAOS Conference Proceedings, 26-29 May 2015, Henri Poincaré Institute, Paris France



or complete lack of knowledge on exact governing equations, as it frequently happens e.g. in Economics, Biology, and Medicine (see e.g. Refs. Zebrowski and Baranowski[15], Chian [16]).

It is interesting to note that the most of the above cited references are devoted to system having more than one dimension. Spite of this, they can be described by one dimensional map. This phenomenon is typical of systems that contract volumen in phase space Ott[17].

All cases of Pomeau and Maneville intermittency has been classified in three types called I, II, and III Schuster and Just[18]. The local laminar dynamics of type-I intermittency evolves in a narrow channel, whereas the laminar behaviour of type-II and type-III intermittencies develops around a fixed point of its generalized Poincare maps.

Another characteristic attribute of intermittency is the *global reinjection mechanism* that maps trajectories of the system from the chaotic region back into the local laminar phase. The reinjection mechanism from the chaotic phase into laminar region dependent on the chaotic phase behaviour, so it is a global property, hence the probability density of reinjection (RPD) of the system back from chaotic burst into points in laminar zone is determined by the dynamics in the chaotic region. Only in a few case it is possible to get an analytical expression for PRD, let say $\phi(x)$. It is also difficult to get PRD experimentally or numerically, because the large number of data needed to cover each small subset of length Δx which belong to the reinjection zone. Because of all this, different approximations have been used in literature to study the intermittency phenomenon. The most comun approximation is to consider PRD uniform and thus independent of the reinjection point Manneville[19], Dubois *et al.*[3], Pikovsky[20], Kim *et al.*[21], Kim *et al.*[22], Kim *et al.*[23], Cho *et al.*[24], Schuster and Just[18].

We described here an overview of a recent theory on the intermittency phenomenon based on a new two-parameter class of PRDs appearing in many maps with intermittency (see for instance: del Rio and Elaskar[25], Elaskar *et al.*[26], del Rio *et al.*[27] and del Rio *et al.*[28]) and the noise effect on this PRD. For a specific values of the parameters, we recover the classical theory developed for uniform PRD.

Firstly let us briefly describe the theoretical framework that accounts for a wide class of dynamical systems exhibiting intermittency. We consider a general 1-D map

$$x_{n+1} = G(x_n), \quad G : \mathbb{R} \rightarrow \mathbb{R} \quad (1)$$

which exhibits intermittency. Note that the map (1) can be coming, for instance, from a Poincare map of a continuous dynamical system. Let us introduce the dynamics corresponding to the three types of intermittencies around the unstable fixed point. The local laminar dynamics of type-I intermittency determined by the Poincare map in the form:

$$x_{n+1} = \varepsilon + x_n + a x_n^p \quad (2)$$

where $a > 0$ accounts for the weight of the nonlinear component and ε is a controlling parameter ($\varepsilon \ll 1$). The laminar behavior of type-II and type-III

intermittencies develops around a fixed point of generalized Poincare maps:

$$x_{n+1} = (1 + \varepsilon)x_n + ax_n^p \quad \text{Type-II} \quad (3)$$

$$x_{n+1} = -(1 + \varepsilon)x_n - ax_n^p \quad \text{Type-III} \quad (4)$$

where $a > 0$ accounts for the weight of the nonlinear component and ε is a controlling parameter ($|\varepsilon| \ll 1$). For $\varepsilon \gtrsim 0$, the fixed point $x_0 = 0$ becomes unstable, and hence trajectories slowly escape from the origin preserving and reversing orientation for type-II and type-III intermittencies. In some pioneer papers devoted to type-I intermittency, the nonlinear component in Eq. (2) is quadratic, (i.e. $p = 2$) and cubic for type-II and type-III, i.e. $p = 3$ in Eq. (3) and Eq. (4) but actually this restriction is not necessary. In any case, for $\varepsilon > 0$, there is a unstable fixed point at $x = 0$ for type-II and type-III and there is not a fixed point at $x = 0$ for type-I, and hence, the trajectories slowly move along the narrow channel formed with the bisecting line as illustrates Fig. 1 where there are indicated two LBR corresponding with two reinjected mechanisms according with the values of γ of Eq. (6).

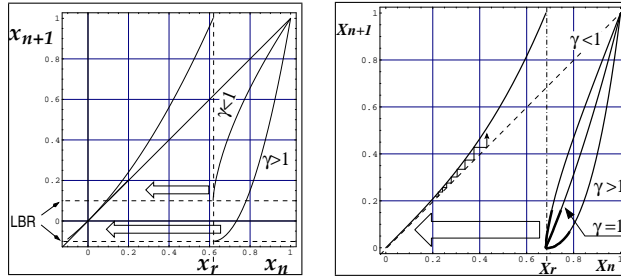


Fig. 1. Map having type-I in- **Fig. 2.** Map having type-II
 intermittency

Figure 2 illustrates a map having type-II intermittency given by the equation

$$x_{n+1} = G(x_n) \equiv \begin{cases} F(x_n) & x_n \leq x_r \\ (F(x_n) - 1)^\gamma & x_n > x_r \end{cases} \quad (5)$$

Here $F(x) = (1 + \varepsilon)x + ax^p$ with $a = 1 - \varepsilon$ and x_r is the root of the equation $F(x_r) = 1$. Note that the map (5) is a generalisation of the map used by Manneville[19], that is, for $\gamma = 1$ the map (5) can be write as $x_{n+1} = (F(x_n) \bmod 1)$ and if $p = 2$ we recover the Manneville map. Three reinjected mechanisms are also indicated in Fig. 2 depending on the values of the parameter γ . For $\varepsilon > 0$, an iterated points x_n of a starting point x_0 closed to the origin, increases in a process driven by parameters ε and p as it is indicated in Fig. 2. When x_n becomes larger than x_r , a chaotic burst occurs that will be interruted when x_n is again mapped into the laminar region, from the region labelled with heavy black segments. This reinjection process is indicated by a big arrow in Fig. 2.

The next modification of the map 5 illustrates the type I intermittency (see Fig. 1)

$$x_{n+1} = G(x_n) = \begin{cases} \varepsilon + x_n + a|x_n|^p & \text{if } x_n < x_r \\ (1 - \hat{x}) \left(\frac{x_n - x_r}{1 - x_r} \right)^\gamma + \hat{x} & \text{otherwise} \end{cases} \quad (6)$$

where x_r is the root of the equation $\varepsilon + x_n + x_n^p = 1$ and the parameter $\gamma > 1$ driven the nonlinear term of the reinjection mechanism. The parameter \hat{x} correspond with the so called lower boundary reinjection point (LBR) and it indicates the limit value for the reinjection form the chaotic region into the laminar one.

Note that ε and p modified the duration of the laminar phase where the dynamics of the system look like periodic and x_n is less than some value, let said c . Note that the function PRD will strongly depend on parameter γ , that determines the curvature of the map in region marked by heavy black segment in Fig. 2. Only points in that region will be mapped inside of the laminar region. Note that when γ increases, also increases the number of points that will be mapped around the unstable fixed point $x = 0$, hence we expect that the classical hypothesis of uniform RPD used to develop the classical intermittency theory does not work. In the next section we study a more general RPD.

2 Assessment of reinjection probability distribution function from data series

The RPD function, determines the statistical distribution of trajectories leaving chaotic region. The key point to solve the problem of model-fitting is to introduce the following integral characteristic:

$$M(x) = \begin{cases} \frac{\int_{x_s}^x \tau \phi(\tau) d\tau}{\int_{x_s}^x \phi(\tau) d\tau} & \text{if } \int_{x_s}^x \phi(\tau) d\tau \neq 0 \\ 0 & \text{otherwise} \end{cases} \quad (7)$$

where x_s is some “starting” point. The interesting property of the function $M(x)$ is that it is a linear function for a wide class of maps, hence the function $M(x)$ is an useful tool to find the parameters determining the RPD. Setting a constant $c > 0$ that limits the laminar region we define the domain of M , i.e. $M : [x_0 - c, x_0 + c] \rightarrow \mathbb{R}$, where x_0 is the fixed point of the map.

As $M(x)$ is an integral characteristic, its numerical estimation is more robust than direct evaluation of $\phi(x)$. This allows reducing statistical fluctuations even for a relatively small data set or data with high level of noise.

2.1 Fitting linear model to data series

To approximate numerically $M(x)$, we notice that it is an average over reinjection points in the interval (x_s, x) , hence we can write

$$M(x) \approx M_j \equiv \frac{1}{j} \sum_{k=1}^j x_k, \quad x_{j-1} < x \leq x_j \quad (8)$$

where the data set (N reinjection points) $\{x_j\}_{j=1}^N$ has been previously ordered, i.e. $x_j \leq x_{j+1}$.

For a wide class of maps exhibiting type-I, type-II or type-III intermittency the numerical and experimental data show that $M(x)$ follows the linear law

$$M(x) = \begin{cases} m(x - \hat{x}) + \hat{x} & \text{if } x \geq \hat{x} \\ 0 & \text{otherwise} \end{cases} \quad (9)$$

where $m \in (0, 1)$ is a free parameter and \hat{x} is the lower boundary of reinjections (LBR), i.e. $\hat{x} \approx \inf\{x_j\}$. Then using (7) we obtain the corresponding RPD:

$$\phi(x) = b(\alpha)(x - \hat{x})^\alpha, \quad \text{with } \alpha = \frac{2m - 1}{1 - m} \quad (10)$$

where $b(\alpha)$ is a constant chosen to satisfy $\int_{-\infty}^{\infty} \phi(x) dx = 1$. At this point, we note that the linear approximation (9) for the numerical or experimental data determines the RPD given by 10. Figure (3) displays different RPD depending

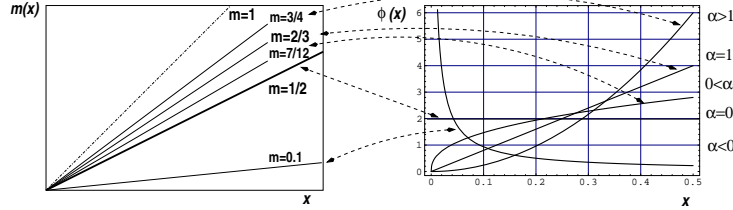


Fig. 3. RPD for different values of α showing decreasing and non-decreasing functions. It is sketched the corresponding slope for the function $M(x)$. Dashes line represents the limit value $m = 1$.

on the exponent α for $\hat{x} = 0$ and $c = 0.5$. It is also shown how the free parameter α depends on the slope m according with Eq. (10). For $m = 1/2$ we recover the most common approach with uniform RPD, i.e. $\phi(x) = \text{const}$, widely considered in the literature. For $m < 1/2$ we have $\alpha < 0$ and the RPD increases without bound for $x \rightarrow 0$ as it is shown in Fig. (3). In the opposite case $m > 1/2$ we have $\phi(0) = 0$. In this last case, the two possibilities for the RPD, concave or convex are separated by the slope $m = 2/3$ (see Fig. 3). The RPD (10) has two limit cases:

$$\phi_0(x) = \lim_{m \rightarrow 0} \phi(x) = \delta(x - \hat{x}) \quad (11)$$

$$\phi_1(x) = \lim_{m \rightarrow 1} \phi(x) = \delta(x - c) \quad (12)$$

(note that $b(\alpha) \rightarrow 0$ in these cases).

From the mathematical RPD shape it is possible to analytically estimate the fundamental characteristic of the intermittency, that is the probability density of the length of laminar phase $\psi(l)$, depending on l , that approximates the number of iterations in the laminar region, i.e. the length of the laminar

phase. Note that the function $\psi(l)$ can be estimated from time series, as it is usual to characterize the intermittency type. The characteristic exponent β , depending on $\psi(l)$, defined through the relation $\bar{l} \rightarrow \varepsilon^{-\beta}$, is also a good indicator of the intermittency behavior.

The next section is devoted to evaluate the RPD, that is the key point to determine the rest of the properties associated with a specific intermittency.

3 Length of laminar phase and characteristic exponent

The probability of finding a laminar phase of length between l and $l + dl$ is $dl\psi(l)$, where the $\psi(l)$ is the duration probability density of the laminar phase. It is useful to characterize the type of intermittency to compare the analytical prediction for $\psi(l)$ with numerical or experimental evaluation of it. We explain how the RPD of Eq.(10) can be modified by the classical result about $\psi(l)$. The method used is similar for the three types of intermittencies studied here, however, whereas for type-II and type-III it is possible to find the analytical solution, for type-I it is not possible in the general case.

Firstly we study type-II. To do this, we introduce the next continuous differential equation to approximate the dynamics of the local map (3) in the laminar region

$$\frac{dx}{dl} = \varepsilon x + a x^p \quad (13)$$

where l approximates the number of iterations in the laminar region, i.e. the length of the laminar phase. After integration it yields

$$l(x, c) = \frac{1}{\varepsilon} \left[\ln\left(\frac{c}{x}\right) - \frac{1}{p-1} \ln\left(\frac{ac^{(p-1)} + \varepsilon}{ax^{(p-1)} + \varepsilon}\right) \right]. \quad (14)$$

Note that Eq. (14) refers to a local behaviour of the map in the laminar region and it determines the length of laminar period, however, the length statistic of the laminar phases, $\psi(l)$, is also affected by the density $\phi(x)$, which is a global property as

$$\psi(l) = \phi(X(l)) \left| \frac{dX(l)}{dl} \right| = \phi(X(l)) |\varepsilon X(l) + a X(l)^p| \quad (15)$$

where $X(l)$ is the inverse function of $l(x, c)$ and we have used the Eq. (16)

Note that $\psi(l)$ depends on the local parameters ε and p , and on the global parameters α and \hat{x} determined by the linear function $M(x)$ according with Eq. (10).

Concerning with type-III intermittency, in the laminar region the sign x_n changes in each mapping. However, $|x|$ can be approximated by Eq. 16, consequently the previous values of β reported for type-II intermittency can be applied also in the case of type-III.

Let us consider now the case of type-I intermittency. In this case, the equivalent to Eq. (16) for type-I is

$$\frac{dx}{dl} = \varepsilon + a x^p, \quad (16)$$

from which we obtain $l = L(x, c)$ as a function of x

$$L(x, c) = \frac{c}{\varepsilon} {}_2F_1\left(\frac{1}{p}, 1; 1 + \frac{1}{p}; -\frac{ac}{\varepsilon}\right) - \frac{x}{\varepsilon} {}_2F_1\left(\frac{1}{p}, 1; 1 + \frac{1}{p}; -\frac{ax}{\varepsilon}\right) \quad (17)$$

in terms of the Gauss hypergeometric function ${}_2F_1(a, b; c; z)$ Abramowitz and Stegun[29]. In the case of $p = 2$, $L(x, c)$ can be given by

$$L(x, c) = \frac{1}{\sqrt{a\varepsilon}} \left[\tan^{-1} \left(\sqrt{\frac{a}{\varepsilon}} c \right) - \tan^{-1} \left(\sqrt{\frac{a}{\varepsilon}} x \right) \right]. \quad (18)$$

In the case of type-I intermittency, the Eq. 15 transforms into the follow

$$\psi(l) = \phi(X(l, c)) \left| \frac{dX(l, c)}{dl} \right| = \phi(X(l, c)) |aX(l, c)^p + \varepsilon| \quad (19)$$

It is interesting to observe that if $\alpha > 0$ we have $\psi(l_{max}) = 0$ and the graphs of $\psi(l)$ given by Eq.(19) are very different from the obtained for the classical $\psi(l)$ that can be seen in Schuster and Just[18] and Hirsch *et al.*[30], for instance. The reader can find all possible shapes for the $\psi(l)$ in del Rio *et al.*[28]. Two of this graphs are displayed in Figs. (4) and (5). Note that $\psi(l)$ in Fig. (4) has

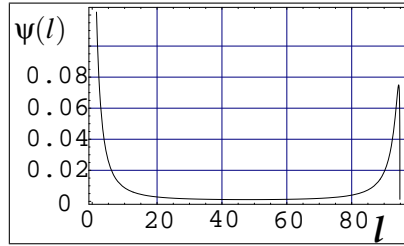


Fig. 4. $\psi(l)$ from Eq.(19) for $\alpha > 0$ and $\hat{x} < 0$

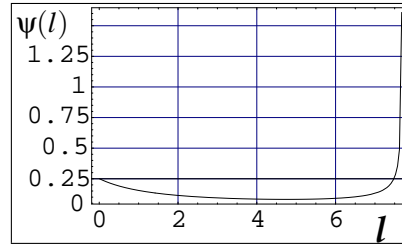


Fig. 5. $\psi(l)$ from Eq.(19) for $\alpha < 0$ and $\hat{x} > 0$

a local maximum, what is a remarkable characteristic does not given by the classical theory on type-I intermittency. We will come back to this point in the noise section.

3.1 Characteristic relations

Let us described the how the characteristic exponent is affected by the RPD of Eq. (10). This exponent, β , defined by the characteristic relation

$$\bar{l} \propto \frac{1}{\varepsilon^\beta} \quad (20)$$

describes, for small values of ε , how fast the length of the laminar phase grows while ε decreases. Traditionally is admitted a single value depending on the intermittency type Schuster and Just[18]. The mean value of l is defined by

$$\bar{l} = \int_0^\infty s\psi(s) ds. \quad (21)$$

Taking into account the function ψ , depending on the parameter \hat{x} and α , (or m) we found that the characteristic exponent β is not a single value as it is usually established. According with Eq. (21), intermittencies type-II and type-III have the same characteristic exponent that are summarized in table 1. In

\hat{x}	m	β
$\hat{x} \approx x_0$	$m \in (0, 1 - \frac{1}{p})$	$\beta = \frac{\alpha+2-p}{1-p} = \frac{1+p(m-1)}{(1-p)(1-m)}$
$\hat{x} \approx x_0$	$m \in [1 - \frac{1}{p}, 1)$	$\beta = 0$
$\hat{x} > x_0$	$m \in (0, 1)$	$\beta = 0$
$\hat{x} < x_0$	$m \in (0, 1)$	$\beta = \frac{p-2}{p-1}$

Table 1. The characteristic exponent β for types II and III.

a similar way, for type-I intermittency we find the cases described in table 2

\hat{x}	m	β
$\hat{x} \approx x_0$	$m \in (0, 1 - \frac{1}{p})$	$\beta = \beta = \frac{p-\alpha-2}{p} = 1 - \frac{1}{(1-m)p}$
$\hat{x} \approx x_0$	$m \in [1 - \frac{1}{p}, 1)$	$\beta = 0$
$\hat{x} > x_0$	$m \in (0, 1)$	$\beta = 0$
$\hat{x} < x_0$	$m \in (\frac{1}{2}, 1)$	$\beta = \frac{p-2}{p}$
$\hat{x} < x_0$	$m \in (0, \frac{1}{2})$	$\beta = \frac{p-1}{p}$

Table 2. The characteristic exponent β for types I.

4 Effect of noise on the RPD

In previous section we have used the function $M(x)$ as a useful tool to study the RPD. In the noisy case, we also use this function to investigate the new noisy RPD, let say NRPD, in systems with intermittency. Figure 6 shows the noise effect on a point near the maximum for the next map having type-III intermittency,

$$x_{n+1} = -(1 + \varepsilon) x_n - a x_n^3 + d x_n^6 \sin(x_n) + \sigma \xi_n, \quad (22)$$

where $-(1 + \varepsilon) x_n - a x_n^3$ ($a > 0$) is the standard local map for type-III intermittency, whereas the term $d x_n^6 \sin(x_n)$ ($d > 0$) provides the reinjection mechanism into the laminar region around the critical point $x_0 = 0$. In the map (22) ξ_n is a noise with $\langle \xi_m, \xi_n \rangle = \delta(m - n)$ and $\langle \xi_n \rangle = 0$ and σ is the noise strength. As Fig. 6 illustrates, the RPD corresponding to the noiseless map is generated around the maximum and minimum of the map by a mechanism that is robust against noise. Following this argument we can obtain the NRPD, let say $\Phi(x)$, from the noiseless RPD according to the convolution

$$\Phi(x) = \int \phi(y)g(x - y, \sigma)dy, \quad (23)$$

where $g(x, \sigma)$ is the probability density of the noise term $\sigma \xi_n$ in Eq.(22) (see del Rio *et al.*[27]).

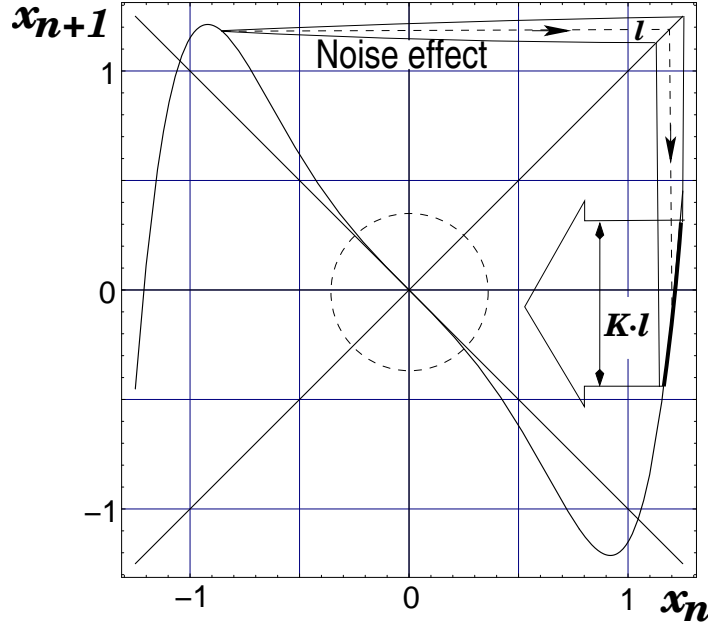


Fig. 6. Noisy map with type-III intermittency. Dashed line between the two solid lines indicate the effect of the noiseless map on a point near the maximum. These solid lines indicate the effect of the noisy map on the same point, that will be mapped on the region shows by a heavy line on the graph of the map. The dashed circle with radius c indicates the laminar region.

In the case of uniform distributed noise, after some algebraic manipulation we get the NRPD as

$$\Phi(x) = \frac{1}{c^{1+\alpha}} \frac{(|x| + K\sigma)^{1+\alpha} - S(|x| - K\sigma)|x| - K\sigma|^{1+\alpha}}{2K\sigma}. \quad (24)$$

where we denote by $S(x)$ the sign function that extracts the sign from its argument. In Eq. (24), the factor K is due to the length amplification indicates in Fig. 6 where the interval of length equal to l is mapped into a new interval of length Kl . We emphasize that, according with Eq. (24), the factor K produces an amplification of the effect of the noise. Note that K should be equal to one in the case on direct reinjection from the maximum o minimum point, as in the case on type-I and II shown in Fig. 1 and Fig. 2. Figure 7 shows in dashed lines a typical noiseless RPD (with $\alpha < 0$) for map of Eq. (22)) with $\sigma = 0$, whereas the solid line corresponds with noisy case according with Eq. (24). Some consequences can be derived from the NRPD of Eq. (24). Firstly, for $|x| \gg K\sigma$ the NRPD approaches to the noiseless RPD and second, for $x \approx x_0$

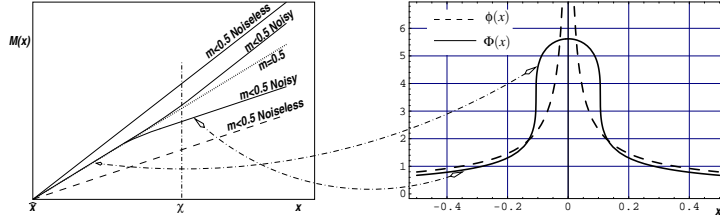


Fig. 7. Comparison between nosily and noiseless case for the RPD and $M(x)$. Dashes arrows connect different regions of the nosily RPD with the corresponding zone of the $M(x)$.

(note that in this example we set $x_0 = 0$) we have a constant function, that is uniform reinjection. The described consequences of Eq. (24) for the NRPD can be better investigated by using the $M(x)$. Figure 7 shows typical shapes of $M(x)$ for noiseless and nosily cases as indicates. The uniform reinjection case with $m = 1/2$ is indicate by dots line. In this figure, dashed line correspond with dashed RPD. Note that now, the noisy $M(x)$ look like a piece linear function with two slopes. The first one corresponding to the noiseless RPD is observed far from the x_0 , that is, on the right side a given value χ in Fig. 7. The second slope approaches to $1/2$ corresponding to uniform reinjection and is observed on the left side of χ . This means that, by the analysis of the noisy data, we can predict the RPD function for the noiseless case. To do this, we proceed like in the noiseless case already explained in the previous sections, but considering only the data on the right side of χ in Fig. 7. That is, by least mean square analysis we can calculate the slope m in Eq.(10), that determines the reinjection function in the noiseless case. Note that now, $K\sigma$ is the single free parameter in Eq. (24).

It is important to note that whereas the noise is applied to the whole map, the function $M(x)$ evidences that, on the right side of χ , the reinjection function is robust against the noise but on the left side of χ , the noise changes the RPD approaching it to the uniform reinjection, at least locally around $x = 0$.

Concerning with the uniform RPD, note that in this case the piece linear function approximation of $M(x)$ shows in Fig. 7 becomes a linear approximation because the two slopes meet in a single one. This meas that the effect of noise on the RPD is not too important for uniform reinjection. Due to this fact, many researches devoted to the noise on the local Poincar map have been published so far, there are only a few study focused on the effect of noise on the RPD. We will find a similar scenario type-II intermitencies.

The case of type-I can be investigated in a similar way, but this type of intermittency presents a different behavior Krause *et al.*[31]. To illustrate this case, let us consider the map of Eq.(6) with $p = 2$ and a noise perturbation, that is

$$x_{n+1} = G(x_n) = \begin{cases} \varepsilon + x_n + ax_n^2 + \sigma\xi_n & \text{if } x_n < x_r \\ (1 - \hat{x}) \left(\frac{x_n - x_r}{1 - x_r} \right)^\gamma + \hat{x} + \sigma\xi_n & \text{otherwise} \end{cases} \quad (25)$$

An important difference with Eq. (22), now the reinjection is not symmetric hence the effect of the noise is to shift the LBR from \hat{x} to $\hat{x} - \sigma$. Other important consequence of the no-symmetric reinjection is that the convolution (23) gives a different results depending on depending on the relation between reinjection parameters. For the simplest case, we have

$$\Phi(x) = \frac{b}{2\sigma(\alpha + 1)} ([x - (\hat{x} - \sigma)]^{\alpha+1} - \Theta[x - (\hat{x} + \sigma)][x + (\hat{x} + \sigma)]^{\alpha+1}) \quad (26)$$

where $\Theta[\cdot]$ represent the Heaviside step function.

Note that in Eq. (14) the position of the LBR is shifted to a new position given by $\hat{x} - \sigma$. In view of this, we split our analysis in two cases according to $\hat{x} - \sigma > -c$ or $\hat{x} - \sigma < -c$. In the first case all points are reinjected directly into the laminar zone and the function $M(x)$ can be approximated by linear function as Fig. 7 shows. This shape is a consequence of Eq.(26). Note that for $x < \hat{x} - \sigma$ the Heaviside function is zero and we recover for $\Phi(x)$ the same power law that for $\phi(x)$ but the parameters are shifted from x to $\hat{x} - \sigma$ and from α to $\alpha + 1$, consequently, the Eq. (9) now can be written as

$$M(x) = m_1(x - \hat{x}_1) + \hat{x}_1 \quad (27)$$

On the other hand, for $x > x + \sigma$, and for small values of σ we can approximate $\Phi(x)$ in Eq. (26) by

$$\Phi(x) \approx b \frac{d}{dx} (x - \hat{x})^{\alpha+1} \quad (28)$$

hence in that region the exponent of $\Phi(x)$ approximates to the exponent of the noiseless density. Note that according to Eq. (10), the two slopes of $M(x)$, m_1 and m_2 , corresponding to the regions with exponents $\alpha + 1$ and α respectively, are related by

$$m_1 = \frac{1}{2 - m_2}. \quad (29)$$

5 Conclusions and discussion

In this work an overview of type-I, II and III intermittecies and a recent method to investigate it are reported.

The main point to described the intermittecy behavior is to determine the probability density of reinjection (RPD). Through the use of M studied in section 2, we have set a way to obtain an analytical description for the RPD, the density of laminar length and the characteristic relations.

The quantity $M(x)$ has a more reliable numerical and experimental access than $\phi(x)$. In a number of cases the linear approximation $M(x) \approx m(x - \hat{x}) + \hat{x}$ fits very well the numerical or experimental data. According with this approximation we have $\phi(x) = b(x - \hat{x})^\alpha$, hence we have found a rich variety of possible profiles for the function $\psi(l)$. Note that the new RPD is a generalization of the usual uniform reinjection approximation which correspond to $\alpha = 0$ or $m = 1/2$.

Because the probability density of the length of laminar phase $\psi(l)$ depends on the RPD, the $\psi(l)$ shapes are qualitatively different from the classical one.

Also it is extended the characteristic relation for type-I, II and III intermitencies. Now, the critical exponent β is determined, through the quantities m , \hat{x} and p as is reported in section 3.1, hence very different RPDs can lead to the same characteristic exponent β .

It is worthy to recall that for $m = 0.5$, the classical uniform reinjection is recovered, together with its corresponding characteristic relation.

Even though, there is certainly many papers devoted to the analysis of the effect of noise on the laminar region, the effect of noise on the reinjection probability density has not been fully considered. Note that the noise effect on the uniform RPD can be neglected if does not change the uniform distribution, however it is not the case for a more general RPD. In section 4, we propose an analytical description of the noisy RPD (NRPD) valid for type-I, II and type-III intermittency. We start making a numerical evaluation of the function $M(x)$. From this knowledge, we obtain the reinjection probability density corresponding to the noiseless map, that is generated around the maximum and minimum of the map. It is also important to note that from the RPD, obtained from noisy data, we have a complete description of the noiseless system.

References

1. P. Manneville, and Y. Pomeau, Intermittency and the Lorenz model, *Phys. Lett. A* **75**, 1-2 (1979).
2. Y. Pomeau, P. Manneville, Intermittent transition to turbulence in dissipative dynamical systems, *Commun. in Math. Phys.* **74** 189-197 (1980).
3. M. Dubois, M. Rubio and P. Berge, Experimental Evidence of Intermittencies Associated with a Subharmonic Bifurcation, *Phys. Rev. Lett.* **51** 1446-1449 (1983).
4. E. del Rio, M.G. Velarde, A. Rodríguez-Lozano, Long Time Data Series and Difficulties with the Characterization of Chaotic Attractors: a Case with Intermittency III *Chaos, Solitons and Fractals* **4** 2169-2179 (1994).
5. S. G. Stavrinos, A. N. Miliou, Th. Laopoulos and A. N. Anagnostopoulos, The Intermittency Route to Chaos of an Electronic Digital Oscillator, *Int. J. of Bifurcation and Chaos* **18** 1561-1566 (2008).
6. G. Krause, S. Elaskar and E. del Rio, type-I intermittency with discontinuous reinjection probability density in a truncation model of the derivative nonlinear Schrodinger equation *Non-linear Dynamics*. **77** 455-466 (2014). DOI 10.1007/s11071-014-1309-1.
7. G. Sanchez-Arriaga, J. Sanmartin and S. Elaskar, Damping models in the truncated derivative nonlinear Schrödinger equation *Physics of Plasmas*. **14**, 082108, (2007)
8. H. Kaplan, Return to type-I intermittency. *Phys. Rev. Lett.* **68**, 553-557, (1992)
9. T. Price, P. Mullin, An experimental observation of a new type of intermittency *Physica D* **48**, 29-52, (1991)
10. N. Platt, E. Spiegel, C. Tresser, On-off intermittency: a mechanism for bursting. *Phys. Rev. Lett.* **70**, 279-282, (1993)
11. A. Pikovsky, G. Osipov, M. Rosenblum, M. Zaks, J. Kurths, Attractor-repeller collision and eyelet intermittency at the transition to phase synchronization *Phys. Rev. Lett.* **79**, 47-50 (1997)

12. K. Lee, Y. Kwak, T. Lim, Phase jumps near a phase synchronization transition in systems of two coupled chaotic oscillators. *Phys. Rev. Lett.* **81**, 321-324, (1998)
13. A. Hramov, A. Koronovskii, M. Kurovskaya, S. Boccaletti, Ring intermittency in coupled chaotic oscillators at the boundary of phase synchronization *Phys. Rev. Lett.* **97**, 114101 (2006)
14. S. Stavrinos, A. Anagnostopoulos, The route from synchronization to desynchronization of chaotic operating circuits and systems. IN: Applications of Chaos and nonlinear dynamics in science and engineering. Banerjee, S., Rondoni, L. (eds.) Springer-Verlag, Berlin (2013)
15. J. Zebrowski and R. Baranowski, Type I intermittency in nonstationary systems Models and human heart rate variability, *Physica A* **336** 74-83 (2004).
16. A. Chian, Complex Systems Approach to Economic Dynamics IN: Lecture Notes in Economics and Mathematical Systems Vol. 592, Springer Berlin Heidelberg, 2007, pp. 39-50.
17. E. Ott, *Chaos in Dynamical Systems*, Cambridge University Press, Cambridge, 2008
18. H. Schuster and W. Just, *Deterministic Chaos. An Introduction*, (WILEY-VCH Verlag GmbH & Co. KGaA, Weinheim, Germany, 2005).
19. P. Manneville, Intermittency, self-similarity and $1/f$ spectrum in dissipative dynamical systems, *Le Journal de Physique* **41** 1235-1243 (1980).
20. Pikovsky A.S. A new type of intermittent transition to chaos, *J. Phys A* **16** L109-L112 (1983).
21. C.M. Kim, O.J. Kwon, Eok-Kyun Lee and Hoyun Lee, New Characteristic Relations in Type-I Intermittency, *Phys. Rev. Lett.* **73** 525-528 (1994).
22. Chil-Min Kim, Geo-Su Yim Jung-Wan Ryu and Young-Jai Park. Characteristic Relations of Type-III Intermittency in an Electronic Circuit, *Phys. Rev. Lett.* **80**, 5317-5320 (1998).
23. C.M. Kim, Geo-Su Yim, Yeon Soo Kim, Jeong-Moog Kim and Lee H. W. "Experimental evidence of characteristic relations of type-I intermittency in an electronic circuit," *Phys. Rev. E* **56**, 2573-2577 (1997).
24. J.H. Cho, M.S. Ko, Y.J. Park, C.M. Kim, Experimental observation of the characteristic relations of Type-I intermittency in the presence of noise, *Phys. Rev. E* **65** 036222 (2002).
25. Ezequiel del Rio and Sergio Elaskar, New Characteristic Relations in Type-II Intermittency, *Int. J. of Bifurcation and Chaos* **20** 1185-1191 (2010).
26. Sergio Elaskar, Ezequiel del Rio and Jose M. Donoso, Reinjection Probability Density in Type-III Intermittency, *Physica A* **390** 2759-2768 (2011).
27. Ezequiel del Rio, Miguel A.F. Sanjuán and Sergio Elaskar, Effect of noise on the reinjection probability density in intermittency, *Commun. Nonlinear Sci. Numer. Simulat.* **17** 3587-3596 (2012).
28. Ezequiel del Rio, Sergio Elaskar and Jose M. Donoso, Laminar length and characteristic relation in Type-I intermittency, to appear in *Commun Nonlinear Sci. Numer. Simulat.* (2013)
29. M. Abramowitz and I. A. Stegun. *Handbook of Mathematical Functions*, Dover, USA, 1970.
30. J. E. Hirsch, B. A. Huberman, and D.J. Scalapino, Theory of intermittency, *Phys. Rev. A* **25** (1982) 519-532.
31. Gustavo Krause, Sergio Elaskar and Ezequiel del Ro. Noise effect on statistical properties of type-I intermittency *Physica A* 402 (2014) 318329

Electrohydrodynamic Stability of an Electrified Jet

Dharmansh and Paresh Chokshi

Department of Chemical Engineering, Indian Institute of Technology Delhi, New
Delhi 110016, India

(E-mail: paresh@chemical.iitd.ac.in)

Abstract. The axisymmetric stability of a straight jet in electrospinning process is examined for a Newtonian fluid using the leaky dielectric model. While the previous studies consider cylindrical jet of uniform radius as the base-state, in the present study the thinning jet profile obtained as the steady-state solution of the 1D slender filament model is treated as the base-state. The linear stability of the thinning jet is analyzed for axisymmetric disturbances, which are believed to be responsible for the bead formation. The eigen-spectrum of the disturbance growth rate is constructed from the governing equations discretized using the Chebyshev collocation method. The most unstable growth rate for thinning jet is significantly different from that for the uniform jet. For the same electrospinning conditions, the thinning jet is found to be stable whereas the uniform radius cylindrical jet is unstable to capillary mode driven by surface tension. The dominant mode for the thinning jet is believed to be an oscillatory conductive mode driven by the accumulation of the surface charge on the perturbed jet. The role of various material and process parameters in the stability behavior is also investigated.

Keywords: Electrospinning, Electrohydrodynamic instability, Linear stability theory.

1 Introduction

In electrospinning process, nano fibers are produced by subjecting fluid to a very high potential difference. The external electric field acting on the charges located at the fluid surface generates a tangential force leading to an electrified jet with strong thinning. The solid fibers, so produced, present tremendous potential for technological applications leading to strong interest in the electrospinning process. Many efforts to produce very thin fibers of size below 100

*8th CHAOS Conference Proceedings, 26-29 May 2015, Henri Poincaré Institute,
Paris France*

© 2015 ISAST



nm suffer from the jet breakup due to surface tension driven capillary instability. In real electrospinning, this instability manifests in the form of bead formation along the fibers. The stability analysis of the electrified jet provides insightful understanding of the conditions under which the instability can be observed.

The early analyses of stability of an electrified cylinder consider either an uncharged jet in an axial electric field [1] or a perfectly conducting jet with a uniform surface charge density but in the absence of an external electric field [2]. In electrospinning, the jet possesses both the surface charge and the tangential electric field which significantly alters the dynamics of the jet due to tangential electric stress on the jet surface. Hohman *et al.* [3] showed that a new mode of instability attributed to the field-charge coupling is introduced for a charged cylinder in the presence of a tangential electric field. This mode, referred to as the conductive mode, is qualitatively different from the surface tension driven Rayleigh-Plateau mode modified by the presence of an electric field. In particular, while increasing the strength of electric field tends to stabilize the capillary mode of instability, it renders the conductive mode unstable. The dominant mode depends strongly on the applied field, surface charge density, jet radius as well as the rheology of the fluid.

Carroll and Joo [4, 5] carried out theoretical and experimental investigation of the axisymmetric instability of an electrically driven viscoelastic jet. Using an Oldroyd-B model to describe the fluid viscoelasticity, linear stability analysis was carried out to obtain growth rate for the axisymmetric instability. The stabilizing role of fluid elasticity has been observed, much in agreement with experiments. However, in all previous studies, the stability is analyzed for a charged cylinder of uniform radius, whereas in electrospinning the charged jet undergoes significant stretching and thinning. While cylindrical jet as base-state simplifies the calculation of the disturbance growth rate, as imposed perturbations can be assumed periodic in axial direction, this simple base-state ignores the variation in radius, and hence the extensional strain rate developed in the fluid. The strong extensional flow in the jet is believed to influence the stability behavior due to the viscous stresses. In the present analysis, we consider the actual thinning jet as the base-state, taking into account the variation in jet radius, velocity, electric field as well as surface charge density along the axial direction. The nonlinear coupling of these jet variables with the disturbance can alter the stability behavior of, an otherwise, cylindrical jet.

2 Problem formulation

We analyze the straight jet emanating from the nozzle in the presence of an axial electric field. The jet is modeled as 1D slender filament. The variables are radius, R , velocity, v , surface charge density, σ and electric field within the jet, E , made non-dimensionalized using nozzle radius, R_0 , velocity at the nozzle, $v_0 = Q/(\pi R_0^2)$, $\sigma_0 = \bar{\epsilon}E_0$, and $E_0 = I/(\pi R_0^2 K)$. Here, Q is the volumetric flow rate, I is the current passing through the jet, $\bar{\epsilon}$ is the air permittivity, and K is the electrical conductivity of the fluid. Additionally, time is non-dimensionalized by R_0/v_0 and stress in the fluid by ρv_0^2 , ρ being the fluid density. In real electrospinning, there exists a non-zero charge density on the surface of the jet, and also the axial-electric field, leading to a strong electric tangential shear force which is responsible for thinning of the jet. The electrical forces in the fluid with finite conductivity is described using the leaky dielectric model. The dimensionless governing equations describing the electrohydrodynamics of the jet are [3, 6]:

$$2R \frac{\partial R}{\partial t} + \frac{\partial R^2 v}{\partial z} = 0, \quad (1)$$

$$\frac{\partial v}{\partial t} + v \frac{\partial v}{\partial z} = \frac{3}{Re} \frac{1}{R^2} \frac{\partial}{\partial z} \left(R^2 \frac{\partial v}{\partial z} \right) + \frac{1}{We} \left(\frac{1}{R^2} \frac{\partial R}{\partial z} + \frac{\partial^3 R}{\partial z^3} \right) + \frac{1}{Fr} + \alpha \left(\sigma \frac{\partial \sigma}{\partial z} + \beta \epsilon \frac{\partial E}{\partial z} + \frac{2E\sigma}{R} \right), \quad (2)$$

$$\frac{\partial(R\sigma)}{\partial t} + \frac{\partial}{\partial z} (ER^2 + PeRv\sigma) = 0, \quad (3)$$

$$E = E_\infty - \ln(\chi) \left(\frac{d(\sigma R)}{dz} - \frac{\beta}{2} \frac{d^2(ER^2)}{dz^2} \right). \quad (4)$$

Here, equation (1) is the mass conservation equation; equation (2) represents the conservation of momentum; equation (3) is the conservation equation for the electrical charge; and equation(4) is the governing equation for the axial-electric field within the jet. The definitions of various dimensionless numbers are given in Table 1.

The electric forces due to Maxwell stresses on the slender filament are obtained using the jump conditions:

$$||\epsilon E_n|| = \bar{\epsilon} \bar{E}_n - \epsilon E_n = \sigma, \quad (5)$$

$$||\epsilon E_t|| = \bar{E}_t - E_t = 0, \quad (6)$$

where the overbar signifies the parameter for the ambient air outside the jet.

Table 1. List of dimensionless groups

Parameter	Dimensionless number	Definition
Pe	Electric Peclet No.	$\frac{2\epsilon v_0}{KR_0}$
Fr	Froude No.	$\frac{v_0^2}{gR_0}$
Re	Reynolds No.	$\frac{\rho v_0 R_0}{\eta}$
We	Weber No.	$\frac{\rho v_0^2 R_0}{\gamma}$
E_0	Initial electric field	$\frac{I}{(\pi R_0^2 K)}$
α	Alpha	$\frac{\epsilon E_0^2}{\rho v_0^2}$
β	Relative permittivity	$\frac{\epsilon}{\epsilon} - 1$
E_∞	Imposed potential difference	$\frac{(\Delta V/d)}{E_0}$
χ	Jet aspect ratio	d/R_0

2.1 Base-state

In previous studies [3], the base-state has been considered to be a cylindrical jet of uniform radius. However, in the present study, we perform linear stability analysis of the thinning jet, representing the actual profile during electrospinning. Therefore, the base-state for the stability analysis is the steady-state solution of the governing equations (1-4), which are solved numerically to obtain the steady profile. The governing equations are supplemented with the following boundary conditions at the top ($z = 0$):

$$R(0) = 1, \quad v(0) = 1. \quad (7)$$

The surface charge density at the nozzle-exit, generally, depends upon the geometry of the top electrode. The simple 1D model employed cannot capture the details of the charge distribution near the electrode. We assume that near the nozzle the free charges are distributed within the bulk of the fluid and hence following boundary condition is enforced [6]:

$$\sigma(0) = 0. \quad (8)$$

As the jet travels towards the bottom electrode, the free charges migrate to the surface of the jet (fluid-air interface) and $\sigma(z)$ becomes non-zero short distance from the nozzle.

In real electrospinning the straight jet undergoes whipping motion after certain distance. Since, we examine only the straight jet, the boundary conditions at the end of the straight jet are naturally unknown. However, far away from

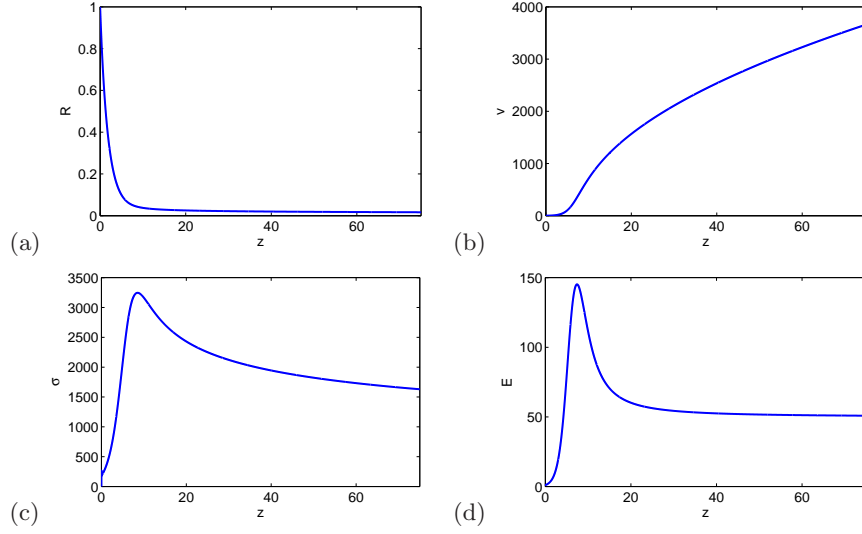


Fig. 1. Steady-state jet profiles: (a) Radius; (b) Velocity; (c) Surface charge density; (d) Electric field. Parameters: $\chi = 75$, $\beta = 50$, $Re = 10^{-3}$, $We = 10^{-3}$, $Fr = 10^{-3}$, $Pe = 10^{-5}$, $\alpha = 0.01$, and $E_\infty = 50$.

the electrode, the electric field may be assumed to reach its imposed value:

$$E(\chi) = E_\infty. \quad (9)$$

[7] derived the asymptotic thinning condition considering that the radius of the jet in the exit condition is very small and the electric forces are comparable to the inertial forces, giving rise to following condition to be imposed at $z = \chi$:

$$R + 4z \frac{dR}{dz} = 0. \quad (10)$$

The steady-state solution of the nonlinear governing equations (1-4) is obtained using the relaxation method. Figure 1 shows the profiles of jet radius ($\bar{R}(z)$), velocity ($\bar{v}(z)$), charge density ($\bar{\sigma}(z)$) and electric field ($\bar{E}(z)$) for a set of dimensionless parameters corresponding to a Newtonian jet of glycerol.

3 Linear stability analysis

3.1 Stability analysis of a uniform jet

For stability analysis, the disturbance can be imposed on a cylindrical jet of uniform radius, as done by [3] and others. In this case, the normal mode disturbance of the following form is superimposed on the steady-state jet variable:

$$\phi(z, t) = \bar{\phi} + \epsilon \phi_\epsilon e^{ikz + \omega t}, \quad (11)$$

where ϕ represents the generic jet variable $\phi = [R, v, \sigma, E]^T$, and $\bar{\phi}$ denotes its steady-state value. k is the axial wavenumber of the disturbance and ω is the temporal growth/decay rate of the imposed disturbance. The steady-state jet radius \bar{R} may be taken as unity, representing jet radius near the capillary or the radius of the thinned jet near the bottom collector plate. For stability analysis of a jet of uniform property, we consider the steady-state variables $\bar{\phi} = [\bar{R}, \bar{v}, \bar{\sigma}, \bar{E}]^T$ corresponding to the thinned jet, *i.e.* $\bar{\phi} = \phi|_{z=\chi}$, as shown in Figure 1. After substituting the superposition equation (11) in the governing equations (1) - (4) and linearizing about the base-state, using ϵ as a small parameter, the algebraic equations for the disturbance dynamics are obtained. The non-trivial solution for disturbance variables ϕ_ϵ results into a dispersion relation for the disturbance growth rate, $\omega = \omega(k)$.

For the perturbations imposed on a cylindrical jet, the base-state profile $\bar{\phi}(z)$ is taken as $\bar{\phi}(\chi)$, a uniform value corresponding to the end-value of the jet variable ϕ . For the steady-state profiles shown in Section 2.1, the base-state variables are $\bar{R} = 1.65 \times 10^{-2}$, $\bar{E} = 50$, and $\bar{\sigma} = 1630$. Considering the reference frame moving with the cylindrical jet, we take $\bar{v} = 0$. For this jet profile, the dispersion relation provides the growth-rate as a function of disturbance wavenumber, as shown in Figure 2. The cylindrical electrified jet is predicted to be unstable with maximum growth rate corresponding to wavenumber $k \approx 0.05$, made non-dimensionalized with capillary radius, R_0 .

3.2 Stability analysis for a thinning jet

Considering the base-state as a cylindrical jet of uniform radius is not appropriate as the jet undergoes strong thinning during the electrospinning. The uniform radius jet ignores the stretching and hence the axial strain rate that is developed in the electrified jet. Since the viscous stresses are important in the jet dynamics, the oversimplification of uniform jet neglects the role of the viscous stresses on the jet instability. The nonlinear coupling of the steady-state extension rate and the disturbance of jet radius is believed to play an important role in the stability behavior. In the present study, we consider the thinning profile $\bar{\phi}(z)$ as the base-state for the linear stability analysis. The generic variable is expanded as steady-state profile superposed with infinitesimal amplitude non-periodic disturbance as follows:

$$\phi(z, t) = \bar{\phi}(z) + \epsilon \tilde{\phi}(z) e^{\omega t}, \quad (12)$$

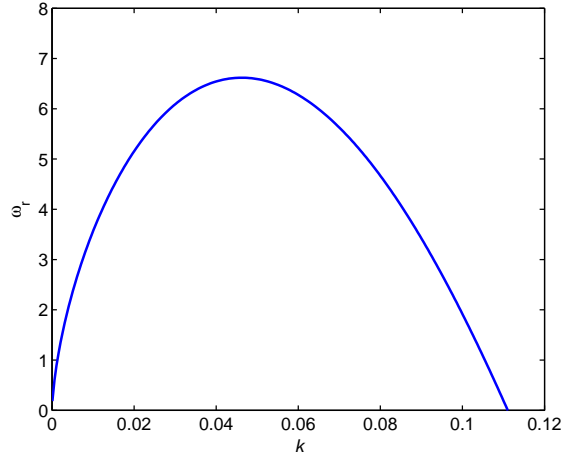


Fig. 2. Real part of the growth rate against disturbance wavenumber for uniform jet superimposed with periodic perturbations. Parameters: $\chi = 75$, $\beta = 50$, $Re = 10^{-3}$, $We = 10^{-3}$, $Fr = 10^{-3}$, $Pe = 10^{-5}$, $\alpha = 0.01$, and $E_\infty = 50$.

where $\bar{\phi}(z)$ is the steady-state jet profile and $\tilde{\phi}z$ denotes the disturbance profile. Upon substituting above superposition in the conservation equations and linearizing to $O(\epsilon)$ terms result into the disturbance governing equations. For the form of non-periodic disturbance imposed, $\tilde{\phi}(z)$, we need to identify boundary conditions for the disturbance variables. The boundary conditions are:

$$\tilde{R}(0) = 0, \quad \tilde{v}(0) = 0, \quad (13)$$

$$\tilde{E}(0) = 0, \quad \tilde{\sigma}(0) = 0. \quad (14)$$

At lower end of the jet, $z = \chi$, we consider following conditions:

$$\tilde{R}(\chi) = 0 \quad \tilde{E}(\chi) = 0. \quad (15)$$

The disturbance equations are discretized using the Chebyshev collocation technique resulting into a generalized eigenvalue problem of the form:

$$\mathcal{A}\tilde{\phi} = \omega \mathcal{B}\tilde{\phi}, \quad (16)$$

where \mathcal{A} and \mathcal{B} are matrices of size $4N \times 4N$, with N being the number of collocation points in the domain $z = (0, \chi)$. The spectrum of complex eigenvalues is obtain using *LAPACK* numerical libraries.

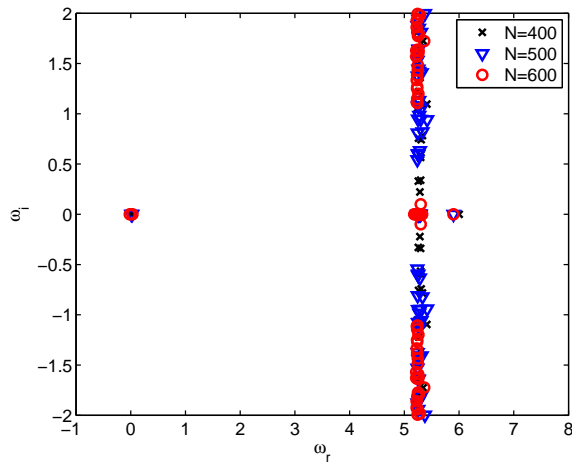


Fig. 3. Eigenspectrum of disturbance growth rate: real part against imaginary part of the growth rate for uniform jet superimposed with non-periodic perturbations. Parameters: $\chi = 75$, $\beta = 50$, $Re = 10^{-3}$, $We = 10^{-3}$, $Fr = 10^{-3}$, $Pe = 10^{-5}$, $\alpha = 0.01$, and $E_\infty = 50$.

In order to validate the numerical scheme, we first obtain the eigenspectrum for the jet of uniform radius, studied in previous section. Figure 3 plots the eigenspectrum showing the real and imaginary parts of the discrete eigenvalues, ω_r and ω_i respectively. As seen, the eigenspectrum is unaffected by the number of Chebyshev collocation points, N , thus eliminating the possibility of any spurious eigenvalues. The most unstable eigenvalue has growth rate $\omega_r \approx 6.04$, which is similar to the maximum ω_r obtained earlier using periodic perturbations as shown in Figure 2. Thus, the discretization technique which constructs the full eigenspectrum has been validated.

So far, we have used the end-values of the jet profile when the jet has sufficiently thinned far away from the capillary, as the base-state upon which the infinitesimal amplitude disturbances are imposed. Thus, considering $\bar{\phi}(z) = \bar{\phi}(\chi)$ in equation (12) ignores the entire thinning profile of the steady-state jet. Next, the disturbances are superimposed on the thinning profile $\bar{\phi}(z)$ taking into account the role of extensional rate in stability behavior. Figure 4 shows the eigenspectrum for the thinning jet using the same set of parameters as used for the cylindrical jet. The eigenspectrum is found to be independent of

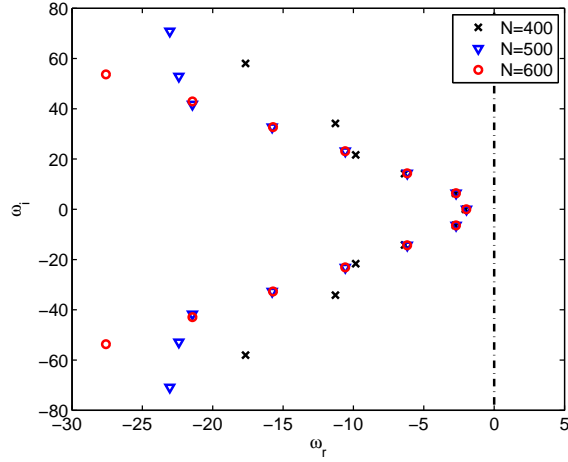


Fig. 4. Eigenspectrum of disturbance growth rate: real part against imaginary part of the growth rate for a thinning jet superimposed with non-periodic perturbations. Parameters: $\chi = 75$, $\beta = 50$, $Re = 10^{-3}$, $We = 10^{-3}$, $Fr = 10^{-3}$, $Pe = 10^{-5}$, $\alpha = 0.01$, and $E_\infty = 50$.

the discretization points, N . Comparing with Figure 3 for the cylindrical jet, the thinning jet is found to be stable as the real part of the growth rate ω_r is negative, $\omega_r \approx -2.1$, for the leading eigenvalue. Therefore, the viscous stresses as well as the variation in the surface charge density along the fiber render stability to the jet.

The effect of various parameters on the leading growth rate is shown in Figure 5. On decreasing the surface tension, *i.e.* increasing Weber number, the real part of the leading growth rate is found to be nearly unaffected, as shown in Figure 5(a). The insensitivity of surface tension to the disturbance growth rate indicates that the leading eigenvalue corresponds to the conductive mode of instability. This instability is driven by the electric field in the presence of non-zero charge density on the jet surface [3]. To further confirm the type of instability mode, the influence of external electric field, E_∞ , is shown in Figure 5(b). As the strength of external field increases, the leading growth rate, ω_r , increases, even though remaining negative. Thus, the electric field tends to weaken the stability of the jet. For the set of parameters employed,

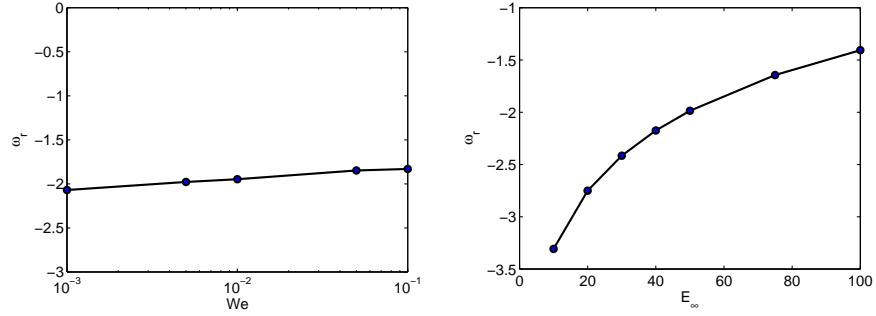


Fig. 5. Effect of various parameters on the real part of the leading growth rate for a thinning jet: (a) Effect of Weber number, for $E_\infty = 50$; (b) Effect of external electric field for $We = 10^{-3}$. Parameters: $\chi = 75$, $\beta = 50$, $Re = 10^{-3}$, $Fr = 10^{-3}$, $Pe = 10^{-5}$, and $\alpha = 0.01$.

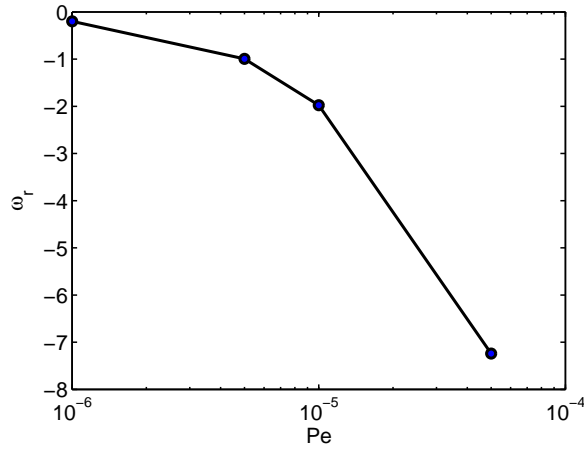


Fig. 6. Effect of electrical conductivity of the fluid on the leading growth rate. Parameters: $\chi = 75$, $\beta = 50$, $Re = 10^{-3}$, $We = 10^{-3}$, $Fr = 10^{-3}$, $\alpha = 0.01$, and $E_\infty = 50$.

the growth rate of the leading disturbance remains negative for a range of electric field strength studied.

Finally, we examine the effect of electrical conductivity of the fluid on the leading growth rate. As seen in Table 1, the conductivity, K , appears in the electric Péclet number, Pe and the definition of initial electric field E_0 , which in turn, affects dimensionless numbers α and E_∞ . Hence, to study the effect

of variation in fluid conductivity, three dimensionless parameters, *viz.* Pe , α and E_∞ are varied, in accordance with their definitions. Figure 6 shows the influence of electrical conductivity of the fluid on the leading growth rate. It should be noted that in addition to Péclet number, α and E_∞ are also varied so that the variation in K is captured keeping other parameters unchanged. With decrease in conductivity (increase in Pe), the surface charge density decreases. Since the leading mode is conductive mode, its growth rate is significantly affected by the surface charge density. Thus, the leading growth rate is found to decrease with increase in Péclet number.

4 Conclusion

The stability of a charged fluid jet under axial electric field is analyzed to understand the bead formation during electrospinning process. Contrary to previous studies in which the jet has been considered cylindrical with uniform radius, the present analysis considers the actual thinning jet as the base-state for stability analysis. Taking into consideration, the gradient of jet radius and other variables along the axial-direction is found to significantly influence the stability behavior of the jet. In particular, we find the thinning profile renders the flow stable to axisymmetric disturbances. Under the same operating and material parameters, while the uniform jet has positive growth rate, the thinning jet is found to be stable with negative growth rate. The leading growth rate appears to be a conductive mode, such that an increase in applied voltage or increase in current tends to have destabilizing effect. However, the growth rate remains negative for the range of parameters studied.

Bibliography

- [1] D. A. Saville. Electrohydrodynamic stability: fluid cylinders in longitudinal electric fields. *Phys. Fluids*, 13, 2987-2994, 1970.
- [2] D. A. Saville. Stability of electrically charged viscous cylinders. *Phys. Fluids*, 14, 1095-1099, 1971.
- [3] M. M. Hohman, M. Shin, G. Rutledge, and M. P. Brenner. Electrospinning and electrically forced jets I: Stability theory. *Phys. Fluids*, 13, 2201-2200, 2001.
- [4] C. P. Carroll and Y. L. Joo. Axisymmetric instabilities of electrically driven viscoelastic jets. *J. Non-Newtonian Fluid Mech.*, 153, 130-148, 2008.
- [5] C. P. Carroll and Y. L. Joo. Axisymmetric instabilities in electrospinning of highly conducting viscoelastic polymer solutions. *Phys. Fluids*, 21, 103101, 2009.
- [6] J. J. Feng. The stretching of an electrified non-Newtonian jet: A model for electrospinning. *Phys. Fluids*, 14, 3912, 2002.
- [7] V. N. Kirichenko, I. V. Petryanov-Sokolov, N. N. Supurn, and A. A. Shutov. Asymptotic radius of a slightly conducting liquid jet in an electric field. *Sov. Phys. Dokl.*, 31, 611, 1986.

Comparison of Nonlinear Dynamics of Parkinsonian and Essential Tremor

Olga E. Dick

Pavlov Institute of Physiology of Russian Academy of Science, nab. Makarova 6, 199034, St. Petersburg, Russia
(E-mail: glazov.holo@mail.ioffe.ru)

Abstract. It is known that wrong clinical diagnosis of Parkinson' disease is about 20 % among patients suffering from pathological tremor. That is why the search of new possibilities to improve the diagnostics has high priority. The aim of the work is to answer the question whether the methods of nonlinear dynamics can be used for the guaranteed differential diagnostics of two main types of pathological tremor (parkinsonian and essential ones). We have analyzed tremor determined as fast involuntary shaking and arising during the performance of the motor task by healthy subjects and two groups of patients with parkinsonian syndrome. The first group has the primary Parkinson's disease and the second group has the essential tremor as finger's shaking during the some movements as the main symptom. Using the wavelet transform modulus maxima method, the calculation of the Hölder exponents as well as the detection of unstable periodic orbits and surrogate data we demonstrate the statistically confirmed differences in dynamical complexity, multifractality degree and number of unstable periodic orbits for the two groups of patients. The results give the positive answer the question rose in the work.

Keywords: Dynamical Complexity, Unstable Periodic Orbits, Multifractality, Parkinson's disease, Essential Tremor.

1 Introduction

In spite of enormous number of works [1, 2] devoted to the study of pathological tremor the topic is of immediate interest because of large number of clinical errors connected with wrong administration of antiparkinsonian drugs for subjects having tremor symptoms but not having Parkinson' disease. For example, parkinsonian tremor and so called essential tremor (or action tremor) when the body parts are involved into involuntary shaking during the movement performance differ by frequency. The frequency in essential tremor, however, declines with age in the side of the parkinsonian tremor frequency [3] so that oldest patients can be objects of clinical errors.

8th CHAOS Conference Proceedings, 26-29 May 2015, Henri Poincaré Institute, Paris France

© 2015 ISAST



The aim of the work is to answer the question whether the methods of nonlinear dynamics can be used for the guaranteed differential diagnostics of two main types of pathological tremor (parkinsonian and essential ones).

We studied involuntary shaking (tremor) of fingers accompanied the performance of the motor task such as sustaining the given effort of human hands under isometric conditions (without finger movement in space). For estimating the tremor features we used the methods of nonlinear dynamics such as the wavelet transform and multifractal analysis as well as recurrence plot technique for detecting unstable periodic orbits and surrogate data. We demonstrate the use of these methods for a diagnostics of the human motor dysfunction.

2 The experimental procedure

We used the results of testing 10 healthy subjects aged 47-54 years, 6 parkinsonian patients with bilateral akinesia and tremor aged 45–62 years and 7 subjects with syndrome of essential tremor and without other symptoms of Parkinson's disease. The motor task was to control the isometric muscle effort with the strength of muscle contraction shown by the positions of marks on a monitor. The subjects sat in front of a monitor standing on a table and pressed on platforms containing stress sensors with their fingers. The sensors transformed the pressure strength of the fingers of each hand into an electric signal. The rigidity of the platforms made it possible to record the effort in the isometric mode, i.e., without noticeable movement of fingers at the points of contact with the sensors. The isometric effort was recorded for 50 s. The subject's fingers sustained an upward muscle effort, with the back of each hand pressing against the base of the platform.

The patients with Parkinson's disease did not take any drugs before the test on the day of testing. Usually, these patients received levodopa, an antiparkinsonian preparation three times a day to compensate for dopamine deficiency. The subjects with syndrome of essential tremor did not have tremor medication.

The recorded trajectory of isometric effort consisted of a slow trend and a fast involuntary component (tremor), which was isolated from the recorded trajectory using the MATLAB software.

3 Wavelet transform and multifractality

3.1 Estimation the global wavelet spectrum of the tremor

To evaluate the difference between physiological and pathological tremors, we used the wavelet transform modulus maxima (WTMM) method [4] based on the continuous wavelet transform of a time series describing the examined tremor $x(t)$:

$$W(a, t_0) = a^{-1/2} \int_{-\infty}^{+\infty} x(t) \psi^*((t-t_0)/a) dt,$$

where a and t_0 are the scale and space parameters, $\psi((t-t_0)/a)$ is the wavelet function obtained from the basic wavelet $\psi(t)$ by scaling and shifting along the time, symbol * means the complex conjugate. As the basic wavelet we use the complex Morlet wavelet:

$$\psi_0(t) = \pi^{-1/4} \exp(-0.5t^2) (\exp(i\omega_0 t) - \exp(-0.5\omega_0^2)),$$

where the second component in brackets can be neglected at $\omega_0=2\pi>0$, the multiplier factor $\exp(i\omega_0 t)$ is a complex form of a harmonic function modulated by the Gaussian $\exp(-0.5t^2)$, the coefficient $\pi^{-1/4}$ is necessary to normalize the wavelet energy. The value $\omega_0=2\pi$ gives the simple relation $f=1/a$ between the scale a and the frequency f of the Fourier spectrum. Then expression has the form:

$$W(f, t_0) = \pi^{-1/4} \sqrt{f} \int_{-\infty}^{+\infty} x(t) \exp(-0.5(t-t_0)^2 f^2) \exp(-i2\pi(t-t_0)f) dt.$$

The modulus of the wavelet spectrum $|W(f, t_0)|$ characterizes the presence and intensity of the frequency f at the moment t_0 in the signal and $|W(f, t_0)|^2$ describes the instantaneous distribution of the tremor energy over frequencies, that is, the local spectrum of the signal energy at the time t_0 .

The value

$$E(f) = \int_{t_1}^{t_2} |W(f, t_0)|^2 dt_0$$

determines the global wavelet spectrum, i.e., the integral distribution of the wavelet spectrum energy over frequency range on the time interval $[t_1, t_2]$.

3.2 Estimation the tremor multifractality

Information about possible multifractal feature of the signal and its localization t_0 reflects in the asymptotic behavior of coefficients $|W(a, t_0)|$ at small a values and large f values, respectively. Abnormal small decrease of the wavelet coefficients at $a \rightarrow 0$ in a neighborhood of the point t_0 testifies about singularity of the signal at the point. Thus, the rate of the change of the modulus of the wavelet coefficients enables to analyze the presence or absence of singularities of the signal.

The degree of singularity of the signal $x(t)$ at the point t_0 is described by the Hölder exponent, $h(t_0)$, the largest exponent such that the analyzed signal in a neighborhood of the point t_0 can be represented as the sum of the regular component (a polynomial $P_n(t)$ of order $n < h(t_0)$) and a member describing a non - regular behavior [4]:

$$x(t) = P_n(t) + c|t - t_0|^{h(t_0)}.$$

The value $h(t_0)$ is the measure of singularity of the signal at the point t_0 since the smaller $h(t_0)$ value, the more singular the signal. The Hölder exponents characterize the presence of correlations of different types in the analyzed process, e.g., anti-correlated ($h < 0.5$) or correlated ($h > 0.5$) dynamics or absence of correlations ($h = 0.5$).

The Hölder exponents are found on the basis of statistical description of local singularities by partition functions [5]. The algorithm consists of the following procedures.

- 1) The continuous wavelet transform of the time series is used.
- 2) A set $L(a)$ of lines of local modulus maxima of the wavelet coefficients is found at each scale a
- 3) The partition functions are calculated by the sum of q powers of the modulus maxima of the wavelet coefficients along the each line at the scales smaller the given value a :

$$Z(q, a) = \sum_{l \in L(a)} \left(\sup_{a' \leq a} |W(a', t_l(a'))| \right)^q,$$

$t_l(a^*)$ determines the position of the maximum corresponding to the line l at this scale

- 4) The partition function is $Z(q, a) \sim a^{\tau(q)}$ at $a \rightarrow 0$ [5], therefore, the scaling exponent can be extracted as

$$\tau(q) \sim \log_{10} Z(q, a) / \log_{10} a.$$

- 5) Choosing different values of the power q one can obtain a linear dependence $\tau(q)$ with a constant value of the Hölder exponent

$$h(q) = d\tau(q)/dq = \text{const}$$

for monofractal signals and nonlinear dependence $\tau(q) = qh(q) - D(h)$ with large number of the Hölder exponents for multifractal signals.

- 6) The singularity spectrum (distribution of the local Hölder exponents) is calculated from the Legendre transform [5]:

$$D(h) = qh(q) - \tau(q).$$

Using the global wavelet spectra and the WWTM algorithm for the different tremor recordings we obtain the maximum of the global tremor energy (E_{\max}) and two multifractal parameters: a) the width of the singularity spectrum

$$\Delta h = h_{\max} - h_{\min},$$

where h_{\max} and h_{\min} are the maximal and minimal values of the Holder exponent corresponding to minimal and maximal tremor fluctuation, respectively; b) the asymmetry of the singularity spectrum

$$\Delta = |\Delta_2 - \Delta_1|,$$

where $\Delta_1 = h_{\max} - h_0$ and $\Delta_2 = h_0 - h_{\min}$, $h_0 = h(q = 0)$.

Smaller Δh indicates that the time series tends to be monofractal and larger Δh testifies the enhancement of multifractality. The asymmetry parameter Δ

characterizes where, in the region of strong singularities ($q > 0$) or in the region of weak singularities ($q < 0$), the singularity spectrum is more concentrated. To compare the mean values in each of the examined group of subjects the Student criterion was applied.

4 Recurrence plot and localization of unstable periodic orbits

The set of unstable periodic orbits (UPOs) which form the skeleton of the chaotic attractor can be found by the recurrence quantification analysis (RQA) [6]. The calculation for the RQA was performed using the CRP Toolbox, available at tocsy.pik-potsdam.de/crp.php.

A recurrence plot (RP) is a graphical representation of a matrix defined as

$$R_{i,j}(m, \epsilon) = \Theta(\epsilon - \|y_i - y_j\|),$$

where ϵ is an error (threshold distance for RP computation), $\theta(\cdot)$ is the Heaviside function, symbol $\|\cdot\|$ denotes a norm and y is a phase space trajectory in a m -dimension phase space [7]. The trajectory can be reconstructed from a time series by using the delay coordinate embedding method [8].

The values $R_{i,j}=1$ and $R_{i,j}=0$ are plotted as gray and white dots, reflecting events that are termed as recurrence and nonrecurrence, respectively.

The recurrence time is defined as the time needed for a trajectory of a dynamical system to return into a previously visited neighborhood [9].

The pattern corresponding to periodic oscillations (periodic orbits) is reflected in the RP by noninterrupted equally spaced diagonal lines. The vertical distance between these lines corresponds to the period of the oscillations. The chaotic pattern leads to the emergence of diagonals which are seemingly shorter. The vertical distances become irregular. When the trajectory of the system comes close to an unstable periodic orbit (UPO), it stays in its vicinity for a certain time interval, whose length depends on how unstable the UPO is [9, 10]. Hence, UPOs can be localized by identifying such windows inside the RP, where the patterns correspond to a periodic movement. If the distance between the diagonal lines varies from one chosen window to the other then various UPOs coexist with different periods.

The period of UPO can be estimated by the vertical distances between the recurrence points in the periodic window multiplied by the sampling time of the data series [9, 11].

The algorithm for finding UPOs consists of the following procedures.

1. A phase space trajectory $y(t)$ is reconstructed from a measured time series $\{x(t)\}$ by the delay coordinate embedding method:

$$y(t) = (x(t), x(t+d), \dots, x(t+(m-1)d),$$

where m is the embedding dimension and d is the delay time. Parameters $m=5$ and $d=2$ were chosen on the basis of first minimum of the mutual information function and the false nearest neighbor method [12].

2. To identify unstable periodic orbits a recurrence plot

$$R_{i,j}(m, \epsilon) = \Theta(\epsilon - \|y_i - y_j\|)$$

is constructed with the threshold distance ϵ equal to 1% of the standard deviation of the data series.

3. The recurrence times of second type [10] are found for the recurrence neighbourhood of radius ϵ . The values of recurrence periods are determined as recurrence times multiplied by the sampling time of the data series. The values are recorded in a histogram. The periods of UPOs are the maxima of the histogram of the recurrence periods.

4. To exclude the noise influence the obtained UPOs are tested for statistical accuracy. For this purpose the procedure is repeated for 30 surrogates obtained as randomized versions of the original data. In the surrogate data the time interval sequences are destroyed by randomly shuffling the locations of the time intervals of original data [13].

The statistical measure of the presence of statistically significant UPOs in the original time series is given by the ratio

$$k = (A - \bar{A}) / \sigma,$$

where A is the value of maximum of the histogram, \bar{A} is the mean of A for surrogates and σ is a standard deviation. The value of k characterizes the existence of statistically significant UPOs in the original data in comparison with its surrogate (noisy) version. The value $k > 2$ means the detection of UPOs with a greater than 95% confidence level.

5 Results and discussion

Examples of fast component of the isometric force trajectory of the human hand (tremor) for the healthy subject, the patient with Parkinson disease and for the subject with essential tremor as well as their global wavelet spectra are given in Fig.1. The healthy and pathological tremors differ by spectra maxima. The maximum (E_{\max}) of the physiological tremor spectrum is in the frequency range of the alpha rhythm [8, 14] Hz. For the pathological tremor E_{\max} is shifted in the theta range [4, 7.5] Hz and it increases in ten times in the parkinsonian tremor and in five times in the essential one as compared with the healthy tremor. The essential tremor spectrum has two peaks as opposed to the parkinsonian tremor but the values of the peaks do not differ significantly.

Figure 2 illustrates the differences in the singularity spectra $D(h)$ for the same subjects. The form of spectrum testifies the multifractality of both physiological and parkinsonian tremor but the spectra differ for the three examples.

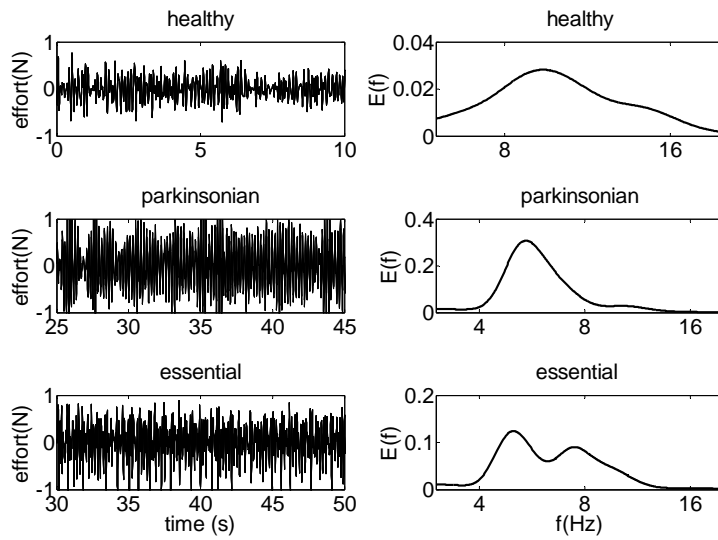


Fig.1 Examples of healthy, parkinsonian and essential tremors (left column) and their global wavelet spectra $E(f)$ (right column)

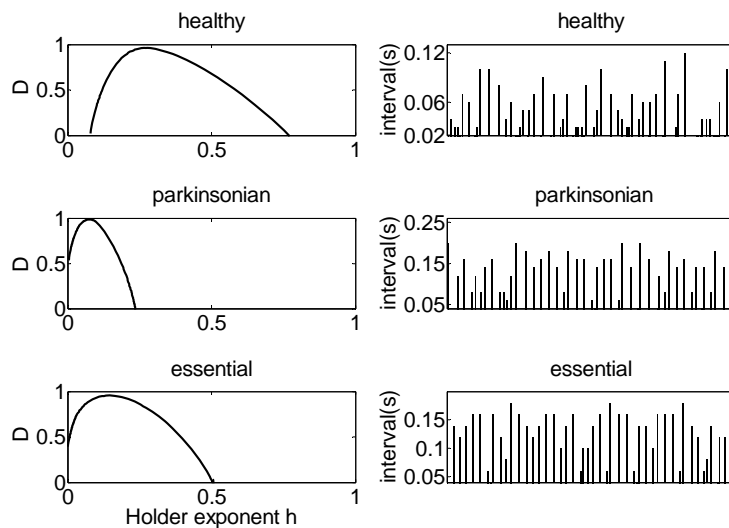


Fig. 2 Examples of the singularity spectra $D(h)$ for the different tremors (left column) and intervals between local maxima of the tremor data (right column)

The healthy tremor is characterized by the largest width Δh of the singularity spectrum and, therefore, by the significant degree of multifractality. The decline in the width of the spectrum shows a fall in the multifractality degree. It means a reduction of nonuniformity of the pathological tremors. We illustrate it in the right column of Figure 2 where intervals between local maxima of the tremor data are depicted.

The parkinsonian tremor is characterized by the smallest width of the singularity spectrum and its smallest asymmetry (Δ). The values of Δh and Δ for the essential tremor are larger than for the parkinsonian one but they do not exceed the values for healthy tremor.

The decrease of the both parameters in pathological tremor is due to decreasing contribution of weak fluctuations (for $q < 0$). These fluctuations lead to the expansion of the singularity spectrum and emergence of both anticorrelated (for $h < 0.5$) and correlated (for $h > 0.5$) dynamics of sequent intervals between local maxima of the tremor data.

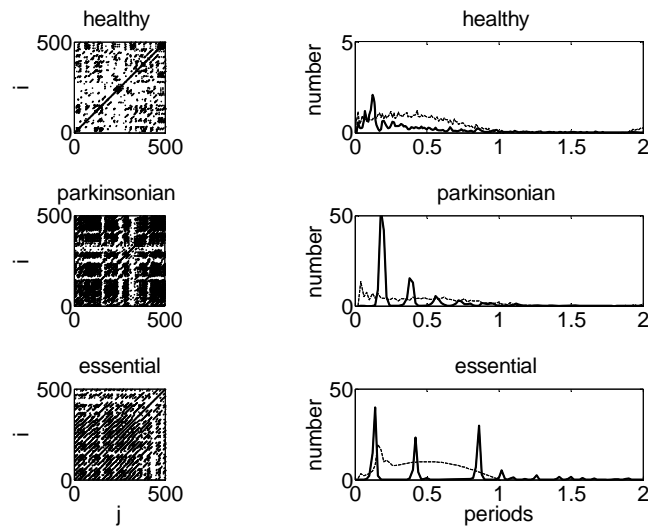


Fig. 3. Examples of recurrence plots for the different tremors (left column) and histograms of recurrence periods for tremor data and their surrogates (right column, solid and dash-and-dot lines, respectively).

Parameters: the embedding dimension $m=5$, the delay time $d=2$, the threshold distance $\epsilon=1\%$ of the standard deviation of the data series.

The recurrence plots depicted in Figure 3 exhibit non-homogeneous but quasi-periodic recurrent structures reflecting in that the distances between the diagonal lines vary in all the three considered tremors. The RP of the healthy

tremor is characterized by small black rectangles, whereas the RPs from the pathological tremors show larger rectangles. These rectangles may reflect time intervals when the trajectory is travelling near the corresponding UPOs [10].

The recurrence times obtained from the RP given in the Figure 3 are clustered in the intervals around the value $i=24$ for the healthy tremor, around $i=36$ and 72 for the parkinsonian one and around $i=28, 84$ and 168 for the essential tremor. Taking into account the value of the sampling rate value $dt=0.005(s)$ the recurrence periods are equal to 0.12 (s) for the healthy data, 0.18 (s) and 0.36 (s) for the parkinsonian data and 0.14 (s), 0.42 (s) and 0.84 (s) for the essential data. These recurrence periods were extracted as peaks of the histograms given in the right column of Figure 3 (solid lines). The periods obtained can be used for localization of UPOs.

Testing surrogate data we excluded the values 0.12 (s) and 0.36 (s) since the statistical measure $k < 1$ in both cases. For other recurrence periods extracted from Figure 3 the value $k > 2$ that supports the detection of UPOs with a greater than 95% confidence level. Thus, for the healthy tremor data represented in Figure 3 there are no statistically significant UPOs. By contrast, the UPO of period 1 ($0,18$ s) is found for the parkinsonian tremor and the UPOs of periods 1, 3 and 6 are obtained for the essential tremor ($0.42/0.14=3, 0.84/0.14=6$).

The similar dynamics of the wavelet and multifractal parameters as well as UPOs localization is observed for all the examined subjects. It enables us to use the common practice of averaging the recordings of all subjects for testing significant variations among the groups.

The values of E_{max} , Δh , Δ and statistical measures k for UPOs of various periods averaged by subjects in every group are given in Table 1.

tremor	hand	healthy	parkinsonian	essential
E_{max}	left	0.029 ± 0.001	0.45 ± 0.02	0.25 ± 0.01
	right	0.037 ± 0.003	0.56 ± 0.04	0.31 ± 0.02
Δh	left	0.83 ± 0.08	0.22 ± 0.02	0.49 ± 0.05
	right	0.76 ± 0.09	0.27 ± 0.02	0.42 ± 0.04
Δ	left	0.46 ± 0.04	0.09 ± 0.01	0.27 ± 0.03
	right	0.38 ± 0.03	0.12 ± 0.01	0.20 ± 0.02
$k(p_1)$	left	< 1	4.9 ± 0.8	5.7 ± 0.9
	right	< 1	3.8 ± 0.6	4.5 ± 0.8
$k(p_2)$	left	< 1	< 1	< 1
	right	< 1	2.1 ± 0.6	< 1
$k(p_3)$	left	< 1	< 1	2.1 ± 0.3
	right	< 1	< 1	2.7 ± 0.3
$k(p_6)$	left	< 1	< 1	3.8 ± 0.4
	right	< 1	< 1	4.1 ± 0.4

Table 1. Comparison of the mean values of wavelet and singularity spectra characteristics and statistical measure of UPOs (averaging over subjects inside the every examined group).

The significant distinctions between the states (pathological or physiological tremor) are identified by all the parameters ($p < 0.03$). The values for the essential and parkinsonian tremors also differ ($p < 0.05$).

The results serve one more verification for the decline of dynamical complexity of time intervals in pathological tremor. It exhibits in the decrease of the multifractality degree, disappearance of long-range correlations and transitions to strongly periodic dynamics including the emergence of unstable periodic orbits in involuntary oscillations of the human hand.

Conclusions

Our study of differences in involuntary oscillations arising during the maintenance of isometric force by the human hand of a subject suffering from Parkinson's disease and a subject having tremor symptoms but not having the disease demonstrates that the multifractal characteristics and number of UPOs can serve useful indicators of a dysfunctional network in the central nervous system.

References

1. J. H. McAuley, C. D. Marsden. Physiological and pathological tremors and rhythmic central motor control. *Brain*, 123, 8, 1545{1567, 2000.
2. A.N. Pavlov, A.N. Tupitsyn, A. Legros, et. al. Using wavelet analysis to detect the influence of low frequency magnetic fields on human physiological tremor, *Physiol. Measurement*, 28, 321{333, 2007.
3. R. J. Elble, C. Higgins, K. Leffler et, al. Factors influencing the amplitude and frequency of essential tremor. *Mov. Disord.*, 9, 589{596, 1994.
4. J. F. Muzy, E. Bacry, A. Arneodo. Multifractal formalism for fractal signals: the structure-function approach versus the wavelet-transform modulus-maxima method. *Phys. Rev. E*, 47, 875{884, 1993.
5. A. Arneodo, E. Bacry, J. F Muzy. The thermodynamics of fractals revisited with wavelets. *Physica A*, 213, 232{275, 1995.
6. J. P. Eckmann, S. Kamphorst, D. Ruelle. Recurrence plots of dynamical systems. *Europhys. Lett.*, 4, 973{977, 1987.
7. N. Marwan, M. C. Romano, M. Thiel, et. al. Recurrence plots for the analysis of complex systems. *Physics Reports*, 438, 237{329, 2007.
8. F. Takens. Detecting strange attractors in turbulence, *Dynamical Systems and Turbulence, Lecture Notes in Mathematics* (D. Rand, L. S. Young, eds.), Springer-Verlag, Berlin 898, 366{381, 1981
9. J. B. Gao. Recurrence time statistics for chaotic systems and their applications. *Phys. Rev. Lett.*, 83, 16, 3178{3181, 1999.
10. E. Bradley, R. Mantilla. Recurrence plots and unstable periodic orbits. *Chaos*, 12, 3, 596{600, 2002.
- 11 E. J. Ngamga, A. Nandi, R. Ramaswamy, et. al., *Phys. Rev. E*, 75, 3 036222{036345, 2007.
12. M. B. Kennel, R. Brown, H. D. Abarbanel. Determining embedding dimension for phase-space reconstruction using a geometrical construction. *Phys. Rev. A*, 45, 6, 3403{3411, 1992.
13. J. Theiler, S. Eubank, A. Longtin, et, al. Testing for nonlinearity in time series: the method of surrogate data. *Physica D*, 58, 77{94, 1992.

The Spectral Chaos in a Spherically Centered Layered Dielectric Cavity Resonator

Zoya E. Eremenko, Ekaterina S. Kuznetsova, Luka D. Shostenko,
Yuriy V. Tarasov, and Igor N. Volovichev

O. Ya. Usikov Institute for Radiophysics and Electronics of National Academy of Sciences of Ukraine, Kharkov, Ukraine
(E-mail:zoya.eremenko@gmail.com)

Abstract. This paper deals with the study of chaotic spectral wave properties of a cavity sphere layered central-symmetric dielectric resonator. The analytical and numerical research was carried out. It is determined that resonant frequencies of a given layered resonator accurately coincide with the resonant frequencies of inhomogeneous resonator with specified oscillation indices if the radius of inner sphere is much less than the outer resonator radius. Increasing the radius of inner sphere these resonant frequencies shift to smaller values and new additional resonances appear, which cannot be identified by the same oscillation indices and it can be considered as possible chaotic presentation. The probability of inter-frequency interval distribution has signs of spectral chaos in studied structure.

Keywords: Sphere dielectric central-symmetric resonator, spectral wave properties, resonant frequencies, oscillation indices, signs of spectral chaos, probability of inter-frequency interval distribution.

1 Introduction

Our aim is to study the chaotic properties of a layered spherical dielectric cavity resonator with a inner centered spherical dielectric sphere. Dielectric resonators are known to be widely used in optics, laser technology, solid-state electronics (see, for example, Refs. [1,2]). The change of the oscillation spectrum of such resonators strongly depends on both inhomogeneities in the dielectric filling and the resonator shape. For practical applications it is extremely important to know the degree of regularity or randomness of the frequency spectrum. The detailed analysis of the spectrum chaotic properties for different resonant systems can be found, for instance, in [3].

The resonators with electromagnetic wave oscillations are often similar to classical dynamic billiards. Spectral properties of classical dynamical billiards have been thoroughly studied to date (see, e. g., the book [4]). The spectral properties of wave billiard systems are the subject of study by the relatively young field of physics, called “quantum (or wave) chaos” [5,6]. Using the terminology given in paper [7], such systems can be called composite billiards.

8th CHAOS Conference Proceedings, 26-29 May 2015, Henri Poincaré Institute, Paris France

© 2015 ISAST



It is necessary to underline that the presence of additional spatial scale in wave billiards — the wavelength λ — results in serious limitations when trying to describe the chaotic properties of their spectra using the ray approach. In particular, there exist the ray splitting on the interface of different edges in the composite billiards [8,9], which cannot be captured by the classical dynamics. Thus, the ray approach is not well-suited to wave billiard-type systems, so their chaotic properties have to be studied, in general, applying of wave equations.

Statistic analysis of the wave system spectrum is mainly based on the methods used in the classical chaos dynamics, for instance, on the study of inter-frequency interval distribution, spectral rigidity and so on [5,6,10]. The goal of the present work is to investigate spectral properties of layered cavity resonators starting from electromagnetic wave approach. To reach this objective we apply the calculation technique consisting of rigorous splitting of oscillation modes by means of the operational method. This technique was used previously for inhomogeneous waveguides and resonators with bulk and surface inhomogeneities [11–14]. The result of the mode splitting in such complicate and conventionally non-integrable systems is the appearance of specific potentials of operator nature in the wave equation. The structure of these potentials gives rise to the possibility of studying the oscillation spectrum both numerically and analytically.

The spectrum of spherical resonator with homogeneous dielectric inside is strongly degenerate due to the central symmetry. The degeneracy leads to the clustering of the probability distribution maximum for inter-frequency intervals near zero value. It is quite natural to expect that when the spherical resonator becomes layered due to the spherical inner dielectric the spectrum degeneracy is removed. This is strongly expected to be so at least in the case of the symmetry violation.

In the present work we attempt to answer the following questions. What is the type of the probability distribution for inter-frequency intervals in the case of composite (layered) spherical resonator with and without the spatial symmetry? What is the qualitative nature of deformation of the probability distribution when spatial symmetry is violated? What are the signatures of classical chaos in this distribution?

2 Problem statement and basic relationships

We are interested in eigen-oscillations of an electromagnetic resonator taken in the form of ideal conducting sphere of radius R_{out} filled with homogeneous dielectric of permittivity ε_{out} , in which a centered inner dielectric sphere of smaller radius R_{in} is placed, whose permittivity is ε_{in} (see Fig. 1).

The electromagnetic field inside the resonator can be expressed through electrical and magnetic Hertz functions, $U(\mathbf{r})$ and $V(\mathbf{r})$ [15]. Using these functions, we can go over to Debye potentials $\Psi_{U,V}(\mathbf{r})$ $\Psi_U(\mathbf{r}) = r^{-1}U(\mathbf{r})$ and

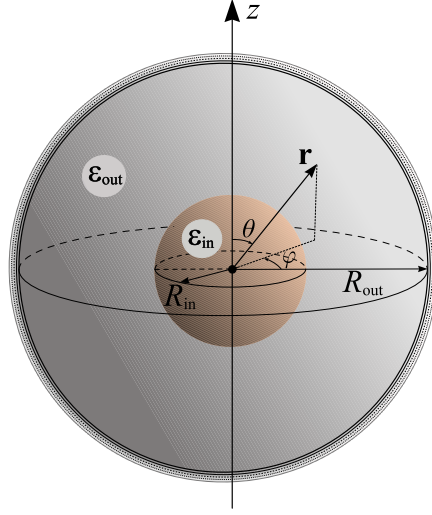


Fig. 1. Composite double-spherical dielectric cavity resonator.

$\Psi_V(\mathbf{r}) = r^{-1}V(\mathbf{r})$ [15,16] both obeying the same Helmholtz equation,

$$\begin{aligned}
 [\Delta + k^2\varepsilon(\mathbf{r})]\Psi(\mathbf{r}) &= \frac{1}{r^2} \frac{\partial}{\partial r} \left(r^2 \frac{\partial \Psi}{\partial r} \right) + \frac{1}{r^2 \sin \vartheta} \frac{\partial}{\partial \vartheta} \left(\sin \vartheta \frac{\partial \Psi}{\partial \vartheta} \right) \\
 &+ \frac{1}{r^2 \sin^2 \vartheta} \frac{\partial^2 \Psi}{\partial \varphi^2} + k^2\varepsilon(\mathbf{r})\Psi = 0
 \end{aligned} \tag{1}$$

(ϑ and φ are polar and azimuthal angle variables), but different independent boundary conditions,

$$\left. \frac{\partial}{\partial r} (r\Psi_U) \right|_{r=R_{\text{out}}} = 0, \tag{2a}$$

$$\left. \Psi_V \right|_{r=R_{\text{out}}} = 0. \tag{2b}$$

The first condition belongs to the class of so-called Robin's boundary conditions (see, e. g., Ref. [17]), the second one is the well-known Dirichlet condition. The conditions (2) for the electrical and magnetic Debye potentials allows to find these potentials independently from each other, which may be interpreted as the possibility to separate electrical and magnetic-type oscillation in the inhomogeneous spherical resonator.

We will consider the resonator inhomogeneity according to quantum-mechanical perturbation approach. If we take the inhomogeneity as a potential in Schrodinger equation we can write the permittivity in the equation (1) as a "weighted" sum of permittivities of inner and outer dielectric spheres,

$$\varepsilon(\mathbf{r}) = \varepsilon_{\text{in}}\Theta(\mathbf{r} \in \Omega_{\text{in}}) + \varepsilon_{\text{out}}\Theta(\mathbf{r} \in \Omega_{\text{out}} \setminus \Omega_{\text{in}}). \tag{3}$$

Here $\Theta(A)$ stands for the logical theta-function determined as

$$\Theta(A) = \begin{cases} 1, & \text{if } A = \text{true} \\ 0, & \text{if } A = \text{false} \end{cases}, \quad (4)$$

Ω_{in} and Ω_{out} are the portions of spatial points belonging to inner and outer spheres, respectively. It is convenient to present function (3) as a sum of its spatially averaged part

$$\bar{\varepsilon} = \frac{\varepsilon_{\text{in}}V_{\text{in}} + \varepsilon_{\text{out}}(V_{\text{out}} - V_{\text{in}})}{V_{\text{out}}}, \quad (5)$$

with $V_{\text{in/out}} = (4\pi/3)R_{\text{in/out}}^3$ being the volumes of inner and outer spheres, and the summand $\Delta\varepsilon(\mathbf{r})$, the integral of which over the whole resonator volume is equal to zero. The solution to Eq. (1) with exact permittivity value instead of its average one given by (5) will be the starting point to build the constructive perturbation theory.

Equation (1) with coordinate-independent permittivity can be solved by the method described in a number of textbooks (see, e.g., Ref. [18]). The general solution can be presented as an expansion in complete orthogonal eigenfunctions of the Laplace operator, which in spherical coordinates have the form [19,20]

$$|\mathbf{r}; \boldsymbol{\mu}\rangle = \frac{D_n^{(l)}}{R} \sqrt{\frac{2}{r}} J_{l+\frac{1}{2}}(\lambda_n^{(l)} r/R) Y_l^m(\vartheta, \varphi) \quad (6)$$

$$(n = 1, 2, \dots, \infty; \quad l = 0, 1, 2, \dots, \infty; \quad m = -l, -l+1, \dots, l-1, l).$$

Here, to simplify the equations we introduce the vector mode index $\boldsymbol{\mu} = \{n, l, m\}$, $J_p(u)$ is the Bessel function of the first kind, $Y_l^m(\vartheta, \varphi)$ is the spherical function,

$$Y_l^m(\vartheta, \varphi) = (-1)^m \left[\frac{(2l+1)}{2} \cdot \frac{(l-m)!}{(l+m)!} \right]^{1/2} P_l^m(\cos \vartheta) \cdot \frac{e^{im\varphi}}{\sqrt{2\pi}}, \quad (7)$$

$P_l^m(t)$ is the Legendre function. The coefficients $\lambda_n^{(l)}$ in the equation (6) are the positive zeros of either the sum $uJ'_{l+\frac{1}{2}}(u) + (1/2)J_{l+\frac{1}{2}}(u)$ (if boundary conditions (BC) (2a) is applied), or the function $J_{l+\frac{1}{2}}(u)$ (in the case of BC (2b)), which are numbered by natural index n in ascending order. Normalization coefficient $D_n^{(l)}$ in relation (6) depends on the particular boundary condition,

$$D_n^{(l)} = \left\{ J_{l+\frac{1}{2}}'^2(\lambda_n^{(l)}) + \left[1 - \left(\frac{l+1/2}{\lambda_n^{(l)}} \right)^2 \right] J_{l+\frac{1}{2}}^2(\lambda_n^{(l)}) \right\}^{-\frac{1}{2}} \quad \text{for BC (2a),} \quad (8a)$$

$$D_n^{(l)} = J_{l+\frac{3}{2}}^{-1}(\lambda_n^{(l)}) \quad \text{for BC (2b).} \quad (8b)$$

The eigenvalue of the Laplace operator, that corresponds to eigenfunction (6), is degenerated over azimuthal index m ,

$$E_{\mu} = -k_{\mu}^2 = - \left(\frac{\lambda_n^{(l)}}{R} \right)^2 . \quad (9)$$

with the degeneracy equal to $2l + 1$.

The spectrum of the resonator with nonuniform permittivity (3) can be found through the calculation of density of states $\nu(k)$ (see, e.g., Ref. [21]). Function $\nu(k)$ can be expressed through the Green function of wave equation (1) with complex-valued frequency account for dissipation in the resonator,

$$\nu(k) = \pi^{-1} \text{Im} \{ \text{Tr} \hat{\mathcal{G}}^{(-)} \} . \quad (10)$$

Here $\hat{\mathcal{G}}^{(-)}$ is the advanced Green operator corresponding the equation (1) with negative imaginary part in the complex frequency plane. The Green function (considered as the coordinate matrix element of operator $\hat{\mathcal{G}}^{(-)}$) obeys the equation

$$[\Delta + \bar{\epsilon}k^2 - i/\tau_d - V(\mathbf{r})] G(\mathbf{r}, \mathbf{r}') = \delta(\mathbf{r} - \mathbf{r}') , \quad (11)$$

where the term $V(\mathbf{r}) = -k^2 \Delta \varepsilon(\mathbf{r})$ will be interpreted as the effective potential (in the quantum-mechanical terminology). In comparison with Eq. (1), equation (11) is supplied with imaginary term i/τ_d which takes phenomenologically into account the dissipation processes in the bulk and on the surface of the resonator. Strictly speaking, the dielectric loss in the resonator depend on the frequency in the general case. Yet now we will neglect this dependence to simplify further investigations.

For the numerical calculation purposes it is suitable to go over from the coordinate representation of Eq. (11) to the momentum representation. Equation (11) then takes the form of an infinite set of coupled algebraic equations,

$$(\bar{\epsilon}k^2 - k_{\mu}^2 - i/\tau_d - \mathcal{V}_{\mu}) G_{\mu\mu'} - \sum_{\nu \neq \mu} \mathcal{U}_{\mu\nu} G_{\nu\mu'} = \delta_{\mu\mu'} . \quad (12)$$

Here the quantities \mathcal{V}_{μ} and $\mathcal{U}_{\mu\nu}$, which we will term the *intramode* and the *intermode* potentials, are the matrix elements of potential $V(\mathbf{r})$ taken in the basis of functions (6),

$$\mathcal{U}_{\mu\nu} = \int_{\Omega} d\mathbf{r} \langle \mathbf{r}; \mu | V(\mathbf{r}) | \mathbf{r}; \nu \rangle = -k^2 (\varepsilon_{\text{in}} - \varepsilon_{\text{out}}) I_{\mu\nu} , \quad (13a)$$

$$\mathcal{V}_{\mu} = \mathcal{U}_{\mu\mu} = -k^2 (\varepsilon_{\text{in}} - \varepsilon_{\text{out}}) [I_{\mu\mu} - V_{\text{in}}/V_{\text{out}}] , \quad (13b)$$

$$I_{\mu\nu} = \int_{\Omega_{\text{in}}} d\mathbf{r} \langle \mathbf{r}; \mu | \mathbf{r}; \nu \rangle .$$

In the case of strictly centered outer and inner dielectric spheres the integrals in the relationships (13) are calculated rigorously, and the result is as follows,

$$I_{\mu\nu}(\Omega_{\text{in}}) = 2\mathcal{Q}\delta_{l_\mu l_\nu}\delta_{m_\mu m_\nu} \frac{D_{n_\mu}^{(l_\mu)} D_{n_\nu}^{(l_\mu)}}{\lambda_{n_\mu}^{(l_\mu)2} - \lambda_{n_\nu}^{(l_\mu)2}} \left[\lambda_{n_\mu}^{(l_\mu)} J_{l_\mu + \frac{3}{2}} \left(\lambda_{n_\mu}^{(l_\mu)} \mathcal{Q} \right) J_{l_\mu + \frac{1}{2}} \left(\lambda_{n_\nu}^{(l_\mu)} \mathcal{Q} \right) - \lambda_{n_\nu}^{(l_\mu)} J_{l_\mu + \frac{1}{2}} \left(\lambda_{n_\mu}^{(l_\mu)} \mathcal{Q} \right) J_{l_\mu + \frac{3}{2}} \left(\lambda_{n_\nu}^{(l_\mu)} \mathcal{Q} \right) \right] \quad (\boldsymbol{\mu} \neq \boldsymbol{\nu}), \quad (14a)$$

$$I_{\mu\mu}(\Omega_{\text{in}}) = \mathcal{Q}^2 \left[D_{n_\mu}^{(l_\mu)} \right]^2 \left[J_{l_\mu + \frac{1}{2}}^2 \left(\lambda_{n_\mu}^{(l_\mu)} \mathcal{Q} \right) - J_{l_\mu - \frac{1}{2}} \left(\lambda_{n_\mu}^{(l_\mu)} \mathcal{Q} \right) J_{l_\mu + \frac{3}{2}} \left(\lambda_{n_\mu}^{(l_\mu)} \mathcal{Q} \right) \right]. \quad (14b)$$

Here we have introduced the scale parameter $\mathcal{Q} = R_{\text{in}}/R_{\text{out}} \leq 1$ that describes the degree of the resonator *geometric* inhomogeneity.

3 Numerical results and discussion

The set of basic equations (12) can, in principle, be solved analytically using the operator technique of mode separation [14]. Yet, in view of the tediousness of that technique, in this study we examine equations (12) numerically. To obtain the solution we have elaborated programming software that calculate the resonator Green function, determine its maxima locations, and also build the inter-frequency distribution function. It is necessary to accentuate that such a calculation task is quite resource-intensive, and it leads to rigid constraint for the number N of oscillation modes taken into account. The computational complexity grows much faster than N^3 . Such a dependence on the number of analyzed oscillations can be explained by the complexity of numerical integration of oscillating functions (Bessel functions, spherical Legendre functions) with the growing number of their zeros on the interval of integration. The main numerical calculations were carried out on the computing cluster at the Institute for Radiophysics and Electronics of National Academy of Sciences of Ukraine, which is a part of the infrastructure of the Ukrainian National Grid (UNG). Based on the available computation resources (CPU clock speed 2.5 GHz, RAM 1.5 Gb/core), we were compelled to limit the number of harmonics by 10,000 and no more than 2000 harmonics for an arbitrary value of heterogeneity. The calculation of each harmonics takes from a few seconds for the long-wavelength modes to tens of minutes for short ones. To speed up the calculations and the possibility to operate with a greater number of harmonics, the parallelization of computational algorithm with the use of MPI technology was implemented. Note that the task under consideration is highly scalable. Thus, the parallel computation provides a performance increase. It is almost proportional to the number of computing nodes involved. All calculations were performed in the standard representation for double-precision real numbers. Relative error of calculation does not exceed 10^6 , and the main source of error was the accuracy of numerical integration and calculation of special functions.

From Eqs. (12) we have calculated all diagonal elements of the Green function matrix $\|G_{\boldsymbol{\mu}\boldsymbol{\mu}'}\|$. In Fig. 2, the density of states (DoS) of the resonator is presented, which is calculated using the definition (10). It can be seen that the

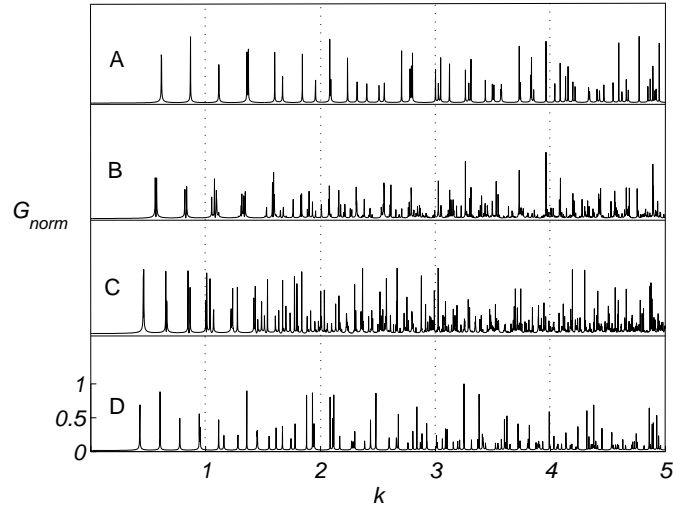


Fig. 2. The whole frequency spectrum as the frequency dependence of the imaginary part of the sum of diagonal Green functions for the composite cavity resonator with centered dielectric spheres: A — $Q=0$; B — $Q=0.583$; C — $Q=0.897$; D — $Q=0.998$. The permittivities of the inner and outer spheres are $\varepsilon_{\text{in}} = 2.08$, $\varepsilon_{\text{out}} = 1.0$. The dissipation value corresponds to $\tau_d = 1000$.

DoS graph becomes thicker with growing the radius of inner dielectric sphere. When the inner radius value goes to the outer one, the DoS is getting thinner. In this case the resonator filling tends to become homogenous with the effective permittivity ε_{out} . Thus, the average DoS maximal value is observed at $Q \rightarrow 1$.

To analyze the oscillation spectrum we examine the probability of the inter-frequency intervals (nearest-neighbor spacings, NNS) between adjacent resonances, $P(S)$. Conventionally, the spectrum unfolding is used for this purpose, implying the normalized mean inter-frequency distance to be equal to unity. Fig. 3 demonstrates distribution $P(S)$ for different inner radii and dissipation values. For $\tau_d = 100000$ (the loss is practically neglected) and $Q=0$ we have convention with Poisson distribution, $P_p(S) = \exp(-S)$. This suggests the resonance frequencies to be completely uncorrelated. With the increase in the dissipation value (for example, $\tau_d = 100$) we obtain the distribution function that tends to Wigner form, $P_w(S) = 0.5\pi S \exp(-\frac{\pi S^2}{4})$. Thus, we are led to conclude that the presence of dissipation in the resonator results in the chaotic behavior of oscillation modes.

The essential difference between NNS distribution of the chaotic spectrum and the regular one is the presence of mode “repulsion” (the downfall of $P(S)$ at low values of S). The repulsion of modes with close frequencies in the chaotic spectrum can be explained as follows. When the resonator infill is homogeneous, different oscillation modes are independent of each other and do not interact with each other even if their own frequencies coincide, i. e. if they are in a degenerate state. Any heterogeneity lifts the degeneracy, and the

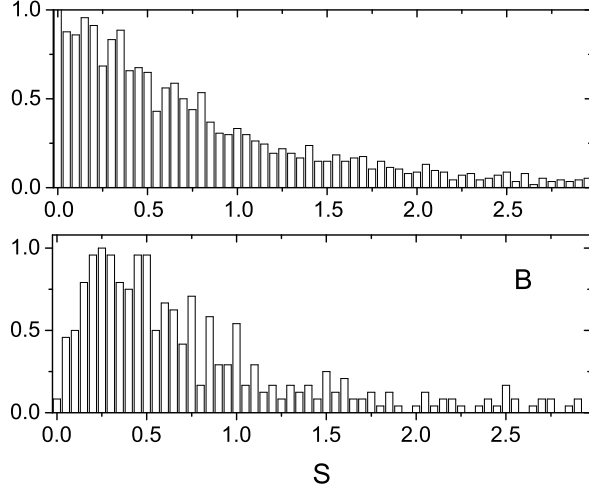


Fig. 3. The probability of inter-frequency interval distribution at different dissipation values and inner radii : A — $\tau_d = 100000$, $Q=0$; B — $\tau_d = 100$, $Q=0.67$.

natural frequencies of different modes change in different ways, depending on the degree of heterogeneity influence. That is, there is a kind of “repulsion” of oscillations modes. The larger the impact of heterogeneity be, the greater is the repulsion effect.

In Fig. 4, the intensity of a partial Green function $G_{\mu\mu}$ from Eq. (12) on wave number is shown for the particular polar and radial indices and different inner sphere radii R_{in} . At $R_{in}=0$ we observe one oscillation mode only. We will call it the main resonance for the selected Green function. With the increase in the inner radius R_{in} , additional resonances appear at the frequencies that coincide with main resonances of the rest of radial modes with the definite polar index.

In Fig. 5, the frequency dependence of the imaginary part of the sum of diagonal Green functions for the oscillations with two different polar indices. As the radius R_{in} increases, we observe that the resonances 1 and 2 interchange their relative position. Thus, we see the occasional and unpredictable oscillations moving. We explain this behavior of resonances as a signature of wave chaos arisen due to inhomogeneity of the resonator.

Thus, we have developed the statistical spectral theory of the centrally symmetric layered cavity resonator with homogeneous and inhomogeneous infill. Numerical investigation of the resonator frequency spectrum was also carried out. The signature of chaotic behavior of the resonator spectrum is demonstrated. We have found out that the homogeneous resonator has inter-frequency interval distribution similar to the Poisson distribution typical for the spectrum with uncorrelated inter-frequency intervals. In the presence of dissipation in

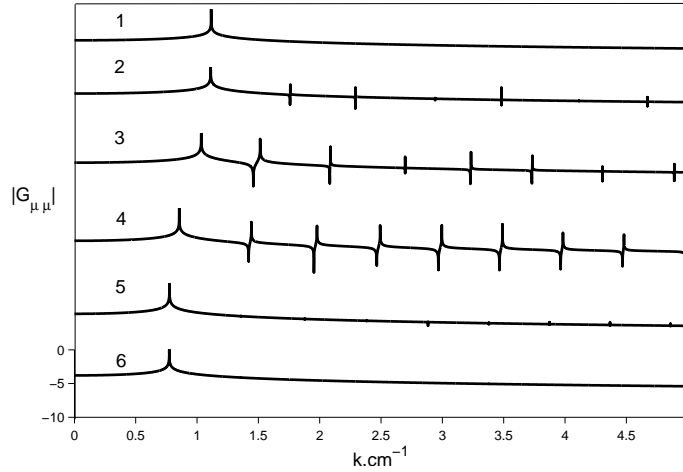


Fig. 4. Frequency dependence of the logarithm of partial normalized Green function for different inner radii: 1 — $Q=0$, 2 — $Q=0.448$, 3 — $Q=0.672$, 4 — $Q=0.8968$, 5 — $Q=0.9977$, 6 — $Q=0.9997$. Polar index is 3, radial index is 1. The permittivities of the inner and outer spheres are $\varepsilon_{\text{in}}=2.08$, $\varepsilon_{\text{out}}=1.0$. The dissipation value corresponds to $\tau_d = 100000$.

the resonator, the NNS distribution tents to the distribution of Wigner form, which clearly demonstrates the effect of “mode repulsion”.

References

1. F. T. Arecchi and R. G. Harrison (eds.). *Instabilities and Chaos in Quantum Optics* (Springer-Verlag, Berlin, 1987).
2. I. O. Kulik and R. Ellialtioglu (eds.). *Quantum mesoscopic phenomena and mesoscopic devices in microelectronics* (Springer Science+Business Media, Dordrecht, 2000).
3. M. C. Gutzwiller. *Resource Letter ICQM-1: The Interplay between Classical and Quantum Mechanics*, Am. J. Phys. **66**, 304 (1998).
4. A. J. Lichtenberg, M. A. Lieberman. *Regular and chaotic dynamics* (Springer-Verlag, New York, 1992).
5. F. Haake. *Quantum Signatures of Chaos* (Springer-Verlag, Berlin, 2010).
6. H.-J. Stöckmann. *Quantum chaos: an introduction* (Cambridge University Press, New York, 1999).
7. V. G. Baryakhtar, V. V. Yanovsky, S. V. Naydenov, and A. V. Kurilo. *Chaos in Composite Billiards*, JETP **103**, 292 (2006).
8. R. Blümel, T. M. Antonsen, B. Georgeot, E. Ott, and R. E. Prange. *Ray Splitting and Quantum Chaos*, **76**, 2476 (1996).
9. R. Blümel, T. M. Antonsen, B. Georgeot, E. Ott, and R. E. Prange. *Ray splitting and quantum chaos*, **53**, 3284 (1996).
10. T. A. Brody, J. Flores, J. B. French, P. A. Mello, A. Pandey, and S. S. M. Wong. *Random-matrix physics: spectrum and strength fluctuations*, **53**, 385 (1981).
11. Yu. V. Tarasov. *Elastic scattering as a cause of quantum dephasing: the conductance of two-dimensional imperfect conductors*, **10**, 395 (2000).

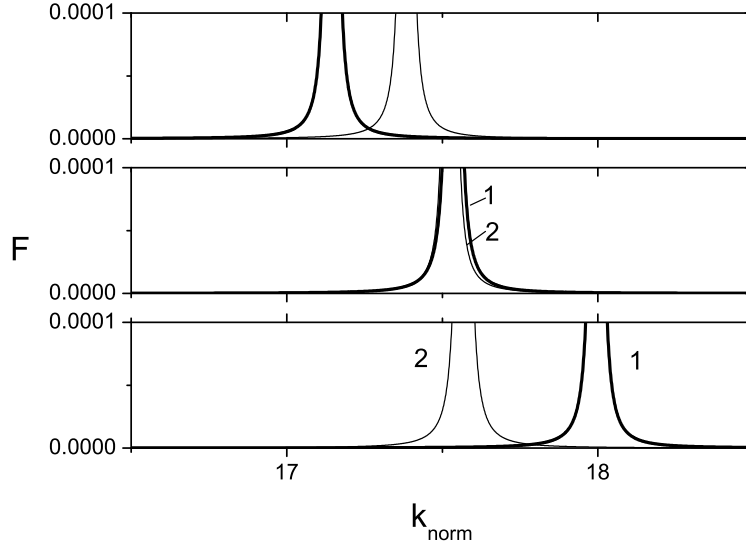


Fig. 5. Frequency dependence of the imaginary part of the sum of diagonal Green functions with fixed polar indices (1 — polar index $l = 1$, 2 — $l = 3$) with different values of radius R_{in} : A — $Q=0.19$, B — $Q=0.21$, C — $Q=0.23$. The permittivities of the inner and outer spheres are $\varepsilon_{in}=2.08$, $\varepsilon_{out}=1.0$. The dissipation value corresponds to $\tau_d = 100000$.

12. E. M. Ganapolskii, Z. E. Eremenko, and Yu. V. Tarasov. *Effect of random surface inhomogeneities on spectral properties of dielectric-disk microresonators: Theory and modeling at millimeter wave range*, **79**, 041136 (2009).
13. E. M. Ganapolskii, Yu. V. Tarasov, and L. D. Shostenko. *Spectral properties of cylindrical quasioptical cavity resonator with random inhomogeneous side boundary*, **84**, 026209 (2011).
14. E. M. Ganapolskii, Z. E. Eremenko, and Yu. V. Tarasov. *Influence of random bulk inhomogeneities on quasioptical cavity resonator spectrum*, **75**, 026212 (2007).
15. L. A. Vajnshtejn. *Electromagnetic Waves* (Radio i Svyaz, Moscow, 1988) (in Russian).
16. A. N. Oraevsky. *Whispering-gallery waves*, Quant. Electron. **32**, 377 (2002).
17. K. Gustafson, T. Abe. *The Third Boundary Condition — Was it Robin's?*, Math. Intell. **20**, 63 (1998).
18. A. Messiah. *Quantum Mechanics*, v. 1 (North-Holland, Amsterdam, 1961).
19. G. N. Watson, *A Treatise on the Theory of Bessel Functions* (Cambridge University Press, 1995).
20. H. Bateman, A. Erdélyi, *Higher transcendental functions*, v. 2 (McGraw Hill, New York, 1953).
21. E. N. Economou. *Green's Functions in Quantum Physics* (Springer-Verlag, Berlin, 2006).

Reachable Sets for a Class of Nonlinear Control Systems with Uncertain Initial States

Tatiana F. Filippova¹, Oxana G. Matviychuk², and Sergey M. Makarov³

¹ Department of Optimal Control of the Institute of Mathematics and Mechanics of the Ural Branch of Russian Academy of Sciences and Ural Federal University, Ekaterinburg, Russian Federation
(E-mail: ftf@imm.uran.ru)

² Department of Optimal Control of the Institute of Mathematics and Mechanics of the Ural Branch of Russian Academy of Sciences and Ural Federal University, Ekaterinburg, Russian Federation
(E-mail: vog@imm.uran.ru)

³ Ural Federal University, Ekaterinburg, Russian Federation
(E-mail: makarovsergey93@mail.ru)

Abstract. We consider the problem of estimating reachable sets of nonlinear dynamical control systems with uncertainty in initial states when we assume that we know only the bounding set for initial system positions and any additional statistical information is not available. We study the case when the system nonlinearity is generated by the combination of two types of functions in related differential equations, one of which is bilinear and the other one is quadratic. The problem may be reformulated as the problem of describing the motion of set-valued states in the state space under nonlinear dynamics with state velocities having bilinear-quadratic kind. Using results of the theory of trajectory tubes of control systems and techniques of differential inclusions theory we find set-valued estimates of related reachable sets of such nonlinear uncertain control system. The algorithms of constructing the ellipsoidal estimates for studied nonlinear systems are given.

Keywords: Nonlinear control systems, Bilinear nonlinearity, Quadratic nonlinearity, Set-membership uncertainty, Ellipsoidal calculus, Funnel equations, Trajectory tubes.

1 Introduction

The problem of parameter estimation for control problems and of the evaluation of related estimating sets describing uncertainty is considered in the paper in the case when a probabilistic description of noise and errors is not available, but only a bound on them is known (Bertsekas and Rhodes[1], Kurzhanski and Valyi[14], Milanese *et al.*[18], Schweppe[20], Walter and Pronzato[22]). Such models may be found in many applied areas ranged from engineering problems in physics to economics as well as to biological and ecological modeling when it occurs that a stochastic nature of the errors is questionable because of limited

8th CHAOS Conference Proceedings, 26-29 May 2015, Henri Poincaré Institute, Paris France

© 2015 ISAST



data or because of nonlinearity of the model. Unlike the classical estimation approach, set-membership estimation is not concerned with minimizing any objective function and instead of finding a single optimal parameter vector, a set of feasible parameters vectors, consistent with the model structure, measurements and bounded uncertainty characterization, should usually be found.

The solution of many control and estimation problems under uncertainty involves constructing reachable sets and their analogs. For models with linear dynamics under such set-membership uncertainty there are several constructive approaches which allow finding effective estimates of reachable sets. We note here two of the most developed approaches to research in this area. The first one is based on ellipsoidal calculus (Chernousko[3], Kurzanski and Valyi[14]) and the second one uses the interval analysis (Walter and Pronzato[22]).

Many applied problems are mostly nonlinear in their parameters and the set of feasible system states is usually non-convex or even non-connected. The key issue in nonlinear set-membership estimation is to find suitable techniques, which produce related bounds for the set of unknown system states without being too computationally demanding. Some approaches to the nonlinear set-membership estimation problems and discrete approximation techniques for differential inclusions through a set-valued analogy of well-known Euler's method were developed in Kurzanski and Varaiya[15], Kurzanski and Filippova[13], Dontchev and Lempio[6], Veliov[21].

In this paper the modified state estimation approaches which use the special quadratic structure of nonlinearity of studied control system and use also the advantages of ellipsoidal calculus (Kurzanski and Valyi[14], Chernousko[3]) are presented. We study here more complicated case than in Filippova and Matviychuk[12] and we assume now that the system nonlinearity is generated by the combination of two types of functions in related differential equations, one of which is bilinear and the other one is quadratic. The problem may be reformulated as the problem of describing the motion of set-valued states in the state space under nonlinear dynamics with state velocities having bilinear-quadratic kind. Using results of the theory of trajectory tubes of control systems and techniques of differential inclusions theory we find set-valued estimates of related reachable sets of such nonlinear uncertain control system. The algorithms of constructing the ellipsoidal estimates for studied nonlinear systems are given. Numerical simulation results related to the proposed techniques and to the presented algorithms are also included.

2 Problem formulation

Let us introduce the following basic notations. Let R^n be the n -dimensional Euclidean space, $compR^n$ is the set of all compact subsets of R^n , $R^{n \times n}$ stands for the set of all $n \times n$ -matrices and $x'y = (x, y) = \sum_{i=1}^n x_i y_i$ be the usual inner product of $x, y \in R^n$ with prime as a transpose, $\|x\| = (x'x)^{1/2}$. We denote as $B(a, r)$ the ball in R^n , $B(a, r) = \{x \in R^n : \|x - a\| \leq r\}$, I is the identity $n \times n$ -matrix. Denote by $E(a, Q) = \{x \in R^n : (Q^{-1}(x - a), (x - a)) \leq 1\}$ the ellipsoid in R^n with a center $a \in R^n$ and a symmetric positive definite

$n \times n$ -matrix Q , $Tr(Y)$ denotes the trace of $n \times n$ -matrix Y (the sum of its diagonal elements). Consider the following system

$$\dot{x} = A(t)x + f(x)d + u(t), \quad x_0 \in X_0, \quad t_0 \leq t \leq T, \quad (1)$$

where $x, d \in R^n$, $\|x\| \leq K$ ($K > 0$), $f(x)$ is the nonlinear function, which is quadratic in x ,

$$f(x) = x' B x,$$

with a given symmetric and positive definite $n \times n$ -matrix B . Control functions $u(t)$ in (1) are assumed Lebesgue measurable on $[t_0, T]$ and satisfying the constraint

$$u(t) \in U, \quad \text{for a.e. } t \in [t_0, T],$$

(here U is a given set, $U \in \text{comp}R^m$). The $n \times n$ -matrix function $A(t)$ in (1) has the form

$$A(t) = A^0 + A^1(t), \quad (2)$$

where the $n \times n$ -matrix A^0 is given and the measurable $n \times n$ -matrix $A^1(t)$ with elements $\{a_{ij}^{(1)}(t)\}$ ($i, j = 1, \dots, n$) is unknown but bounded

$$A^1(t) \in \mathcal{A} = \{A = \{a_{ij}\} \in R^{n \times n} : |a_{ij}| \leq c_{ij}, \quad i, j = 1, \dots, n\}, \quad t \in [t_0, T], \quad (3)$$

where $c_{ij} \geq 0$ ($i, j = 1, \dots, n$) are given.

We will assume that X_0 in (1) is an ellipsoid, $X_0 = E(a_0, Q_0)$, with a symmetric and positive definite matrix Q_0 and with a center a_0 .

Let the absolutely continuous function $x(t) = x(t; u(\cdot), A^1(\cdot), x_0)$ be a solution to dynamical system (1)–(3) with initial state $x_0 \in X_0$, with admissible control $u(\cdot)$ and with a matrix $A^1(\cdot)$ satisfying (2)–(3). The reachable set $X(t)$ at time t ($t_0 < t \leq T$) of system (1)–(3) is defined as the following set

$$X(t) = \{ x \in R^n : \exists x_0 \in X_0, \exists u(\cdot) \in U, \exists A^1(\cdot) \in \mathcal{A} \text{ such that}$$

$$x = x(t) = x(t; u(\cdot), A^1(\cdot), x_0) \}, \quad t_0 < t \leq T.$$

The main problem of the paper is to find the external ellipsoidal estimate $E(a^+(t), Q^+(t))$ (with respect to the inclusion of sets) of the reachable set $X(t)$ ($t_0 < t \leq T$) by using the analysis of a special type of nonlinear control systems with uncertain initial data.

3 Preliminaries

In this section we present some auxiliary results on the properties of reachable sets for different types of dynamical systems which we will need in the sequel.

3.1 Bilinear system

Bilinear dynamic systems are a special kind of nonlinear systems representing a variety of important physical processes. A great number of results related to control problems for such systems has been developed over past decades, among them we mention here Brockett[2], Chernousko[4,5], Polyak *et al.*[19], Kurzhanski and Varaiya[15], Kurzhanski and Filippova[13], Mazurenko[17], Filippova[7,11]. Reachable sets of bilinear systems in general are not convex, but have special properties (for example, are star-shaped). We, however, consider here the guaranteed state estimation problem and use ellipsoidal calculus for the construction of external estimates of reachable sets of such systems.

Consider the bilinear system

$$\dot{x} = A(t)x, \quad t_0 \leq t \leq T, \quad (4)$$

$$x_0 \in X_0 = E(a_0, Q_0), \quad (5)$$

where $x, a_0 \in R^n$, Q_0 is symmetric and positive definite. The unknown matrix function $A(t) \in R^{n \times n}$ is assumed to be of the form (2) with the assumption (3).

The external ellipsoidal estimate of reachable set $X(T)$ of the system (4)-(5) can be found by applying the following theorem.

Theorem 1 (Chernousko[4]). *Let $a^+(t)$ and $Q^+(t)$ be the solutions of the following system of nonlinear differential equations*

$$\dot{a}^+ = A^0 a^+, \quad a^+(t_0) = a_0, \quad t_0 \leq t \leq T, \quad (6)$$

$$\dot{Q}^+ = A^0 Q^+ + Q^+ A^{0'} + qQ^+ + q^{-1}G, \quad Q^+(t_0) = Q_0, \quad t_0 \leq t \leq T, \quad (7)$$

where

$$q = (n^{-1} \text{Tr}((Q^+)^{-1}G))^{1/2}, \quad (8)$$

$$G = \text{diag} \left\{ (n-v) \left[\sum_{i=1}^n c_{ji} |a_i^+| + \left(\max_{\sigma=\{\sigma_{ij}\}} \sum_{p,q=1}^n Q_{pq}^+ c_{jp} c_{jq} \sigma_{jp} \sigma_{jq} \right)^{1/2} \right]^2 \right\}, \quad (9)$$

the maximum in (9) is taken over all $\sigma_{ij} = \pm 1$, $i, j = 1, \dots, n$, such that $c_{ij} \neq 0$ and v is a number of such indices i for which we have: $c_{ij} = 0$ for all $j = 1, \dots, n$. Then the following external estimate for the reachable set $X(t)$ of the system (4)-(5) is true

$$X(t) \subseteq E(a^+(t), Q^+(t)), \quad t_0 \leq t \leq T. \quad (10)$$

Corollary 1. *Under conditions of the Theorem 1 the following inclusion holds*

$$\begin{aligned} X(t_0 + \sigma) &\subseteq (I + \sigma A) X_0 + o_1(\sigma) B(0, 1) \subseteq \\ &E(a^+(t_0 + \sigma), Q^+(t_0 + \sigma)) + o_2(\sigma) B(0, 1), \end{aligned} \quad (11)$$

where $\sigma^{-1} o_i(\sigma) \rightarrow 0$ for $\sigma \rightarrow +0$ ($i = 1, 2$) and

$$(I + \sigma A) X_0 = \bigcup_{x \in X_0} \bigcup_{A \in \mathcal{A}} \{x + \sigma Ax\}.$$

Proof. The inclusion (11) follows directly from (10) and presents a special case of the inclusion related to the discrete version of the integral funnel equation for the system (4)-(5) (Kurzhanski and Varaiya[15], Kurzhanski and Filippova[13]).

The following example illustrates the result of Theorem 1.

Example 1. Consider the following system

$$\begin{cases} \dot{x}_1 = x_2, \\ \dot{x}_2 = (c(t) - 1)x_1, \end{cases} \quad 0 \leq t \leq 1, \quad x_0 \in X_0 = B(0, 1) \quad (12)$$

where $c(t)$ is an unknown but bounded measurable function with $|c(t)| \leq 0.8$ ($0 \leq t \leq 1$). The trajectory tube $X(t)$ and its external ellipsoidal estimate $E(a^+(t), Q^+(t))$ found by Theorem 1 are shown in Figure 1.

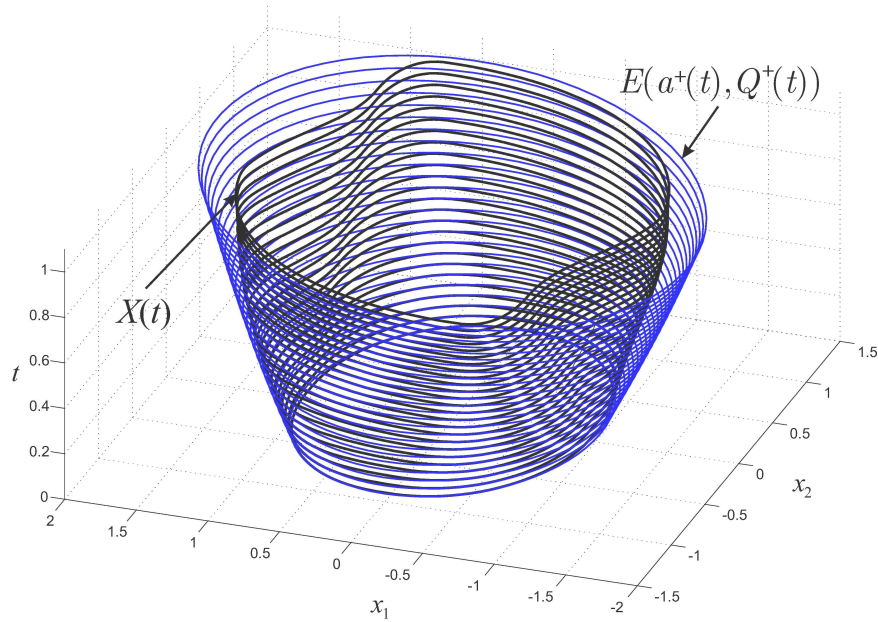


Fig. 1. Trajectory tube $X(t)$ and its ellipsoidal estimating tube $E(a^+(t), Q^+(t))$ for the bilinear control system with uncertain initial states.

We see here that the trajectory tube $X(t)$ of bilinear system (12), issued from the convex set $X_0 = B(0, 1)$, loses the convexity over time. External ellipsoidal tube $E(a^+(t), Q^+(t))$ contains the reachable set $X(t)$ and in some points is enough accurate (it touches the boundary of $X(t)$).

3.2 Systems with quadratic nonlinearity

Consider the control system of type (1) but with a known matrix $A = A^0$

$$\dot{x} = A^0 x + f(x)d + u(t), \quad x_0 \in X_0 = E(a_0, Q_0), \quad t_0 \leq t \leq T. \quad (13)$$

We assume here that $u(t) \in U = E(\hat{a}, \hat{Q})$, vectors d, a_0, \hat{a} are given, a scalar function $f(x)$ has a form $f(x) = x'Bx$, matrices B, Q_0, \hat{Q} are symmetric and positive definite.

Denote the maximal eigenvalue of the matrix $B^{1/2}Q_0B^{1/2}$ by k^2 , it is easy to see this k^2 is the smallest number for which the inclusion $X_0 \subseteq E(a_0, k^2B^{-1})$ is true. The following result describes the external ellipsoidal estimate of the reachable set $X(t) = X(t; t_0, X_0)$ ($t_0 \leq t \leq T$).

Theorem 2 (Filippova[10]). *The inclusion is true for any $t \in [t_0, T]$*

$$X(t; t_0, X_0) \subseteq E(a^+(t), r^+(t)B^{-1}), \quad (14)$$

where functions $a^+(t), r^+(t)$ are the solutions of the following system of ordinary differential equations

$$\dot{a}^+(t) = A^0 a^+(t) + ((a^+(t))' B a^+(t) + r^+(t))d + \hat{a}, \quad t_0 \leq t \leq T, \quad (15)$$

$$\begin{aligned} \dot{r}^+(t) = \max_{\|l\|=1} \left\{ l' (2r^+(t)B^{1/2}(A^0 + 2d \cdot (a^+(t))' B)B^{-1/2} + \right. \\ \left. q^{-1}(r^+(t))B^{1/2}\hat{Q}B^{1/2})l \right\} + q(r^+(t))r^+(t), \quad (16) \\ q(r) = ((nr)^{-1} \text{Tr}(B\hat{Q}))^{1/2}, \end{aligned}$$

with initial state

$$a^+(t_0) = a_0, \quad r^+(t_0) = k^2.$$

Corollary 2 (Filippova[8]). *The following upper estimate for $X(t_0 + \sigma) = X(t_0 + \sigma; t_0, X_0)$ ($\sigma > 0$) holds*

$$X(t_0 + \sigma) \subseteq E(a^+(\sigma), Q^+(\sigma)) + o(\sigma)B(0, 1), \quad (17)$$

where $\sigma^{-1}o(\sigma) \rightarrow 0$ when $\sigma \rightarrow +0$ and

$$a^+(\sigma) = a(\sigma) + \sigma\hat{a}, \quad a(\sigma) = a_0 + \sigma(A^0 a_0 + a_0' B a_0 d + k^2 d), \quad (18)$$

$$\begin{aligned} Q^+(\sigma) &= (p^{-1} + 1)Q(\sigma) + (p + 1)\sigma^2\hat{Q}, \\ Q(\sigma) &= k^2(I + \sigma R)B^{-1}(I + \sigma R)', \quad R = A^0 + 2d \cdot a_0' B \end{aligned} \quad (19)$$

and p is the unique positive root of the equation

$$\sum_{i=1}^n \frac{1}{p + \alpha_i} = \frac{n}{p(p + 1)}$$

with $\alpha_i \geq 0$ ($i = 1, \dots, n$) being the roots of the following equation $|Q(\sigma) - \alpha\sigma^2\hat{Q}| = 0$.

Numerical algorithms basing on Theorem 2 and producing the discrete-time external ellipsoidal tube estimating the reachable set of the system (13) (together with related examples) are given in Filippova[10], Filippova and Matviy-chuk[12].

4 Main results

Consider the general case

$$\dot{x} = A(t)x + x'Bx \cdot d + u(t), \quad t_0 \leq t \leq T, \quad (20)$$

with initial state

$$x_0 \in X_0 = E(a_0, Q_0) \quad (21)$$

and control constraints

$$u(t) \in U = E(\hat{a}, \hat{Q}), \quad (22)$$

and with the uncertain matrix

$$A(t) = A^0 + A^1(t), \quad A^1(t) \in \mathcal{A}, \quad (23)$$

where the set \mathcal{A} is defined in (3). As before we assume that matrices B , \hat{Q} and Q_0 are symmetric and positive definite.

The next theorem describes discrete external ellipsoidal estimates of reachable sets $X(t)$ of the uncertain control system (20)–(23), containing both bilinear and quadratic nonlinearities.

Theorem 3. *The following external ellipsoidal estimate holds*

$$X(t_0 + \sigma) \subseteq E(a^*(t_0 + \sigma), Q^*(t_0 + \sigma)) + o(\sigma)B(0, 1) \quad (24)$$

where $\sigma^{-1}o(\sigma) \rightarrow 0$ for $\sigma \rightarrow +0$ and where

$$a^*(t_0 + \sigma) = \tilde{a}(t_0 + \sigma) + \sigma(\hat{a} + a'_0 B a_0 \cdot d + k^2 d), \quad (25)$$

$$Q^*(t_0 + \sigma) = (p^{-1} + 1)\tilde{Q}(t_0 + \sigma) + (p + 1)\sigma^2 \hat{Q}, \quad (26)$$

with functions $\tilde{a}(t)$, $\tilde{Q}(t)$ calculated as $a^+(t)$, $Q^+(t)$ in Theorem 1 but when we replace matrices Q_0 and A^0 in (6)–(9) by

$$\tilde{Q}_0 = k^2 B^{-1}, \quad \tilde{A}^0 = A^0 + 2d \cdot a'_0 B \quad (27)$$

respectively, and p is the unique positive root of the equation

$$\sum_{i=1}^n \frac{1}{p + \alpha_i} = \frac{n}{p(p + 1)} \quad (28)$$

with $\alpha_i \geq 0$ ($i = 1, \dots, n$) being the roots of the following equation $|Q(t_0 + \sigma) - \alpha\sigma^2 \hat{Q}| = 0$.

Proof. Analyzing both results of Theorem 1 and Theorem 2 and of their corollaries and using the general scheme of the proof of Theorem 2 in Filippova[8] (see also techniques in Filippova[9]) we obtain the formulas (24)–(28) of the Theorem.

The following iterative algorithm basing on Theorem 3 may be used to produce the external ellipsoidal tube estimating the reachable set $X(t)$ on the whole time interval $t \in [t_0, T]$.

Algorithm. Subdivide the time segment $[t_0, T]$ into subsegments $[t_i, t_{i+1}]$ where $t_i = t_0 + ih$ ($i = 1, \dots, m$), $h = (T - t_0)/m$, $t_m = T$.

- Given $X_0 = E(a_0, Q_0)$, find the smallest $k = k_0 > 0$ such that

$$E(a_0, Q_0) \subseteq E(a_0, k^2 B^{-1})$$

(k^2 is the maximal eigenvalue of the matrix $B^{1/2}Q_0B^{1/2}$).

- Take $\sigma = h$ and define by Theorem 3 the external ellipsoid $E(a_1, Q_1)$ such that

$$X(t_1) \subseteq E(a_1, Q_1) = E(a^*(t_0 + \sigma), Q^*(t_0 + \sigma)).$$

- Consider the system on the next subsegment $[t_1, t_2]$ with $E(a_1, Q_1)$ as the initial ellipsoid at instant t_1 .
- Next steps continue iterations 1-3. At the end of the process we will get the external estimate $E(a(t), Q(t))$ of the tube $X(t)$ with accuracy tending to zero when $m \rightarrow \infty$.

Example 2. Consider the following control system

$$\begin{cases} \dot{x}_1 = x_2 + u_1, \\ \dot{x}_2 = -x_1 + c(t)x_1 + x_1^2 + x_2^2 + u_2, \end{cases} \quad x_0 \in X_0, \quad t_0 \leq t \leq T. \quad (29)$$

Here we take $t_0 = 0$, $T = 0.35$, $X_0 = B(0, 1)$ and $U = B(0, 0.1)$, the uncertain but bounded measurable function $c(t)$ satisfies the inequality $|c(t)| \leq 0.8$ ($t_0 \leq t \leq T$). The trajectory tube $X(t)$ and its external ellipsoidal estimating tube $E(a^*(t), Q^*(t))$ calculated by the Algorithm are given in Figure 2.

5 Conclusions

The paper deals with the problems of state estimation for uncertain dynamical control systems for which we assume that the initial state is unknown but bounded with given constraints and the matrix in the linear part of state velocities is also unknown but bounded.

We study here the case when the system nonlinearity is generated by the combination of two types of functions in related differential equations, one of which is bilinear and the other one is quadratic. The problem may be reformulated as the problem of describing the motion of set-valued states in the state space under nonlinear dynamics with state velocities having bilinear-quadratic type.

Basing on results of ellipsoidal calculus developed earlier for some classes of uncertain systems we present the modified state estimation approach which uses the special structure of nonlinearity and uncertainty in the control system and allows constructing the external ellipsoidal estimates of reachable sets.

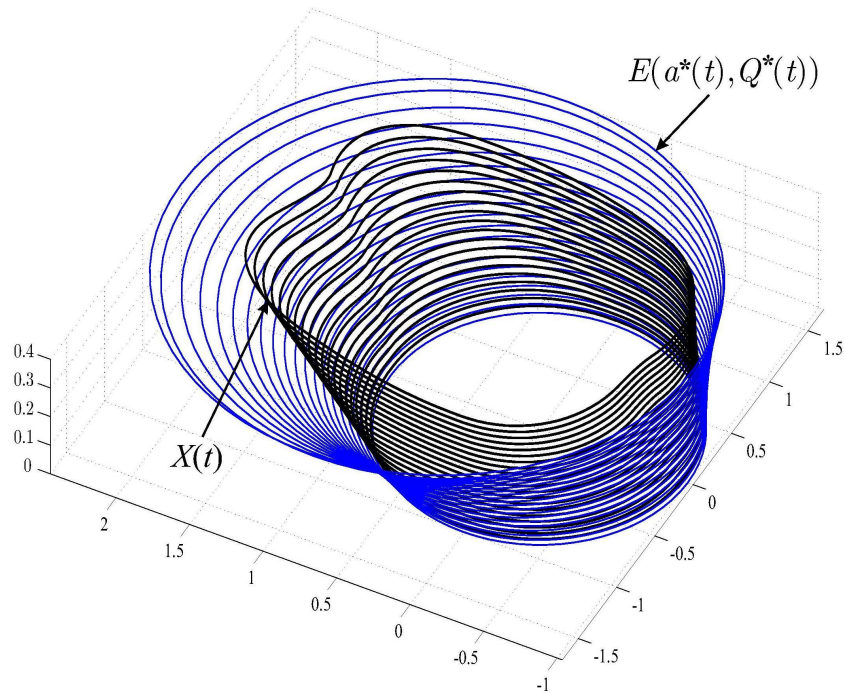


Fig. 2. Trajectory tube $X(t)$ and its ellipsoidal estimating tube $E(a^*(t), Q^*(t))$ for the system with bilinear and quadratic nonlinearities.

Acknowledgements

The research was supported by the Russian Foundation for Basic Researches (RFBR) under Project 15-01-02368a, by the Fundamental Research Program (Project 15-16-1-8) of the Presidium of Russian Academy of Sciences (RAS) with the support of Ural Branch of RAS and by the Program “State Support of the Leading Scientific School” (NS-2692.2014.1).

References

1. D. P. Bertsekas and I. B. Rhodes. Recursive state estimation for a set-membership description of uncertainty. *IEEE Transactions on Automatic Control*, 16, 117–128, 1971.
2. R. W. Brockett. On the reachable set for bilinear systems. *Lecture Notes in Economics and Mathematical Systems*, 111, 54–63, 1975.
3. F. L. Chernousko. *State Estimation for Dynamic Systems*. CRC Press. Boca Raton, 1994.
4. F. L. Chernousko. Ellipsoidal approximation of the reachable sets of linear systems with an indeterminate matrix. *Applied Mathematics and Mechanics*, 60, 6, 940–950, 1996.

5. F. L. Chernousko, D. Ya. Rokityanskii. Ellipsoidal bounds on reachable sets of dynamical systems with matrices subjected to uncertain perturbations. *Journ. of Optimiz. Theory and Appl.*, 104, 1, 1-19, 2000.
6. A. L. Dontchev and F. Lempio. Difference methods for differential inclusions: a survey. *SIAM Review*, 34, 263–294, 1992.
7. T. F. Filippova. A note on the evolution property of the assembly of viable solutions to a differential inclusion. *Computers & Mathematics with Applications*, 25, 2, 115–121, 1993.
8. T. F. Filippova. Estimates of Trajectory Tubes of Uncertain Nonlinear Control Systems. *Lect. Notes in Comput. Sci.*, 5910, 272–279, 2010.
9. T. F. Filippova. Trajectory tubes of nonlinear differential inclusions and state estimation problems. *J. of Concrete and Applicable Mathematics, Eudoxus Press, LLC*, 8, 454–469, 2010.
10. T. F. Filippova. Set-valued dynamics in problems of mathematical theory of control processes. *International Journal of Modern Physics, Series B (IJMPB)*, 26, 25, 1–8, 2012.
11. T. F. Filippova, D. V. Lisin. On the Estimation of Trajectory Tubes of Differential Inclusions. *Proc. Steclov Inst. Math.: Problems Control Dynam. Systems. Suppl. Issue 2*, S28–S37, 2000.
12. T. F. Filippova and O. G. Matviychuk. Algorithms of Estimating Reachable Sets of Nonlinear Control Systems with Uncertainty. In: *Proceedings of the 7th Chaotic Modeling and Simulation International Conference (Lisbon, Portugal: 7-10 June, 2014). Published by ISAST: International Society for the Advancement of Science and Technology, Christos H Skiadas (Ed.)*, 115–124, Portugal, 2014.
13. A. B. Kurzhanski and T. F. Filippova. On the theory of trajectory tubes a mathematical formalism for uncertain dynamics, viability and control. In: *Advances in Nonlinear Dynamics and Control: a Report from Russia, Progress in Systems and Control Theory*, A. B. Kurzhanski (Ed.), 17, 22–188. Birkhauser, Boston, 1993.
14. A. B. Kurzhanski and I. Valyi. *Ellipsoidal Calculus for Estimation and Control*. Birkhauser, Boston, 1997.
15. A. B. Kurzhanski and P. Varaiya. *Dynamics and Control of Trajectory Tubes. Theory and Computation*. Springer-Verlag, New York, 2014.
16. O. G. Matviychuk. Estimation Problem for Impulsive Control Systems under Ellipsoidal State Bounds and with Cone Constraint on the Control. *AIP Conf. Proc.*, 1497, 3–12, 2012.
17. S. S. Mazurenko. A differential equation for the gauge function of the star-shaped attainability set of a differential inclusion. *Doklady Mathematics*, 86, 1, 476–479, 2012.
18. M. Milanese, J. P. Norton, H. Piet-Lahanier and E. Walter (Eds.). *Bounding Approaches to System Identification*. Plenum Press, New York, 1996.
19. B. T. Polyak, S. A. Nazin S.A., C. Durieu, E. Walter. Ellipsoidal parameter or state estimation under model uncertainty. *Automatica*, 40, 1171-1179, 2004.
20. F. Schweppe. *Uncertain Dynamic Systems*. Prentice-Hall, Englewood Cliffs, New Jersey, 1973.
21. V. M. Veliov. Second order discrete approximations to strongly convex differential inclusion. *Systems and Control Letters*, 13, 263–269, 1989.
22. E. Walter and L. Pronzato. *Identification of parametric models from experimental data*. Springer-Verlag, Heidelberg, 1997.